

**Characterization of Tuba, a Novel Ena/VASP Ligand, and Function of Ena/VASP
Proteins in Mouse Development**

by

Adam Vincent Kwiatkowski

B.S. Biology
Cornell University, 1996

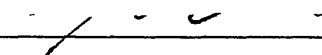
Submitted to the Department of Biology in Partial Fulfillment of the Requirement
for the Degree of

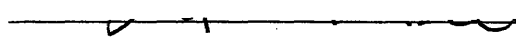
Doctor of Philosophy in Biology
at the
Massachusetts Institute of Technology

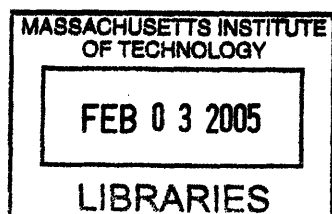
February 2005

©2004 Massachusetts Institute of Technology. All Rights Reserved.

Signature of Author:  Department of Biology
December 15, 2004

Certified by:  Frank Gertler
Associate Professor of Biology
Thesis Supervisor

Accepted by:  Stephen Bell
Professor of Biology
Chair, Committee for Graduate Students



ARCHIVES

**Characterization of Tuba, a Novel Ena/VASP Ligand, and Function of Ena/VASP
Proteins in Mouse Development**

by

Adam Vincent Kwiatkowski

Submitted to the Department of Biology on December 15, 2004
in Partial Fulfillment of the Requirements for the Degree of Doctor
of Philosophy in Biology

Abstract

Regulated actin assembly drives cells movement, adhesion and shape change. The Ena/VASP family of proteins controls actin filament elongation and are important regulators of axon guidance and cell motility. In vertebrates, the family consists of Mena (Mammalian Enabled), VASP (Vasodilator Stimulated Phosphoprotein), and EVL (Ena-VASP-Like). This thesis work focused on understanding the vertebrate Ena/VASP protein family by discovering pathways that regulate Ena/VASP function and by defining the role of Ena/VASP proteins in vertebrate development. Characterization of the EVL locus revealed a new EVL isoform. A protein interaction screen for new Ena/VASP ligands produced Tuba, a novel scaffold protein that associates with Ena/VASP proteins *in vivo*. Tuba is a unique guanine nucleotide exchange factor (GEF) for Cdc42 that binds dynamin and a number of actin regulatory proteins in addition to Ena/VASP proteins. A knockout of EVL was made to determine the requirement for EVL in mouse development. Genetic analysis of Ena/VASP function in the mouse revealed a requirement for Ena/VASP proteins in neuronal layering, spinal and cranial nerve formation, and cardiovascular development.

Thesis Supervisor: Frank Gertler
Title: Associate Professor of Biology

Table of Contents

Title Page	1
Abstract	2
Table of Contents	3
Acknowledgements	4
Chapter 1. Introduction	5
Chapter 2. Molecular Characterization of Ena/VASP-Like (EVL)	37
Chapter 3. Tuba is a Novel Rho-Family Guanine Nucleotide Exchange Factor (GEF) That Binds Ena/VASP Proteins and Links Dynammin to Regulation of the Actin Cytoskeleton	56
Chapter 4. The Role of Ena/VASP Proteins in Mouse Development	102
Chapter 5. Future Directions	140

Acknowledgements

There are many people to thank. I have had the amazing good fortune of meeting and interacting with many wonderful and interesting people during my years as a graduate student, all of whom impacted my life here at MIT in some manner. I will never forget my time here, and although trying at times, it has been a memorable journey.

First of all, thank you so much Frank. For all of your help, guidance, inspiration and motivation through the years. You have had an immeasurable impact on my development as scientist, and for that, I am forever grateful.

In no particular order, many thank yous to...

Dan – for your enthusiasm and hard work on the two hybrid screen. My first and only UROP, you taught me a lot, and I hope you learned a thing or two from me.

Jon - without your help, there would be EVL knockout mice. You came along just in the nick of time and helped me keep this project going when I had just about given up. Your hard work and determination made it happen.

Doug – what can I say, I owe you big. You have been invaluable in moving the knockout project forward. I have enjoyed working with you over the last year, and eagerly await the day when we can reap the benefits of our hard work. And stop setting up plugs.

Joe – for everything over the years. You have been a great friend and labmate, and were always there when I needed you most. You too have had an immeasurable impact on my development as a scientist.

Bronson – your help with the analysis of the knockout mice has been great.

Angelique, Kara, and Gretchen – an extra big thank you for all the help with genotyping and other mouse issues!

Jill, Caroline, Jen and the rest of the wonderful DCM staff – thank you for all the great work you do keeping our mice happy and healthy.

Jim and Matthias– for all the help and guidance over the years.

Members of my committee – for all the helpful advice over the years.

Labmates – you have made my time in the Gertler lab interesting and unforgettable.

And last but certainly not least, my family – for the unconditional love and support over the years. I couldn't have done it without you.

Chapter 1

Introduction

Chapter 1

Regulated cell movement is required for normal development and physiology. Cell movement is driven largely by dynamic changes in the underlying actin cytoskeleton that affect cell morphology and adhesion. A growing list of proteins are known to regulate actin assembly, stability, and disassembly, many of which are thought to play an important role in regulating cell motility. Included in this list are the Ena/VASP proteins, a highly conserved protein family that controls actin filament elongation and regulates cell movement. The thesis work presented is a molecular, cell biological, and genetic analysis of Ena/VASP proteins. It begins in Chapter Two with the molecular characterization of one of three vertebrate Ena/VASP proteins, Ena-VASP-Like (EVL). Chapter Three describes the discovery and characterization of a novel Ena/VASP ligand, Tuba, that links Ena/VASP proteins to Rho-family GTPases. Finally, Chapter 4 details a genetic analysis of Ena/VASP proteins that reveals new requirements for Ena/VASP function in the developing mouse.

Actin dynamics in cell motility

Cell motility can be broken down into 4 steps: protrusion, adhesion, retraction, and de-adhesion. The first step, protrusion, is characterized by the forward extension of a lamellipodium in the direction of cell movement. The

Chapter 1

lamellipodium contains a branched network of actin filaments that provides the mechanical force for membrane extension. Filamentous actin (F-actin) is made up of individual globular actin (G-actin) monomers. Actin filaments are polar, having a barbed or plus end and pointed or minus end. Actin monomers incorporate more readily onto the barbed end of the actin filament. Within the extending lamellipodium, actin filaments are oriented with fast-growing barbed ends facing towards the membrane (Pollard and Borisy, 2003).

A dendritic nucleation model has been proposed to account for the formation of the actin filament network within lamellipodia (Pollard and Borisy, 2003; Svitkina and Borisy, 1999). In this model, a defined set of proteins work in concert at the front or leading edge of the extending lamellipodium to regulate actin dynamics. Though cells possess a large number of proteins that bind actin or regulate actin assembly, basic actin assembly can be achieved with a small set of core proteins (Pantaloni et al., 2001). They are actin, profilin, the Arp2/3 complex, an activator of the Arp2/3 complex, heterodimeric capping protein (CP), and cofilin. The role of these proteins in a dendritic nucleation model of lamellipodial protrusion is discussed in detail below.

Cells contain a large pool of monomeric actin, most of which is bound to sequestering proteins, such as profilin. Profilin is a small protein found in all cell types that binds to actin monomer and inhibits spontaneous nucleation (Carlsson et al., 1977). Importantly, profilin catalyzes the exchange of ADP for ATP in the bound monomer (Goldschmidt-Clermont et al., 1992). This ATP-bound actin

Chapter 1

monomer is primed for incorporation onto the growing barbed end of an actin filament. Thus, it is thought that profilin functions to maintain a pool of unpolymerized actin ready for addition to newly created filaments during protrusion.

Protrusion can be initiated when extracellular migratory cues bind to cell surface receptors. Receptor activation initiates signaling pathways that stimulate PIP2 and Rho-family GTPases (Pollard and Borisy, 2003). The importance of both PIP2 and Rho GTPases in the regulation of the actin cytoskeleton is well documented, and Rho family GTPases are discussed later in this chapter.

PIP2 and activated Rho GTPases function to stimulate members of the WASP/WAVE superfamily of proteins. This protein family activates the actin nucleating Arp2/3 complex. The Arp2/3 complex is an assembly of seven proteins, including the two actin-related proteins Arp2 and Arp3 (Machesky et al., 1994). PIP2 and Cdc42, a Rho family GTPase, bind to N-WASP and release it from an auto-inhibited state (Prehoda et al., 2000). The C-terminus of N-WASP contains a binding site for actin monomer and an acidic region that activates the Arp2/3 complex and induces actin nucleation (Machesky and Insall, 1998).

The complex of N-WASP, Arp2/3 and monomeric actin binds to the sides of existing actin filaments and promotes the formation of new actin filaments through the nucleating activity of the Arp2/3 complex. New filament growth at the barbed end is supported through the pool of profilin-actin complexes. In this model, filament growth by actin monomer addition provides the mechanical force for

Chapter 1

membrane protrusion (Pollard and Borisy, 2003). Filament growth is quickly terminated by the binding of CP to the barbed end, functioning to maintain filament length and number, an important principle in this model (Cooper and Schafer, 2000).

Newly incorporated actin subunits hydrolyze their bound ATP and slowly release the gamma-phosphate. Release of the gamma-phosphate induces filament disassembly and promotes the severing activity of ADF/cofilin at or near the pointed end. Freshly released ADP-actin monomers are bound by profilin, which promotes the exchange of ADP for ATP and replenishes the pool of ATP actin that is primed for another cycle of filament assembly at the leading edge. The cycle of Arp2/3 activation, *de novo* branch formation and elongation, filament capping, and filament disassembly continues as the lamellipodium is protruding (Pollard and Borisy, 2003). Other actin-based structures, such as filopodia and contractile rings, can be generated by variations on this mechanism or through distinct activities (Mejillano et al., 2004).

As mentioned above, cells possess a large number of proteins that are thought to have some role in regulating actin assembly. While it is possible to reconstitute actin-driven motility *in vitro* with a small, defined set of proteins, the extending lamellipodium of a cell is far more complex, and proper formation and regulation of the actin network within the lamellipodium is likely to require a number of additional proteins. One such family of proteins now thought to play an

integral role in the regulation of lamellipodial protrusion, as well as other actin-dependent processes, are the Ena/VASP family of proteins.

The Ena/VASP protein family

Ena/VASP proteins have emerged as important regulators of actin dynamics, and are thought to link different signaling pathways to changes in cell morphology. The Ena/VASP family includes the three highly related vertebrate proteins Mena (**Mammalian Enabled**), VASP (**Vasodilator Stimulated Phosphoprotein**), and EVL (**Ena-VASP-Like**), as well as the invertebrate orthologs *D. melanogaster* Ena (**Enabled**) and *C. elegans* UNC-34, and an ortholog in the mycetozoan *D. discoideum* (DdVASP) (Fig. 1). All members of the family share a highly conserved domain structure: a proline-rich core (PRO) flanked by two distinct regions called Ena-VASP Homology domains (EVH1 and EVH2, respectively). In addition, all vertebrate Ena/VASP proteins are substrates for the cyclic nucleotide dependent kinases PKA/PKG (Krause et al., 2003). The importance of the various domains and phosphorylation to the function and regulation of Ena/VASP proteins is discussed later in this chapter.

The founding members of the family, Ena and VASP, were discovered as key players in two independent, actin-dependent processes. Ena was originally identified as a dose-dependent suppressor of Abelson (Abl)-dependent phenotypes in *Drosophila* (Gertler et al., 1990). Abl is a cytoplasmic tyrosine kinase required for axon outgrowth and guidance in *Drosophila* that can phosphorylate Ena (Gertler

Chapter 1

et al., 1995). Reduction in Ena gene dosage from two to one alleviates all known Abl-dependent phenotypes (Gertler et al., 1990). Mutations in Ena cause a recessive lethal phenotype that includes defects in the embryonic nervous system (Gertler et al., 1995; Wills et al., 1999). VASP was originally identified as a major

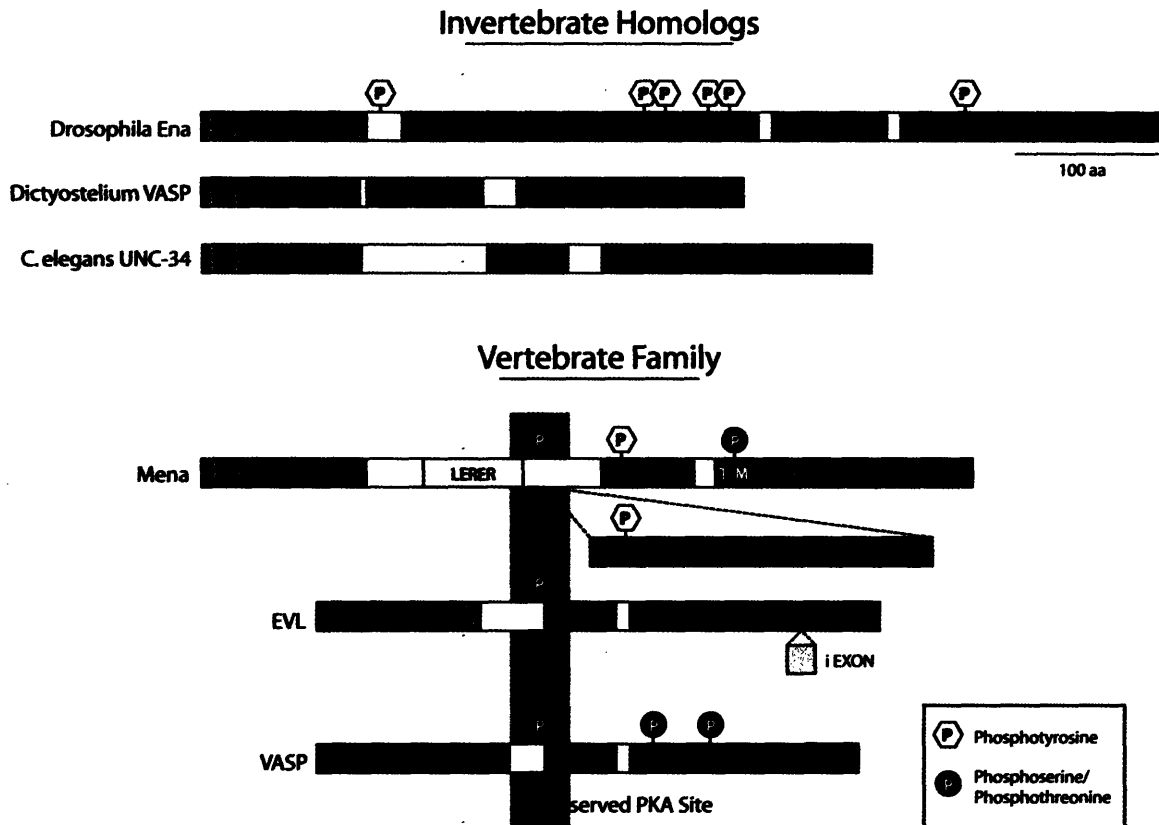


Figure 1. The Ena/VASP Family of Proteins

substrate cyclic-nucleotide dependent kinases in platelets; phosphorylation of VASP correlates with inhibition of platelet activation (Halbrugge and Walter, 1989; Waldmann et al., 1987). Platelet activation is associated with actin-dependent changes cell morphology and adhesion that promote aggregation necessary for clot formation. The role of VASP in platelet activation is discussed in more detail below.

Chapter 1

A number of biochemical studies have implicated Ena/VASP proteins in regulating actin dynamics and cell motility. First, Ena/VASP proteins localize to the tips of filopodia and lamellipodia, highly dynamic actin-rich structures (Fig. 2).

Ena/VASP proteins are also found along stress fibers, thick actin filament bundles that stretch across the cell, at focal adhesions, sites of signaling between the cytoskeleton and the extracellular matrix, and sites of cell-cell contact (Gertler et al., 1996; Lambrechts et al., 2000;

Lanier et al., 1999; Rottner et al., 1999; Vasioukhin et al., 2000).

Second, Ena/VASP proteins bind profilin (Gertler et al., 1996;

Lambrechts et al., 2000). Third, Ena/VASP proteins bind both G-

and F-actin, and can promote actin filament elongation and bundling *in vitro* (Bachmann et al., 1999; Harbeck et al., 2000; Huttelmaier et al., 1999; Lambrechts et al., 2000; Walders-Harbeck et al., 2002). Finally, Ena/VASP proteins bind ActA, a surface protein of the intracellular pathogen *Listeria monocytogenes*, and are

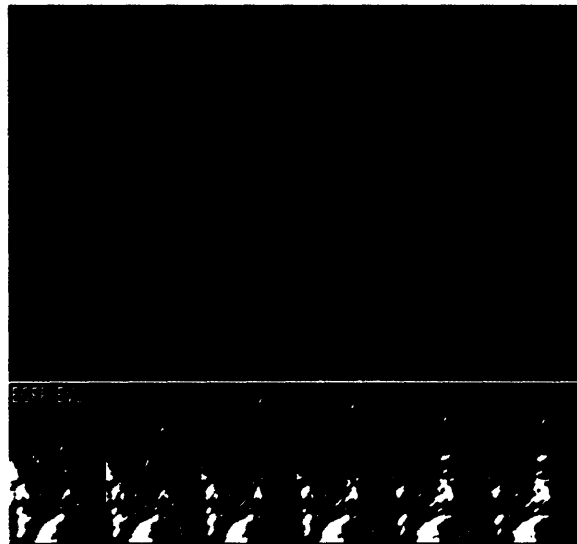


Figure 2. Localization of Ena/VASP proteins. Top panel – an extending fibroblast lamellipodium fixed and stained for VASP and F-actin. Note the enrichment of VAP at the leading edge of the lamellipodium. Bottom panel – time lapse series from a cell expressing EGFP-EVL. Dynamic localization to the tips of filopodia and lamellipodia and focal adhesions is observed. EGFP-EVL localization to the tip of one filopodium is denoted by a white arrow in each frame.

required for ActA-dependent actin polymerization and *Listeria* motility (Laurent et al., 1999).

Ena/VASP proteins regulate cell motility

The first evidence for how Ena/VASP proteins might regulate cell motility came from studies of fibroblast migration (Bear et al., 2000). Loss of Ena/VASP function, through genetic deletion or inhibition via mislocalization, causes net cell speed to increase. Conversely, overexpression of Ena/VASP proteins leads to slower cell movement. Furthermore, localization to the tips of lamellipodia is required for Ena/VASP-dependent regulation of cell speed. Selective delocalization of Ena/VASP proteins from focal adhesions, but not from the leading edge, does not affect fibroblast migration, and Ena/VASP-deficient cells do not show any reduction in the number, morphology, or protein composition of focal adhesions (Bear et al., 2000).

Ena/VASP proteins were later discovered to regulate lamellipodial protrusion by controlling the actin network geometry within the lamellipodium (Bear et al., 2002). Closer examination of lamellipodial extension in Ena/VASP-deficient cells revealed that lamellipodia protruded slower, but were more persistent. Conversely, in cells overexpressing Ena/VASP proteins, lamellipodia protruded faster but were less persistent. Loss of Ena/VASP proteins produced lamellipodia containing a network of shorter, more highly-branched filaments than in controls. Overexpression of Ena/VASP proteins, on the other hand, produced longer, less-

Chapter 1

branched filaments. These changes in the actin network geometry ultimately produce the changes in lamellipodial dynamics (Bear et al., 2002).

Actin filament length and branching must be tightly controlled to drive protrusion. In a dendritic nucleation model, filament capping by CP is important for controlling filament length and number. However, Ena/VASP activity can affect actin filament length and branching in cells. Further experiments showed that Ena/VASP proteins localize at or near the barbed end in cells, and can be displaced by drugs that bind directly to the barbed end. *In vitro*, VASP can inhibit capping by CP during actin filament polymerization (Bear et al., 2002). Therefore, one function of Ena/VASP proteins is to protect actin filaments from CP, thus promoting filament elongation.

Ena/VASP proteins also regulate filopodia formation and dynamics. Filopodia are thin cellular extensions made up of long, bundled actin filaments, and though found in many cell types, are classically associated with the growth cone of neurons. Filopodia are thought to play both sensory and mechanical roles in locomotion (Dickson, 2002). Ena/VASP proteins localize to the tips of filopodia in neurons and fibroblasts, and have been implicated in many filopodial-dependent processes (Lanier et al., 1999; Vasioukhin et al., 2000). Inhibition of Ena/VASP proteins in hippocampal neurons causes a dramatic reduction in the number and length of filopodia (Lebrand et al., 2004).

The importance of Ena/VASP proteins in filopodial formation could be due to the anti-capping activity demonstrated in fibroblasts, or it could be due to

Chapter 1

another activity of Ena/VASP proteins, or both. Additional studies in fibroblasts seem to suggest that it could be both. Loss of CP in fibroblasts eliminates lamellipodial formation and causes a dramatic increase in filopodia formation. However, in Ena/VASP-deficient cells, loss of CP causes extensive ruffling, not filopodia formation. This suggests that, in addition to functioning as antagonists of CP, Ena/VASP proteins can promote filopodia formation (Mejillano et al., 2004). The filopodia forming activity of Ena/VASP proteins could involve their ability to tetramerize and bundle actin filaments. The structural properties of Ena/VASP proteins are discussed in the next section.

Structural requirements for Ena/VASP function

The EVH1 domain

The EVH1 domain is the most highly conserved region in Ena/VASP proteins and binds directly to a proline-rich consensus motif, (D/E)-FPPPP-X(D/E)(D/E). The EVH1 domain plays an essential role in subcellular targeting of Ena/VASP proteins. A number of cellular proteins contain FPPPP motifs and are known to bind Ena/VASP proteins, including the focal adhesion proteins zyxin and vinculin, the axon guidance receptor roundabout (Robo) (Prehoda et al., 1999), and the Fyn-binding and SLP-76 associated protein (Fyb/SLAP) that functions in T-cell activation (Krause et al., 2000). The *Listeria* protein ActA contain four FPPPP motifs, and recruitment of Ena/VASP proteins is required for optimal *Listeria* motility (Laurent et al., 1999; Niebuhr et al., 1997).

Chapter 1

Ena/VASP localization to the leading edge, required for Ena/VASP function in cell motility, is in part mediated by EVH1 ligand binding. The Lamellipodin(Lpd)/RIAM family of proteins are EVH1 ligands of Ena/VASP proteins that localize to the leading edge. Both Lpd and RIAM regulate lamellipodial dynamics, and are thought to cooperate with Ena/VASP proteins to link extracellular signals to changes in actin dynamics (Krause et al., 2004; Lafuente et al., 2004).

The proline-rich region

The proline-rich(PRO) region of Ena/VASP proteins contains binding sites for profilin and a growing list of SH3 and WW domains, including those found in Abl, IRSp53, and FE65 (Kwiatkowski et al., 2003). Deletion of the PRO-region has no effect on the ability of Ena/VASP proteins to localize or to support normal rates of fibroblast movement, suggesting that this region is dispensable for the Ena/VASP-dependent regulation of cell motility (Loureiro et al., 2002). Interestingly, the same mutant provides only a limited stimulatory effect on *Listeria* movement (Geese et al., 2002). Therefore, interactions with ligands for the PRO region play an important role in the ability of Ena/VASP to support *Listeria* movement, but the requirement for such interactions in lamellipodia is unclear.

Though profilin-binding is not required for Ena/VASP-dependent regulation of whole cell motility, under certain circumstances or in specific processes, profilin levels may become limiting and expose a requirement for Ena/VASP-profilin

Chapter 1

interactions. In fact, a requirement for Mena and profilin-I has been observed genetically (Gertler et al., 1996)(discussed in Chapter 4). Alternatively, deletion of the PRO region in Ena/VASP proteins may render them constitutively active or somehow obviate a requirement for profilin binding.

Outside of profilin recruitment, the physiological significance of interactions mediated by the PRO-rich region remains unclear. It has been suggested that SH3-mediated interactions between the Rho-family effector protein IRSp53 and the PRO region of Mena stimulates filopodial formation (Krugmann et al., 2001). A second report, however, found that interactions with Mena were not required for IRSp53 localization to lamellipodia and filopodia, and that Ena/VASP proteins were not essential for filopodial formation in response to activation of pathways thought to use IRSp53 (Nakagawa et al., 2003). Given the potent genetic interactions between Ena and Abl in flies, it is possible that physical interactions between the PRO-region and the SH3 domain of Abl might play a role in connecting Abl signaling to Ena/VASP function. Identifying additional ligands to the PRO-rich region will better define the importance of the PRO region for Ena/VASP function. In addition, ligands to the PRO region are expected to link Ena/VASP proteins to molecular complexes and signaling pathways that might regulate Ena/VASP activity. An SH3-containing protein that binds to the PRO region and links Ena/VASP proteins to other regulators of the actin cytoskeleton is described in Chapter 3.

The EVH2 domain

The EVH2 domain contains three highly conserved regions of interest: a G-actin binding region (also known as the TLM, or Thymosin-Like-Motif), an F-actin binding region (FAB), and a coiled-coil region (COCO). Mena and VASP possess one and two PKA/PKG sites, respectively, within the EVH2 domain (Fig. X). *In vitro*, the EVH2 domain has been shown to bind both G-actin and F-actin, induce actin filament nucleation, promote filament bundling, and mediate oligomerization (Bachmann et al., 1999; Harbeck et al., 2000; Huttelmaier et al., 1999; Lambrechts et al., 2000; Walders-Harbeck et al., 2002).

The FAB region binds F-actin, and is required for Ena/VASP-dependent actin nucleation *in vitro* (Lambrechts et al., 2000). The ability to bind F-actin is crucial for Ena/VASP proteins to retain anti-capping activity in cells (Bear et al., 2002). In Ena/VASP-deficient fibroblasts, the FAB motif is necessary for both leading edge targeting and proper regulation of cell motility (Loureiro et al., 2002).

The coiled-coil region (COCO) in Ena/VASP proteins mediates oligomerization, and oligomerization has been shown to be important for both *in vitro* actin nucleation and binding to some Ena/VASP ligands (Ahern-Djamali et al., 1998; Bachmann et al., 1999; Walders-Harbeck et al., 2002). One loss of function allele of *Drosophila Ena* was found to lack just the COCO motif, indicating that this region is important for function *in vivo*. Consistent with this, a mutant form of Mena lacking the COCO region localized poorly to the leading edge and failed to function effectively in cell motility assays (Loureiro et al., 2002).

Chapter 1

The dispensability of the PRO region along with the requirement of the FAB and COCO regions for both localization and cell motility suggests that the EVH2 domain plays a prominent, profilin-independent, role in Ena/VASP function. When expressed in fibroblasts, the EVH2 domain localizes to the edges of lamellipodia, though demonstrating a broader distribution pattern than wild type Mena (Nakagawa et al., 2001). However, the EVH2 domain functions similar to wild type protein cell motility assay, suggesting that the EVH2 domain contains the features required to regulate lamellipodial dynamics during fibroblast movement.

Three properties have been ascribed to the EVH2 domain – G- actin binding, F-actin binding, and oligomerization – and others might exist. Interestingly, VASP contains two PKA/PKG sites in the EVH2 domain, Mena has one, but EVL lacks any known PKA/PKG site in the EVH2 domain. It has been postulated that the conserved N-terminal PKA/PKG site found in all three vertebrate Ena/VASP proteins is the most critical for the regulation of Ena/VASP function (Loureiro et al., 2002). However, there is evidence to support that phosphorylation in the EVH2 domain can affect Ena/VASP activities *in vitro* (Harbeck et al., 2000). The absence of PKA/PKG sites in EVL is puzzling, but the discovery of an alternate spliceform of EVL discussed in Chapter 2 might point to an additional means of regulation.

Ena/VASP phosphorylation and actin dynamics

Chapter 1

The discovery and initial characterization of Ena/VASP proteins focused on their role as substrates for specific kinases implicated in cell signaling. The *Drosophila* ortholog of the family, *Ena*, originally identified as a dominant suppressor of the non-receptor tyrosine kinase D-Abelson (*D-Abl*) (Gertler et al., 1990), was later shown to be a D-Abl substrate (Gertler et al., 1995). VASP was initially identified as an abundant substrate for cyclic-nucleotide dependent kinases in platelets (Halbrugge et al., 1990; Reinhard et al., 1992). Further studies showed that all vertebrate members of the Ena/VASP family are substrates for both cAMP and cGMP-induced protein kinases (PKA and PKG) (Butt et al., 1994; Gertler et al., 1996; Lambrechts et al., 2000). VASP possesses three PKA/PKG phosphorylation sites that flank the central proline-rich region. Mena contains two such sites, while EVL has just one. The lone N-terminal PKA/PKG site in EVL is structurally and functionally conserved in both Mena and VASP, and is the preferred site of PKA.

Evidence for how phosphorylation might alter specific properties of Ena/VASP proteins has come mainly from *in vitro* studies that have focused on the role of phosphorylation in regulating Ena/VASP affinities for actin and ligand binding. Phosphorylation affects Ena/VASP interactions with F-actin, although exactly how is unclear (Harbeck et al., 2000; Laurent et al., 1999). Phosphorylation of Ena/VASP proteins is known to interfere with G-actin binding and filament elongation *in vitro* (Lambrechts et al., 2000; Walders-Harbeck et al., 2002).

Phosphorylation at the first PKA/PKG site also affects interactions between the adjacent proline-rich region and a number of SH3 domains (including the Abl SH3 domain), but does not affect binding to profilin *in vitro* (Lambrechts et al., 2000). In cells, VASP and Abl can be detected in complexes that are disrupted under conditions that promote VASP phosphorylation (Howe et al., 2002). PKA phosphorylation does not appear to affect ligand binding to the EVH1 domain, nor does it interfere with the ability of Ena/VASP proteins to oligomerize (Harbeck et al., 2000).

Ena/VASP proteins - PKA/PKG signaling and adhesion

VASP was originally identified as a major substrate for PKA and PKG in platelets, and phosphorylation of VASP correlates with inhibition of platelet activation. In platelets, production of cyclic nucleotides and concomitant increase in PKA activity leads to inhibition of platelet activation, an actin-dependent process that promotes blood clotting. Mice lacking VASP are completely viable and fertile, and do not display any gross morphological abnormalities. However, *in vitro* analysis of platelets derived from VASP-deficient mice revealed that PKA/PKG-dependent inhibition of platelet aggregation was significantly reduced, suggesting VASP plays a key role in mediating this PKA-dependent function (Aszodi et al., 1999; Hauser et al., 1999). Interestingly, PKA-dependent phosphorylation of Ena/VASP proteins has also been shown to correlate with changes in cell adhesion in fibroblasts. Cellular detachment induces rapid PKA-dependent phosphorylation

of VASP. Reattachment results in immediate dephosphorylation of VASP, followed by intermediate levels of phosphorylation during spreading (Howe et al., 2002).

Ena/VASP proteins bind the focal adhesion proteins zyxin and vinculin and are enriched at sites of cell-substratum contact. In fibroblasts, the function of Ena/VASP in focal contacts and adhesions is unclear since removal of Ena/VASP from these structures, but not the leading edge, has no effect on cell motility or the average number and morphology of focal contacts/adhesions (Bear et al., 2000). VASP-deficient platelets, however, exhibit increased affinity for fibrinogen (Aszodi et al., 1999). Fibrinogen binding is important for cross-linking platelets at sites of injury, and is mediated by integrin $\alpha\text{IIb}\beta\text{3}$ switching from a resting to an active conformation, a process called “inside-out” signaling. Thus, one role for VASP might be to regulate inside-out signaling by integrins in response to cyclic nucleotides.

Ena/VASP proteins – cell-cell adhesion

Epithelia cells adhere tightly to each other to form sheets of cells that function as physical boundaries. Adhesion is mediated by three main types of cell-cell junctions in epithelial cells: adherens junctions, tight junctions, and desmosomes. Adherens junctions are cadherin-dependent adhesions connected to the actin cytoskeleton, and in their absence, other cell-cell junctions are reduced (Vasioukhin and Fuchs, 2001). Ena/VASP proteins localize to adherens junctions, and it has been proposed that Ena/VASP proteins function in the “filopodia-zipper”

Chapter 1

model of adherens junction formation. Overexpression of the coiled-coil region of VASP that mediates oligomerization was reported to prevent adherens junction formation in keratinocytes and cause skin blisters in mice (Vasioukhin et al., 2000). However, it is unclear if this approach interferes specifically with Ena/VASP proteins. Furthermore, analysis of mice that lack all Ena/VASP proteins has not revealed a defect in skin development (discussed in Chapter 4). Studies in *Drosophila* have revealed that Ena can affect epithelial cell biology. Ena interacts genetically with both Abl and *Drosophila* cadherin (armadillo) in epithelial sheet morphogenesis (Grevengoed et al., 2001).

Tight junctions, like adherens junctions, are connected to the actin cytoskeleton and function as a physical barrier between the apical and basolateral regions of the cell. Zona occludens-1 (ZO-1) is a marker of tight junctions, and VASP was found to co-immunoprecipitate with ZO-1 from endothelial cells (Comerford et al., 2002). Endothelial cells provide an important barrier as the lining cells of blood vessels. This barrier function is mediated through cell-cell contacts, and is regulated by PKA (Wojciak-Stothard and Ridley, 2002). It has been postulated that Ena/VASP proteins, as components of cell-cell adhesions and substrates of PKA, are important for regulating barrier function in endothelial cells (Comerford et al., 2002). A possible role for Ena/VASP proteins in endothelial biology is discussed in Chapter 4.

Ena/VASP proteins – axon guidance

Chapter 1

Genetic studies of invertebrate Ena/VASP orthologs has suggested that Ena/VASP proteins function downstream of known axon guidance signaling pathways. The founding member of the Ena/VASP family, Ena was originally identified as a dominant suppressor of lethality and central nervous system (CNS) defects associated with loss of D-Abl (Gertler et al., 1990). Loss of Ena in the fly produces defects in CNS and motor axon pathways (Gertler et al., 1995; Wills et al., 1999). Further genetic experiments suggests that Ena and D-Abl both act downstream of the repulsive axon guidance receptor roundabout (Robo). Interestingly, Ena and D-Abl appear to play opposing roles in Robo signaling, with Ena being required for Robo-dependent repulsion and D-Abl antagonizing Robo signaling (Bashaw et al., 2000). The *C. elegans* Ena/VASP ortholog Unc-34 has also been shown to be required for Sax3(Robo) repulsion (Yu et al., 2002). Consistent with the genetic data, biochemical experiments revealed that Ena/VASP proteins can bind to the cytoplasmic tail of Robo (Bashaw et al., 2000).

Ena/VASP proteins also function downstream of netrin guidance cues. The axon guidance molecule netrin binds to the receptor DCC/Unc-40, and netrin signaling promotes axonal outgrowth and turning. In the worm, gain of function mutations in DCC/Unc-40 cause defects in axon outgrowth, branching, and guidance. Genetic experiments revealed that loss of function mutations in Unc-34 suppressed the gain of function mutation in DCC/Unc-40, indicating that Unc-34 functions downstream of the DCC/Unc-40 receptor in netrin signaling (Gitai et al., 2003). Ena/VASP proteins have also been shown to function downstream of Netrin

Chapter 1

in cultured mouse neurons. Inhibition of Ena/VASP activity in neuron blocked Netrin mediated filopodia formation (Lebrand et al., 2004).

Consistent with the invertebrate models for Ena/VASP function, loss of Mena in mice causes defects in axon guidance. Of the three vertebrate family members, Mena is most highly expressed in the developing nervous system and adult brain. Mena-deficient mice are viable and fertile, but close examination of brain architecture reveals severe defects in formation of the corpus callosum, the major fiber tract that connects the two hemispheres of the brain. Mice lacking Mena also display defects in the formation of the hippocampal commissure and pontocerebellar fiber bundles (Lanier et al., 1999). The loss of Mena also disrupts formation of the optic chiasm (Menziés et al., 2004). These results suggest that the formation of major axonal pathways require Mena for proper formation, and that Mena, and by extension, Ena/VASP proteins play an important role in axon guidance.

As mentioned earlier, Ena/VASP proteins are required for proper filopodia formation and outgrowth in cultured neurons. Filopodia are thought to be critical for detecting guidance cues and promoting growth cone motility. The pathfinding phenotypes observed in Mena-deficient mice could reflect the requirement of Mena in these neurons for filopodia formation. However, the perturbation of specific axonal pathways suggests that Mena is not required for all axon guidance pathways. Three possibilities exist to explain this. The first is that the requirement of Mena in correctly targeted neurons is masked by the presence of VASP and EVL.

Chapter 1

Both VASP and EVL are expressed in the developing nervous system, and previous biochemical data as well as results presented in this thesis (Chapter 2) suggest that Ena/VASP proteins can function interchangeably. In support of this, analysis of mice lacking both Mena and VASP revealed defects not observed in single mutants (Menzies et al., 2004). Some guidance pathways are clearly disrupted in the absence of Mena (Lanier et al., 1999), suggesting that either Mena is the only Ena/VASP protein expressed in these neurons or that Mena possesses a unique function that neither VASP nor EVL possess.

The second possibility is that Ena/VASP proteins are not required for filopodia formation and growth cone motility in all neurons. Though the mechanism of Ena/VASP function in filopodia formation is not clear, it is likely to partially involve its role as a barbed end actin filament anti-capper. Recently, another class of molecules have been proposed to bind at the barbed end of actin filaments, the formins (Romero et al., 2004). A large family of proteins conserved from yeast to man, all formins possess a conserved formin homology 1 (FH1) domain that can induce actin nucleation *in vitro* and a formin homology 2 (FH2) domain that can bind profilin and is required for function *in vivo* (Zigmond, 2004). Formins bind the barbed end of actin filaments, but unlike CP, allow for the addition of actin monomer and have thus been termed “leaky cappers” (Zigmond et al., 2003). Mechanistically, formins can promote actin filament growth by accelerating the rate of ATP hydrolysis at the barbed end, a process that requires profilin (Romero et al., 2004). Formins have been proposed to be involved in

filopodia formation, and it is possible that this family of proteins, or proteins with a similar function, could compensate for the absence of Ena/VASP proteins in growth cone motility or other Ena/VASP-regulated actin processes.

The third possibility is that filopodia are not essential for all axon guidance. Though filopodia have long been implicated in sensing guidance cues and directing growth cone movement, it is possible that some growth cones do not require filopodia for movement. Instead, these growth cones could exercise a more lamellipodia-like motility, similar to a fibroblasts.

Signaling to the cytoskeleton – Rho family GTPases

A large number of molecules have been implicated in signaling to the cytoskeleton and regulating actin dynamics. In addition to the aforementioned serine/threonine kinases such as PKA and PKG, they include tyrosine kinases, MAPK kinases, lipid kinases, scaffold proteins, Ras and Rho family GTPases. The Rho family of GTPases in particular are well known to regulate pathways that control actin dynamics. Rho GTPases have been implicated in the control of polarity, vesicle trafficking, endocytosis, and growth cone guidance (Raftopoulou and Hall, 2004). Their role in the regulation of cell motility is discussed below.

Rho GTPases function as molecular switches, cycling between a GDP-bound inactive state and a GTP-bound active state. In their active state, they bind to downstream effectors and initiate a variety of cellular responses. Upstream of Rho GTPases are three separate classes of proteins that tightly regulate GTPase

Chapter 1

activity. Guanine nucleotide exchange factors (GEFs) promote the exchange of GDP for GTP, and function to maintain GTPases in the active form. GTPase activating proteins (GAPs) stimulate GTPase activity, and promote the inactive, GDP-bound form. Finally, guanine nucleotide dissociation inhibitors block function by sequestering the GTPase protein. Upstream signals activate one or more of these proteins to modulate the activity of a specific Rho GTPase (Raftopoulou and Hall, 2004).

In mammals, over 20 Rho family GTPases have been identified to date. The three best characterized GTPases are Rho, Rac and Cdc42, and all play an important role in regulating cell motility. Earlier studies in fibroblasts suggested that the three GTPases control the formation of specific actin structures. Rho regulates the assembly of stress fibers and focal adhesions, Rac controls the formation of lamellipodia, and Cdc42 regulates the production of filopodia (Nobes and Hall, 1995; Ridley and Hall, 1992; Ridley et al., 1992). Together, the three proteins function to regulate all the classic steps of cell movement.

The downstream targets of Rho GTPases are of great interest, particularly those that induce changes in the actin cytoskeleton. Some of the best characterized are members of the WASP/WAVE family of proteins. As described earlier, this family of proteins can stimulate the Arp2/3 complex and induce actin nucleation. Activated Cdc42 binds directly to and activates N-WASP in cooperation with PI(4,5)P₂, which in turns leads to Arp2/3 activation and actin nucleation (Rohatgi et al., 2001). Activated Rac does not interact with the WAVE

Chapter 1

family of proteins directly, but instead regulates a WAVE-containing molecular complex that regulates WAVE-induced Arp2/3 activation (Eden et al., 2002).

In *Drosophila*, a genetic interaction has been noted between the ortholog of Trio, which in mammals is a GEF for Rac and Cdc42, and the Ena/VASP ortholog Ena (Liebl et al., 2000). However, the significance of this interaction remains unknown. Identifying and establishing a molecular link or links between Ena/VASP proteins and Rho family GTPases will help to define how the two families of proteins cooperate to regulate actin dynamics. A protein that links Ena/VASP proteins to Rho GTPase signaling is discussed in Chapter 3.

References

- Ahern-Djamali, S. M., Comer, A. R., Bachmann, C., Kastenmeier, A. S., Reddy, S. K., Beckerle, M. C., Walter, U., and Hoffmann, F. M. (1998). Mutations in *Drosophila* enabled and rescue by human vasodilator-stimulated phosphoprotein (VASP) indicate important functional roles for Ena/VASP homology domain 1 (EVH1) and EVH2 domains. *Mol Biol Cell* 9, 2157-2171.
- Aszodi, A., Pfeifer, A., Ahmad, M., Glauner, M., Zhou, X. H., Ny, L., Andersson, K. E., Kehrel, B., Offermanns, S., and Fassler, R. (1999). The vasodilator-stimulated phosphoprotein (VASP) is involved in cGMP- and cAMP-mediated inhibition of agonist-induced platelet aggregation, but is dispensable for smooth muscle function. *Embo J* 18, 37-48.
- Bachmann, C., Fischer, L., Walter, U., and Reinhard, M. (1999). The EVH2 domain of the vasodilator-stimulated phosphoprotein mediates tetramerization, F-actin binding, and actin bundle formation. *J Biol Chem* 274, 23549-23557.
- Bashaw, G. J., Kidd, T., Murray, D., Pawson, T., and Goodman, C. S. (2000). Repulsive axon guidance: Abelson and Enabled play opposing roles downstream of the roundabout receptor. *Cell* 101, 703-715.
- Bear, J. E., Loureiro, J. J., Libova, I., Fassler, R., Wehland, J., and Gertler, F. B. (2000). Negative regulation of fibroblast motility by Ena/VASP proteins. *Cell* 101, 717-728.
- Bear, J. E., Svitkina, T. M., Krause, M., Schafer, D. A., Loureiro, J. J., Strasser, G. A., Maly, I. V., Chaga, O. Y., Cooper, J. A., Borisy, G. G., and Gertler, F. B. (2002). Antagonism between Ena/VASP proteins and actin filament capping regulates fibroblast motility. *Cell* 109, 509-521.
- Butt, E., Abel, K., Krieger, M., Palm, D., Hoppe, V., Hoppe, J., and Walter, U. (1994). cAMP- and cGMP-dependent protein kinase phosphorylation sites of the focal adhesion vasodilator-stimulated phosphoprotein (VASP) in vitro and in intact human platelets. *J Biol Chem* 269, 14509-14517.
- Carlsson, L., Nystrom, L. E., Sundkvist, I., Markey, F., and Lindberg, U. (1977). Actin polymerizability is influenced by profilin, a low molecular weight protein in non-muscle cells. *J Mol Biol* 115, 465-483.
- Comerford, K. M., Lawrence, D. W., Synnestvedt, K., Levi, B. P., and Colgan, S. P. (2002). Role of vasodilator-stimulated phosphoprotein in PKA-induced changes in endothelial junctional permeability. *Faseb J* 16, 583-585.

Chapter 1

Cooper, J. A., and Schafer, D. A. (2000). Control of actin assembly and disassembly at filament ends. *Curr Opin Cell Biol* 12, 97-103.

Dickson, B. J. (2002). Molecular mechanisms of axon guidance. *Science* 298, 1959-1964.

Eden, S., Rohatgi, R., Podtelejnikov, A. V., Mann, M., and Kirschner, M. W. (2002). Mechanism of regulation of WAVE1-induced actin nucleation by Rac1 and Nck. *Nature* 418, 790-793.

Geese, M., Loureiro, J. J., Bear, J. E., Wehland, J., Gertler, F. B., and Sechi, A. S. (2002). Contribution of Ena/VASP proteins to intracellular motility of listeria requires phosphorylation and proline-rich core but not F-actin binding or multimerization. *Mol Biol Cell* 13, 2383-2396.

Gertler, F. B., Comer, A. R., Juang, J. L., Ahern, S. M., Clark, M. J., Liebl, E. C., and Hoffmann, F. M. (1995). enabled, a dosage-sensitive suppressor of mutations in the Drosophila Abl tyrosine kinase, encodes an Abl substrate with SH3 domain-binding properties. *Genes Dev* 9, 521-533.

Gertler, F. B., Doctor, J. S., and Hoffmann, F. M. (1990). Genetic suppression of mutations in the Drosophila abl proto-oncogene homolog. *Science* 248, 857-860.

Gertler, F. B., Niebuhr, K., Reinhard, M., Wehland, J., and Soriano, P. (1996). Mena, a relative of VASP and Drosophila Enabled, is implicated in the control of microfilament dynamics. *Cell* 87, 227-239.

Gitai, Z., Yu, T. W., Lundquist, E. A., Tessier-Lavigne, M., and Bargmann, C. I. (2003). The netrin receptor UNC-40/DCC stimulates axon attraction and outgrowth through enabled and, in parallel, Rac and UNC-115/ABLIM. *Neuron* 37, 53-65.

Goldschmidt-Clermont, P. J., Furman, M. I., Wachsstock, D., Safer, D., Nachmias, V. T., and Pollard, T. D. (1992). The control of actin nucleotide exchange by thymosin beta 4 and profilin. A potential regulatory mechanism for actin polymerization in cells. *Mol Biol Cell* 3, 1015-1024.

Grevengoed, E. E., Loureiro, J. J., Jesse, T. L., and Peifer, M. (2001). Abelson kinase regulates epithelial morphogenesis in Drosophila. *J Cell Biol* 155, 1185-1198.

Halbrugge, M., Friedrich, C., Eigenthaler, M., Schanzenbacher, P., and Walter, U. (1990). Stoichiometric and reversible phosphorylation of a 46-kDa protein in human platelets in response to cGMP- and cAMP-elevating vasodilators. *J Biol Chem* 265, 3088-3093.

Chapter 1

- Halbrugge, M., and Walter, U. (1989). Purification of a vasodilator-regulated phosphoprotein from human platelets. *Eur J Biochem* 185, 41-50.
- Harbeck, B., Huttelmaier, S., Schluter, K., Jockusch, B. M., and Illenberger, S. (2000). Phosphorylation of the vasodilator-stimulated phosphoprotein regulates its interaction with actin. *J Biol Chem* 275, 30817-30825.
- Hauser, W., Knobloch, K. P., Eigenthaler, M., Gambaryan, S., Krenn, V., Geiger, J., Glazova, M., Rohde, E., Horak, I., Walter, U., and Zimmer, M. (1999). Megakaryocyte hyperplasia and enhanced agonist-induced platelet activation in vasodilator-stimulated phosphoprotein knockout mice. *Proc Natl Acad Sci U S A* 96, 8120-8125.
- Howe, A. K., Hogan, B. P., and Juliano, R. L. (2002). Regulation of vasodilator-stimulated phosphoprotein phosphorylation and interaction with Abl by protein kinase A and cell adhesion. *J Biol Chem* 277, 38121-38126.
- Huttelmaier, S., Harbeck, B., Steffens, O., Messerschmidt, T., Illenberger, S., and Jockusch, B. M. (1999). Characterization of the actin binding properties of the vasodilator-stimulated phosphoprotein VASP. *FEBS Lett* 451, 68-74.
- Krause, M., Dent, E. W., Bear, J. E., Loureiro, J. J., and Gertler, F. B. (2003). Ena/VASP proteins: regulators of the actin cytoskeleton and cell migration. *Annu Rev Cell Dev Biol* 19, 541-564.
- Krause, M., Leslie, J. D., Stewart, M., Lafuente, E. M., Valderrama, F., Jagannathan, R., Strasser, G. A., Rubinson, D. A., Liu, H., Way, M., et al. (2004). Lamellipodin, an Ena/VASP Ligand, Is Implicated in the Regulation of Lamellipodial Dynamics. *Dev Cell* 7, 571-583.
- Krause, M., Sechi, A. S., Konradt, M., Monner, D., Gertler, F. B., and Wehland, J. (2000). Fyn-binding protein (Fyb)/SLP-76-associated protein (SLAP), Ena/vasodilator-stimulated phosphoprotein (VASP) proteins and the Arp2/3 complex link T cell receptor (TCR) signaling to the actin cytoskeleton. *J Cell Biol* 149, 181-194.
- Krugmann, S., Jordens, I., Gevaert, K., Driessens, M., Vandekerckhove, J., and Hall, A. (2001). Cdc42 induces filopodia by promoting the formation of an IRSp53:Mena complex. *Curr Biol* 11, 1645-1655.
- Kwiatkowski, A. V., Gertler, F. B., and Loureiro, J. J. (2003). Function and regulation of Ena/VASP proteins. *Trends Cell Biol* 13, 386-392.
- Lafuente, E. M., van Puijenbroek, A. A., Krause, M., Carman, C. V., Freeman, G. J., Berezovskaya, A., Constantine, E., Springer, T. A., Gertler, F. B., and Boussiotis, V.

Chapter 1

A. (2004). RIAM, an Ena/VASP and Profilin Ligand, Interacts with Rap1-GTP and Mediates Rap1-Induced Adhesion. *Dev Cell* 7, 585-595.

Lambrechts, A., Kwiatkowski, A. V., Lanier, L. M., Bear, J. E., Vandekerckhove, J., Ampe, C., and Gertler, F. B. (2000). cAMP-dependent protein kinase phosphorylation of EVL, a Mena/VASP relative, regulates its interaction with actin and SH3 domains. *J Biol Chem* 275, 36143-36151.

Lanier, L. M., Gates, M. A., Witke, W., Menzies, A. S., Wehman, A. M., Macklis, J. D., Kwiatkowski, D., Soriano, P., and Gertler, F. B. (1999). Mena is required for neurulation and commissure formation. *Neuron* 22, 313-325.

Laurent, V., Loisel, T. P., Harbeck, B., Wehman, A., Grobe, L., Jockusch, B. M., Wehland, J., Gertler, F. B., and Carlier, M. F. (1999). Role of proteins of the Ena/VASP family in actin-based motility of *Listeria monocytogenes*. *J Cell Biol* 144, 1245-1258.

Lebrand, C., Dent, E. W., Strasser, G. A., Lanier, L. M., Krause, M., Svitkina, T. M., Borisy, G. G., and Gertler, F. B. (2004). Critical role of Ena/VASP proteins for filopodia formation in neurons and in function downstream of netrin-1. *Neuron* 42, 37-49.

Liebl, E. C., Forsthoefel, D. J., Franco, L. S., Sample, S. H., Hess, J. E., Cowger, J. A., Chandler, M. P., Shupert, A. M., and Seeger, M. A. (2000). Dosage-sensitive, reciprocal genetic interactions between the Abl tyrosine kinase and the putative GEF trio reveal trio's role in axon pathfinding [see comments]. *Neuron* 26, 107-118.

Loureiro, J. J., Rubinson, D. A., Bear, J. E., Baltus, G. A., Kwiatkowski, A. V., and Gertler, F. B. (2002). Critical roles of phosphorylation and actin binding motifs, but not the central proline-rich region, for Ena/vasodilator-stimulated phosphoprotein (VASP) function during cell migration. *Mol Biol Cell* 13, 2533-2546.

Machesky, L. M., Atkinson, S. J., Ampe, C., Vandekerckhove, J., and Pollard, T. D. (1994). Purification of a cortical complex containing two unconventional actins from *Acanthamoeba* by affinity chromatography on profilin-agarose. *J Cell Biol* 127, 107-115.

Machesky, L. M., and Insall, R. H. (1998). Scar1 and the related Wiskott-Aldrich syndrome protein, WASP, regulate the actin cytoskeleton through the Arp2/3 complex. *Curr Biol* 8, 1347-1356.

Mejillano, M. R., Kojima, S., Applewhite, D. A., Gertler, F. B., Svitkina, T. M., and Borisy, G. G. (2004). Lamellipodial versus filopodial mode of the actin nanomachinery: pivotal role of the filament barbed end. *Cell* 118, 363-373.

Chapter 1

Menzies, A. S., Aszodi, A., Williams, S. E., Pfeifer, A., Wehman, A. M., Goh, K. L., Mason, C. A., Fassler, R., and Gertler, F. B. (2004). Mena and vasodilator-stimulated phosphoprotein are required for multiple actin-dependent processes that shape the vertebrate nervous system. *J Neurosci* 24, 8029-8038.

Nakagawa, H., Miki, H., Ito, M., Ohashi, K., Takenawa, T., and Miyamoto, S. (2001). N-WASP, WAVE and Mena play different roles in the organization of actin cytoskeleton in lamellipodia. *J Cell Sci* 114, 1555-1565.

Nakagawa, H., Miki, H., Nozumi, M., Takenawa, T., Miyamoto, S., Wehland, J., and Small, J. V. (2003). IRSp53 is colocalised with WAVE2 at the tips of protruding lamellipodia and filopodia independently of Mena. *J Cell Sci* 116, 2577-2583.

Niebuhr, K., Ebel, F., Frank, R., Reinhard, M., Domann, E., Carl, U. D., Walter, U., Gertler, F. B., Wehland, J., and Chakraborty, T. (1997). A novel proline-rich motif present in ActA of *Listeria monocytogenes* and cytoskeletal proteins is the ligand for the EVH1 domain, a protein module present in the Ena/VASP family. *Embo J* 16, 5433-5444.

Nobes, C. D., and Hall, A. (1995). Rho, rac, and cdc42 GTPases regulate the assembly of multimolecular focal complexes associated with actin stress fibers, lamellipodia, and filopodia. *Cell* 81, 53-62.

Pantaloni, D., Le Clairche, C., and Carlier, M. F. (2001). Mechanism of actin-based motility. *Science* 292, 1502-1506.

Pollard, T. D., and Borisy, G. G. (2003). Cellular motility driven by assembly and disassembly of actin filaments. *Cell* 112, 453-465.

Prehoda, K. E., Lee, D. J., and Lim, W. A. (1999). Structure of the enabled/VASP homology 1 domain-peptide complex: a key component in the spatial control of actin assembly. *Cell* 97, 471-480.

Prehoda, K. E., Scott, J. A., Dyche Mullins, R., and Lim, W. A. (2000). Integration of multiple signals through cooperative regulation of the N- WASP-Arp2/3 complex. *Science* 290, 801-806.

Raftopoulou, M., and Hall, A. (2004). Cell migration: Rho GTPases lead the way. *Dev Biol* 265, 23-32.

Reinhard, M., Halbrugge, M., Scheer, U., Wiegand, C., Jockusch, B. M., and Walter, U. (1992). The 46/50 kDa phosphoprotein VASP purified from human platelets is a novel protein associated with actin filaments and focal contacts. *Embo J* 11, 2063-2070.

Chapter 1

Ridley, A. J., and Hall, A. (1992). The small GTP-binding protein rho regulates the assembly of focal adhesions and actin stress fibers in response to growth factors. *Cell* 70, 389-399.

Ridley, A. J., Paterson, H. F., Johnston, C. L., Diekmann, D., and Hall, A. (1992). The small GTP-binding protein rac regulates growth factor-induced membrane ruffling. *Cell* 70, 401-410.

Rohatgi, R., Nollau, P., Ho, H. Y., Kirschner, M. W., and Mayer, B. J. (2001). Nck and Phosphatidylinositol 4,5-bisphosphate synergistically activate actin polymerization through the N-WASP-Arp2/3 pathway. *J Biol Chem* 276, 4, 4.

Romero, S., Le Clainche, C., Didry, D., Egile, C., Pantaloni, D., and Carlier, M. F. (2004). Formin Is a Processive Motor that Requires Profilin to Accelerate Actin Assembly and Associated ATP Hydrolysis. *Cell* 119, 419-429.

Rottner, K., Behrendt, B., Small, J. V., and Wehland, J. (1999). VASP dynamics during lamellipodia protrusion. *Nat Cell Biol* 1, 321-322.

Svitkina, T. M., and Borisy, G. G. (1999). Arp2/3 complex and actin depolymerizing factor/cofilin in dendritic organization and treadmilling of actin filament array in lamellipodia. *J Cell Biol* 145, 1009-1026.

Vasioukhin, V., Bauer, C., Yin, M., and Fuchs, E. (2000). Directed actin polymerization is the driving force for epithelial cell-cell adhesion. *Cell* 100, 209-219.

Vasioukhin, V., and Fuchs, E. (2001). Actin dynamics and cell-cell adhesion in epithelia. *Curr Opin Cell Biol* 13, 76-84.

Walders-Harbeck, B., Khaitlina, S. Y., Hinssen, H., Jockusch, B. M., and Illenberger, S. (2002). The vasodilator-stimulated phosphoprotein promotes actin polymerisation through direct binding to monomeric actin. *FEBS Lett* 529, 275-280.

Waldmann, R., Nieberding, M., and Walter, U. (1987). Vasodilator-stimulated protein phosphorylation in platelets is mediated by cAMP- and cGMP-dependent protein kinases. *Eur J Biochem* 167, 441-448.

Wills, Z., Bateman, J., Korey, C. A., Comer, A., and Van Vactor, D. (1999). The tyrosine kinase Abl and its substrate enabled collaborate with the receptor phosphatase Dlar to control motor axon guidance. *Neuron* 22, 301-312.

Wojciak-Stothard, B., and Ridley, A. J. (2002). Rho GTPases and the regulation of endothelial permeability. *Vascul Pharmacol* 39, 187-199.

Chapter 1

Yu, T. W., Hao, J. C., Lim, W., Tessier-Lavigne, M., and Bargmann, C. I. (2002). Shared receptors in axon guidance: SAX-3/Robo signals via UNC-34/Enabled and a Netrin-independent UNC-40/DCC function. *Nat Neurosci* 5, 1147-1154.

Zigmond, S. H. (2004). Formin-induced nucleation of actin filaments. *Curr Opin Cell Biol* 16, 99-105.

Zigmond, S. H., Evangelista, M., Boone, C., Yang, C., Dar, A. C., Sicheri, F., Forkey, J., and Pring, M. (2003). Formin leaky cap allows elongation in the presence of tight capping proteins. *Curr Biol* 13, 1820-1823.

Chapter 2

Molecular Characterization of Ena/VASP-Like (EVL)

The results described in this chapter contributed to two manuscripts:

Lambrechts, A., Kwiatkowski, A. V., Lanier, L. M., Bear, J. E., Vandekerckhove, J., Ampe, C., and Gertler, F. B. (2000). cAMP-dependent protein kinase phosphorylation of EVL, a Mena/VASP relative, regulates its interaction with actin and SH3 domains. *J Biol Chem* 275, 36143-36151.

Loureiro, J. J., Rubinson, D. A., Bear, J. E., Baltus, G. A., Kwiatkowski, A. V., and Gertler, F. B. (2002). Critical roles of phosphorylation and actin binding motifs, but not the central proline-rich region, for Ena/vasodilator-stimulated phosphoprotein (VASP) function during cell migration. *Mol Biol Cell* 13, 2533-2546.

Abstract

There are three Ena/VASP proteins in vertebrates, Mena, VASP and EVL. Compared to Mena and EVL, relatively little is known about VASP. Analysis of genomic and EST databases revealed the presence of three alternate starts to the VASP coding sequence. Additional analysis revealed the presence of an alternatively spliced exon between the F-actin binding and coiled-coil regions of EVH2 domain of VASP. This exon has been named the I-exon, and is postulated to affect EVH2 regulation and/or function. A similar exon is also found in Mena. Expression of VASP in Ena/VASP-deficient fibroblasts rescues the Ena/VASP-dependent cell motility phenotype, indicating that VASP can substitute for Mena in regulating cell motility.

Introduction

Most work on vertebrate Ena/VASP proteins has focused on Mena and VASP. The third vertebrate Ena/VASP protein, EVL, has not been well characterized. EVL was originally identified as an expressed sequence tag (EST) with similarity to Mena (Gertler et al., 1996). The murine protein is 393 amino acids in length and shares the same domain organization as Mena and VASP. The N-terminal EVH1 domain and C-terminal EVH2 domain of EVL are highly related to Mena and VASP, but the central proline rich region is more divergent. EVL also appears to have only one conserved site for cyclic nucleotide-dependent kinase phosphorylation, compared to three for VASP and two for Mena. EVL is most highly expressed in the developing nervous system and immune system (Lanier et al., 1999). I have conducted a molecular investigation of EVL to better characterize the protein and determine if it functions similar to Mena and VASP.

Results

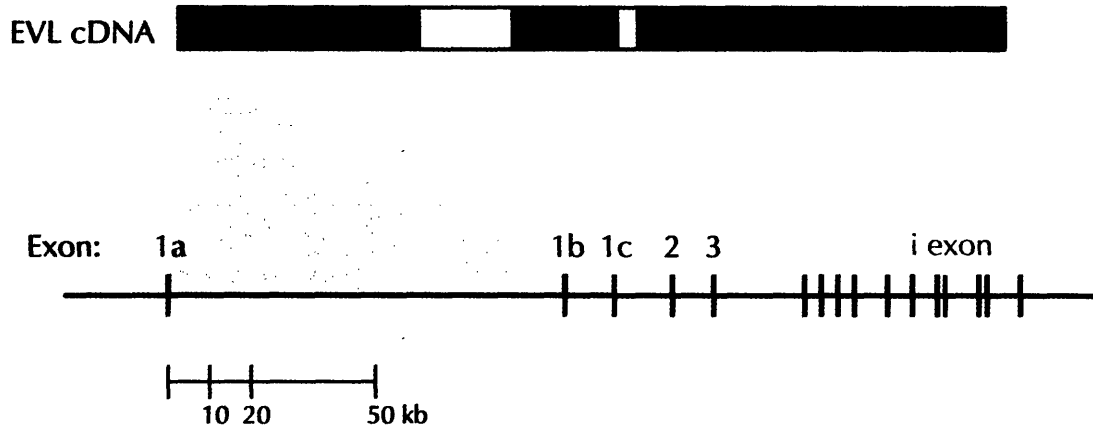
Genomic organization of EVL

BLAT searches (genome.ucsc.edu) against the mouse genome using the mouse protein sequence of EVL revealed that the EVL locus is located on chromosome 12 in mouse (Zimmer et al., 1996). A similar search against the human genome indicated that EVL is found on chromosome 14 in humans. The

Chapter 2

EVL protein is encoded by 13 exons, and the exon-intron organization is similar to both the VASP(Zimmer et al., 1996) and Mena loci (data not shown) (Fig. 1A).

A.



B.

1a. MSEQSICQARA...
1b. MFAFEEFSEQSICQARA...
1c. MVPGEQSICQARA...

Figure 1. Genomic organization of EVL. The EVL locus is located on chromosome 12 in mouse and chromosome 14 in humans, and the exon-intron organization is similar in both species. A total of 13 exons comprise the EVL gene, with one additional exon, the I exon, contributing to the alternatively spliced EVL-I gene. EST analysis suggest there are three alternative starts to EVL, encoded by three small independent exons, labeled as 1a, 1b, and 1c. Each exon 1 encodes a methionine and produces a slightly different EVL N-terminus. Exon 1a appears to be the most commonly used start.

The discovery of a 14th alternatively-spliced exon is discussed below. Exon 1 contains only 5 bps of coding sequence, and was not found in initial searches. BLAT searches using the cloned EVL cDNA (Gertler et al., 1996) that contains approximately 150 bp of 5' UTR revealed that exon 1 is located nearly 100 kb upstream of exon 2 (labeled exon 1a in Fig. 1A). More recently, ESTs encoding EVL from mouse and human sources appear to contain divergent 5' UTRs. These

Chapter 2

new ESTs group into two independent classes. To determine if these new ESTs represented alternative 5' starts or splicing errors, the two groups were aligned to the mouse genome. Interestingly, two additional starts to EVL were discovered, encoded by alternate first exons, denoted as 1b and 1c in Fig. 1A. The alternate start exons are predicted to encode different N-termini (Fig. 1B). The significance of these differences is unknown, as is the prevalence of the two alternate starts. Based on EST data, Exon 1a is the most often used start codon. Identifying both the location and number of start exons, as well as the exon-intron organization of the EVL locus, was important for targeting vector construction during the creation of the EVL knockout mouse (discussed in Chapter 4).

Discovery and characterization of EVL-I

Initial western blot analysis of EVL expression in embryonic and adult tissues revealed two protein bands of 48 and 52 kDa (Lanier et al., 1999). Similar to VASP, it was assumed initially that the 52 kDa band represented the phosphorylated version of the 48 kDa band. EVL contains just one PKA/PKG site, Serine 156, that is conserved in all vertebrate Ena/VASP proteins, and phosphorylation of this site in VASP causes a mobility shift from 46 to 50 kDa (Butt et al., 1994). However, when cell extracts were treated with PKA *in vitro*, western blot analysis revealed that both bands were shifted slightly upward, rather than a complete shift from the lower "dephosphorylated" form to the slower migrating upper "phosphorylated" form. Likewise, treatment of cell extracts with lambda-

Chapter 2

protein phosphatase did not cause a detectable shift from the 52 kDa form to the 48 kDa (Lambrechts et al., 2000).

It was postulated that the larger, 52 kDa form of EVL might represent a larger isoform of EVL produced by the inclusion of either an alternate and/or additional exon. Closer examination of released human and mouse ESTs and genomes revealed the presence of an extra small exon. Consistent with western blot expression data, this additional exon was found in ESTs from a variety of tissue sources and lies between exons 10 and 11 in the mouse genome (Fig. 1A). The exon was named the "I-exon", and the EVL isoform that contains it EVL-I. The I exon is 21 amino acids in length and found between Serine 339 and Arginine 340 of murine EVL. Located in the conserved EVH2 domain, the I exon is found between two regions required for Ena/VASP function in cell motility, the F-actin binding (FAB) region and the coiled-coil (COCO) region (Fig. 2A) (Loureiro et al., 2002). The amino acid sequence of the I exon is shown in Figure 2B. To determine if the addition of the I exon produces the larger 52 kDa form of EVL, an EVL and EVL-I cDNA were expressed in Rat2 fibroblasts. Western blot analysis of lysates prepared from these cells and adult mouse tissues indicated that the EVL-I isoform comigrated with the larger band present in spleen and thymus (Fig 2C). Thus, inclusion of the I exon and not phosphorylation produces the larger form of EVL.

Chapter 2

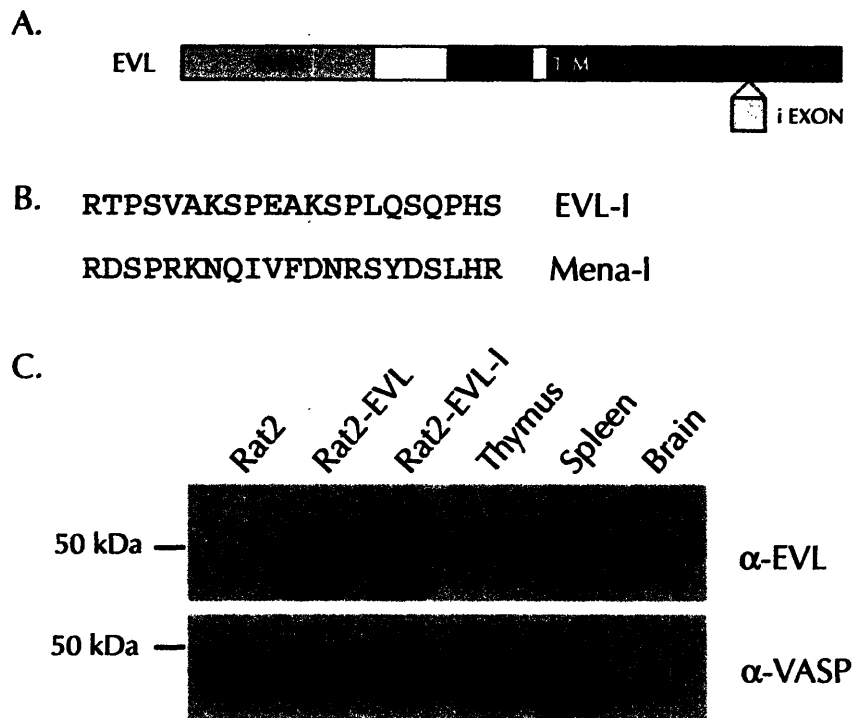


Figure 2. EVL-I is an alternatively spliced form of EVL. A. The I exon is located between Serine 339 and Arginine 340 of EVL, placing it between the F-actin binding (FAB) binding region and coiled-coil (COCO) region in the EVH2 domain. B. The I exon in EVL is 21 amino acids in length, and contains potential phosphorylation sites. An exon of the same length is located in a similar region in Mena, between Arginine 513 and Proline 514. C. Western blot analysis of transfected Rat2 fibroblasts and tissue lysates indicates that addition of the I exon produces the larger, 50 kDa form of EVL, now termed EVL-I.

Two human ESTs encoding the 3' end of Mena that contain an insert in the EVH2 domain were also discovered. Located between Arginine 513 and Proline 514 of human Mena, the 21 amino acid insert is identical in size and location to the I exon of EVL. The amino acid sequence of this insert is shown in Figure 2B. Though divergent in sequence from the I exon in EVL, the location and size of this exon led us to postulate that it is the equivalent of the I exon in EVL. Interestingly, an 88 kDa form of Mena has been observed in embryo lysates and some cultured cell line extracts, but the additional sequence that produces this isoform has

Chapter 2

remained unknown. It is possible that the addition of this exon in Mena could produce this 88 kDa form, but this remains to be tested.

The I-exon does not affect EVL localization

Intracellular Ena/VASP localization is mediated by a combination of EVH1 and EVH2 ligand binding (Bear et al., 2000; Bear et al., 2002; Loureiro et al., 2002). Within the EVH2 domain, both the FAB region and the COCO region are required for EVH2- mediated localization to the leading edge of lamellipodia (Loureiro et al., 2002). Since the I exon is located in between these two important regions, we questioned whether its presence might interfere with EVL localization to the leading edge. Rat2 fibroblasts that lack endogenous EVL were stably infected with retrovirus expressing EVL-I-IRES-EGFP and sorted by FACS for uniform GFP signal. EVL-I localization in fixed cells was identical to EVL (Fig. 3). Furthermore, EGFP-EVL-I displayed the same dynamic localization as EGFP-EVL in live cells (data not shown). Together, these results suggest that the I exon does not affect subcellular targeting.

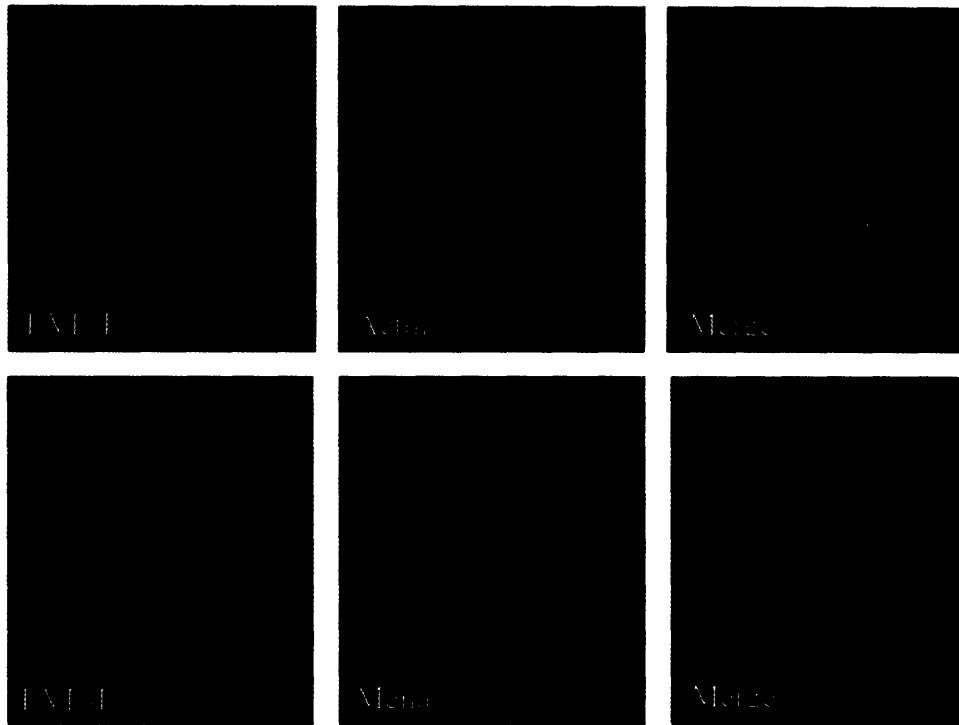


Figure 3. Immunolocalization of EVL-I in Rat2 cells. Rat2 cells expressing exogenous EVL-I were stained with monoclonal antibody 84A5 for EVL, polyclonal 2197 for Mena, and Oregon Green 488 Phalloidin. A. EVL-I localizes to focal adhesions and the leading edge of lamella. B. EVL-I colocalizes with Mena, as expected.

EVL functions interchangeably with Mena and VASP to regulate fibroblast motility

Ena/VASP proteins display a broad and overlapping pattern of expression in the developing and adult mouse (Lanier et al., 1999), and a number of biochemical and genetic experiments suggest that they can function interchangeably (Ahern-Djamali et al., 1998; Geese et al., 2002; Loureiro et al., 2002). One of best studied functions of Ena/VASP proteins is their involvement in fibroblast motility, discussed in Chapter 1. Fibroblastic cells that lack Ena/VASP expression (MV^{D7}) move more rapidly than MV^{D7} cells that express physiological levels of Mena (Bear et al., 2000). EVL is not typically found in most fibroblastic cells lines (data not shown).

Chapter 2

Therefore, we wondered whether EVL could function similar to Mena in regulating cell motility.

EGFP-EVL was stably inserted by retroviral infection into the Ena/VASP-deficient MV^{D7} cell line and sorted by FACS for EGFP expression. In addition, stable MV^{D7} cell lines expressing EGFP-VASP and EGFP-Ena, the sole *Drosophila* Ena/VASP ortholog, were generated. MV^{D7} cells expressing EGFP-Mena were made previously. All cell lines were sorted by FACS for equal EGFP expression. Western blot analysis indicated that all fusion proteins were expressed at equal levels (Loureiro et al., 2002). Finally, all four Ena/VASP fusions displayed similar subcellular distributions, concentrating at the tips of filopodia, the leading of lamellipodia, and focal adhesions (Loureiro et al., 2002).

Time-lapse video microscopy was used to analyze the ability of EVL and the other Ena/VASP proteins to restore normal motility to MV^{D7} cells (Fig. 4A). Cell speeds were quantitated by tracking individual cells over 4 hours, calculating the average speed of each cell, and comparing the population against the MV^{D7} control group (Fig. 4B). As was shown previously, expression of EGFP-Mena at physiological levels in MV^{D7} cells reduced cell speed. Expression of EGFP-EVL had a similar effect, as did the expression of EGFP-VASP, suggesting that the three vertebrate Ena/VASP proteins can function interchangeably in the regulation of whole cell motility (Fig. 4C). Interestingly, EGFP-Ena failed to complement the Ena/VASP motility phenotype, suggesting that the *Drosophila* Ena proteins lacks some key feature for function in cell movement.

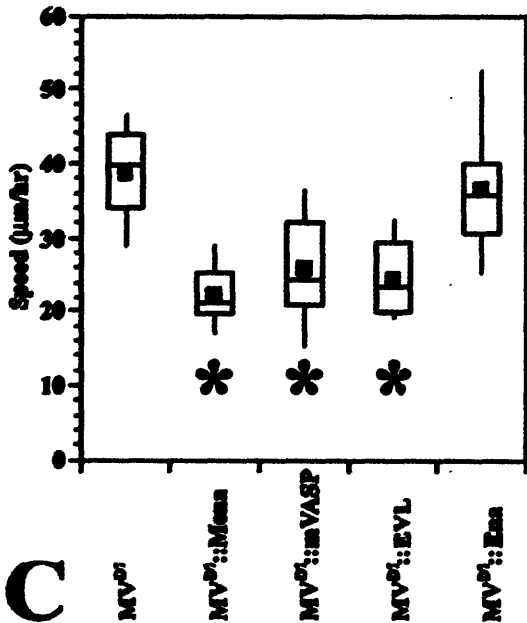
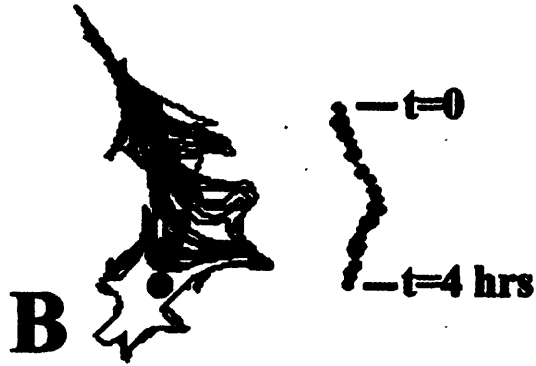
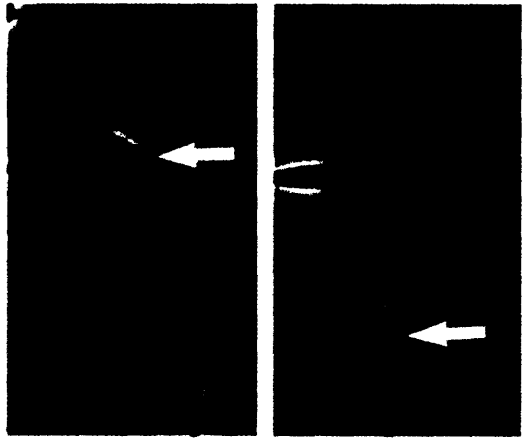


Figure 4. EVL rescues the Ena/VASP-deficient whole cell motility defect. A. Example of MV^{D7} cell movement. Time lapse movies were generated at 5 minute intervals for at least 4 hours. Frames from the beginning (t=0) and the end (t=4 hrs) of one movie are shown. The white arrow points to the same cell at the two time points. B. Cell movement is determined digitally by outlining the cell perimeter in each frame of the movie. Shown on the left is the overlay of all the time points from one cell. On the right, the area-based centroid is calculated from the outline of each cell to generate a cell path. Average cell speed is calculated from this data set and presented in a Box and Whisker format. In this format, the top of the upper line marks the 90th percentile, the top of the rectangle marks the 75th percentile, the bottom of the rectangle marks the 25th percentile, and the bottom of the lower line marks the 10th percentile. Within the rectangle, the black box is the mean and the line is the median. C. EGFP-EVL complements the MV^{D7} whole cell motility defect similar to EGFP-VASP and EGFP-Mena, whereas EGFP-Ena does not.

Discussion

Comparing 5' ESTs of EVL to the genomic region containing the EVL locus revealed what appear to be three independent start exons. The three start exons encode slightly different N-termini, and are thus expected to produce at least three different variants. At present, only two isoforms of EVL have been observed by western – EVL (48 kDa) and EVL-I (52 kDa) – and the difference in size is due to the insertion of the I exon in the EVH2 domain (discussed in more detail below). However, the size difference between alternate starting exons is only a few amino acids, and not easily resolved by SDS-PAGE and visualized by western blotting. Furthermore, over 90% of EVL ESTs found in databases contain exon 1a, suggesting that the alternate start exons, 1b and 1c, are used infrequently. A broader analysis of EVL expression in various tissues and cell types might reveal the presence of these N-terminal variants.

What function(s) might these alternate starts and variable N-termini serve?

The EVH1 domain of Ena/VASP proteins specifically recognizes specific proline rich ligands and is critical for Ena/VASP localization and function (Ball et al., 2000; Huttelmaier et al., 1998; Niebuhr et al., 1997). It is also the most highly conserved portion of Ena/VASP proteins (Gertler et al., 1996). The crystal structures of the N-terminal EVH1 domains of Mena and EVL have been solved (Fedorov et al., 1999; Ishiguro and Xavier, 2004; Prehoda et al., 1999). The EVH1 domain is structurally similar to pleckstrin homology (PH) and phosphotyrosine-binding (PTB) domains. Though conserved between Mena and EVL, the first few amino acids of the N-

Chapter 2

terminus do not appear to be critical for either peptide binding or maintaining structure. However, it is possible that the addition of amino acids at the N-terminus could alter the structure to increase or decrease ligand binding, or it may affect intramolecular interactions. Cloning and characterization of these potential N-terminal EVL variants may yield new information on Ena/VASP ligand binding and localization.

As noted above, one alternatively spliced variant of EVL was confirmed in this study, EVL-I. The I exon is 21 amino acids in length and inserted in the EVH2 domain between the FAB and COCO regions. The insertion of the I exon produces the larger 52 kDa form of EVL. Expression of the two EVL isoforms appears to be regulated in a tissue-dependent manner. For instance, both EVL and EVL-I are expressed robustly in the adult spleen and thymus, whereas EVL is the predominant form in the adult brain (Lanier et al., 1999). Inclusion of the I exon does not affect subcellular targeting, as EVL-I was found to colocalize with Mena in Rat2 cells.

The location of the I exon in the EVH2 domain suggests that it might alter EVH2 domain functions such as F-actin binding or oligomerization, both of which are required for Ena/VASP function in regulating cell motility. It is also possible that the I exon might provide additional sites for ligand binding or regulation. Unlike Mena and VASP, EVL does not contain any PKA/PKG sites in the EVH2 domain, sites that are thought to affect VASP actin *in vitro* (Harbeck et al., 2000; Walders-Harbeck et al., 2002). The I exon in EVL contains 5 serines, and a number of predicted phosphorylation sites (scansite.mit.edu), further raising the possibility

Chapter 2

that the I exon functions to add a level of regulation not present in EVL. Further experiments will be necessary to determine the functional differences between EVL and EVL-I.

An alternatively spliced exon of the same size and relative location was also discovered in Mena. Interestingly, the sequences of the two alternate exons are quite different. This alternate exon in Mena, similar to the I exon of EVL, does contain three serines and one tyrosine, suggesting that it too may function to provide additional sites for phospho-regulation. The inclusion of this exon in Mena may give rise to the 88 kDa form of Mena. This isoform of Mena is expressed during development, but is not found in adult tissues, and the additional exon(s) that produce this variant of Mena have remained undiscovered. Studying the role of this exon in Mena, combined with experiments addressing the importance of the I exon in EVL, will hopefully shed new light on the regulation and function of the EVH2 domain.

EVL functions similar to Mena and VASP in restoring the Ena/VASP loss of function cell motility phenotype in MV^{D7} fibroblasts. This observation suggests that all Ena/VASP proteins can function interchangeably in the regulation of cell movement. Other experiments have indicated all Ena/VASP proteins share the same basic functions, including the ability to support *Listeria* motility and bind actin and profilin (Gertler et al., 1996; Harbeck et al., 2000; Lambrechts et al., 2000; Laurent et al., 1999). This has important implications when conducting and interpreting loss of function experiments *in vivo*. Most tissues and cell types tested

Chapter 2

to date express at least two of the three Ena/VASP proteins. If Ena/VASP proteins are functionally interchangeable, the absence of one Ena/VASP protein would be masked by the presence of another. In support of this, animals lacking only one Ena/VASP protein display relatively subtle phenotypes (Aszodi et al., 1999; Hauser et al., 1999; Lanier et al., 1999). Therefore, to uncover Ena/VASP-dependent processes in vertebrate development and physiology, two or more Ena/VASP proteins must be deleted or inactivated (Goh et al., 2002; Menzies et al., 2004). The role of Ena/VASP proteins in mouse development is analyzed and discussed in Chapter 4.

Materials and Methods

Cloning

A fragment from mouse EST W91012 that encoded the 3' end of EVL containing the I exon was ligated to 5' end of the EVL cDNA to create a new EVL-I cDNA. The EVL-I cDNA was cloned into pIRES-EGFP using standard techniques. EVL, VASP and Ena were subcloned into the pMSCV-EGFP retroviral plasmid using standard techniques.

Immunofluorescence

Immunofluorescence staining of fibroblastic cell lines was performed essentially as described (Gertler et al., 1996). Antibodies used were anti-EVL polyclonal serum 1404, anti-Mena polyclonal antiserum 2197. Labeled secondary

Chapter 2

antibodies were purchased from Jackson Immuno Research. Images were collected on a Deltavision microscope and digitally deconvolved using Softworx software (Applied Percision).

Cell Culture

Rat2 fibroblasts were cultured as previously described (Gertler et al., 1996). The MVD7 fibroblastic cell line was isolated in Bear et al. (2000). MVD7 cell lines were cultured at 32 C in DME plus 15% fetal calf serum, penicillin/streptomycin, L-glutamine, and 50 U/ml recombinant mouse interferon- γ (Invitrogen).

Stable transfection of fibroblasts

Retroviral plasmids were transiently transfected in Bosc23 packaging cells, and supernatant collected after 48 hours. Rat2 and MVD7 cells were grown to approximately 50% confluence for infection. Retrovirus-containing supernatant supplemented with 4 μ g/ml polybrene was added to cells for 24 hours. Cells were sorted for EGFP expression by FACS.

Western blot analysis

Cells and tissues were lysed in NP-40 buffer plus protease and phosphatase inhibitors and cleared at 10,000 g for 15 minutes. Protein concentrations were measured using the BCA assay (Pierce). SDS-PAGE and western blotting were performed using standard techniques. Anti-EVL polyclonal antiserum 1404 was used for blotting.

References

- Ahern-Djamali, S. M., Comer, A. R., Bachmann, C., Kastenmeier, A. S., Reddy, S. K., Beckerle, M. C., Walter, U., and Hoffmann, F. M. (1998). Mutations in *Drosophila* enabled and rescue by human vasodilator-stimulated phosphoprotein (VASP) indicate important functional roles for Ena/VASP homology domain 1 (EVH1) and EVH2 domains. *Mol Biol Cell* 9, 2157-2171.
- Aszodi, A., Pfeifer, A., Ahmad, M., Glauner, M., Zhou, X. H., Ny, L., Andersson, K. E., Kehrel, B., Offermanns, S., and Fassler, R. (1999). The vasodilator-stimulated phosphoprotein (VASP) is involved in cGMP- and cAMP-mediated inhibition of agonist-induced platelet aggregation, but is dispensable for smooth muscle function. *Embo J* 18, 37-48.
- Ball, L. J., Kuhne, R., Hoffmann, B., Hafner, A., Schmieder, P., Volkmer-Engert, R., Hof, M., Wahl, M., Schneider-Mergener, J., Walter, U., *et al.* (2000). Dual epitope recognition by the VASP EVH1 domain modulates polyproline ligand specificity and binding affinity. *Embo J* 19, 4903-4914.
- Bear, J. E., Loureiro, J. J., Libova, I., Fassler, R., Wehland, J., and Gertler, F. B. (2000). Negative regulation of fibroblast motility by Ena/VASP proteins. *Cell* 101, 717-728.
- Bear, J. E., Svitkina, T. M., Krause, M., Schafer, D. A., Loureiro, J. J., Strasser, G. A., Maly, I. V., Chaga, O. Y., Cooper, J. A., Borisy, G. G., and Gertler, F. B. (2002). Antagonism between Ena/VASP proteins and actin filament capping regulates fibroblast motility. *Cell* 109, 509-521.
- Butt, E., Abel, K., Krieger, M., Palm, D., Hoppe, V., Hoppe, J., and Walter, U. (1994). cAMP- and cGMP-dependent protein kinase phosphorylation sites of the focal adhesion vasodilator-stimulated phosphoprotein (VASP) in vitro and in intact human platelets. *J Biol Chem* 269, 14509-14517.
- Fedorov, A. A., Fedorov, E., Gertler, F., and Almo, S. C. (1999). Structure of EVH1, a novel proline-rich ligand-binding module involved in cytoskeletal dynamics and neural function. *Nat Struct Biol* 6, 661-665.
- Geese, M., Loureiro, J. J., Bear, J. E., Wehland, J., Gertler, F. B., and Sechi, A. S. (2002). Contribution of Ena/VASP proteins to intracellular motility of *listeria* requires phosphorylation and proline-rich core but not F-actin binding or multimerization. *Mol Biol Cell* 13, 2383-2396.

Chapter 2

- Gertler, F. B., Niebuhr, K., Reinhard, M., Wehland, J., and Soriano, P. (1996). Mena, a relative of VASP and Drosophila Enabled, is implicated in the control of microfilament dynamics. *Cell* 87, 227-239.
- Goh, K. L., Cai, L., Cepko, C. L., and Gertler, F. B. (2002). Ena/VASP proteins regulate cortical neuronal positioning. *Curr Biol* 12, 565-569.
- Harbeck, B., Huttelmaier, S., Schluter, K., Jockusch, B. M., and Illenberger, S. (2000). Phosphorylation of the vasodilator-stimulated phosphoprotein regulates its interaction with actin. *J Biol Chem* 275, 30817-30825.
- Hauser, W., Knobloch, K. P., Eigenthaler, M., Gambaryan, S., Krenn, V., Geiger, J., Glazova, M., Rohde, E., Horak, I., Walter, U., and Zimmer, M. (1999). Megakaryocyte hyperplasia and enhanced agonist-induced platelet activation in vasodilator-stimulated phosphoprotein knockout mice. *Proc Natl Acad Sci U S A* 96, 8120-8125.
- Huttelmaier, S., Mayboroda, O., Harbeck, B., Jarchau, T., Jockusch, B. M., and Rudiger, M. (1998). The interaction of the cell-contact proteins VASP and vinculin is regulated by phosphatidylinositol-4,5-bisphosphate. *Curr Biol* 8, 479-488.
- Ishiguro, K., and Xavier, R. (2004). Homer-3 regulates activation of serum response element in T cells via its EVH1 domain. *Blood* 103, 2248-2256.
- Lambrechts, A., Kwiatkowski, A. V., Lanier, L. M., Bear, J. E., Vandekerckhove, J., Ampe, C., and Gertler, F. B. (2000). cAMP-dependent protein kinase phosphorylation of EVL, a Mena/VASP relative, regulates its interaction with actin and SH3 domains. *J Biol Chem* 275, 36143-36151.
- Lanier, L. M., Gates, M. A., Witke, W., Menzies, A. S., Wehman, A. M., Macklis, J. D., Kwiatkowski, D., Soriano, P., and Gertler, F. B. (1999). Mena is required for neurulation and commissure formation. *Neuron* 22, 313-325.
- Laurent, V., Loisel, T. P., Harbeck, B., Wehman, A., Grobe, L., Jockusch, B. M., Wehland, J., Gertler, F. B., and Carlier, M. F. (1999). Role of proteins of the Ena/VASP family in actin-based motility of *Listeria monocytogenes*. *J Cell Biol* 144, 1245-1258.
- Loureiro, J. J., Rubinson, D. A., Bear, J. E., Baltus, G. A., Kwiatkowski, A. V., and Gertler, F. B. (2002). Critical roles of phosphorylation and actin binding motifs, but not the central proline-rich region, for Ena/vasodilator-stimulated phosphoprotein (VASP) function during cell migration. *Mol Biol Cell* 13, 2533-2546.
- Menzies, A. S., Aszodi, A., Williams, S. E., Pfeifer, A., Wehman, A. M., Goh, K. L., Mason, C. A., Fassler, R., and Gertler, F. B. (2004). Mena and vasodilator-

Chapter 2

stimulated phosphoprotein are required for multiple actin-dependent processes that shape the vertebrate nervous system. *J Neurosci* 24, 8029-8038.

Niebuhr, K., Ebel, F., Frank, R., Reinhard, M., Domann, E., Carl, U. D., Walter, U., Gertler, F. B., Wehland, J., and Chakraborty, T. (1997). A novel proline-rich motif present in ActA of *Listeria monocytogenes* and cytoskeletal proteins is the ligand for the EVH1 domain, a protein module present in the Ena/VASP family. *Embo J* 16, 5433-5444.

Prehoda, K. E., Lee, D. J., and Lim, W. A. (1999). Structure of the enabled/VASP homology 1 domain-peptide complex: a key component in the spatial control of actin assembly. *Cell* 97, 471-480.

Walders-Harbeck, B., Khaitlina, S. Y., Hinssen, H., Jockusch, B. M., and Illenberger, S. (2002). The vasodilator-stimulated phosphoprotein promotes actin polymerisation through direct binding to monomeric actin. *FEBS Lett* 529, 275-280.

Zimmer, M., Fink, T., Fischer, L., Hauser, W., Scherer, K., Lichter, P., and Walter, U. (1996). Cloning of the VASP (vasodilator-stimulated phosphoprotein) genes in human and mouse: structure, sequence, and chromosomal localization. *Genomics* 36, 227-233.

Chapter 3

Tuba is a Novel Rho-Family Guanine Nucleotide Exchange Factor (GEF) That Binds Ena/VASP Proteins and Links Dynamin to Regulation of the Actin Cytoskeleton

Note: Many of the results discussed in this chapter were reported in the following paper, on which I am co-first author:

Salazar, M. A., Kwiatkowski, A. V., Pellegrini, L., Cestra, G., Butler, M. H., Rossman, K. L., Serna, D. M., Sondek, J., Gertler, F. B., and De Camilli, P. (2003). Tuba: A novel protein containing bin/amphiphysin/Rvs (BAR) and Dbl homology domains, links dynamin to regulation of the actin cytoskeleton. *J Biol Chem* 278, 49031-49043.

The following figures in this chapter were generated by our collaborators, namely Marco Salazar and Pietro DeCamilli: Figures 3, 5, 6, 10 and 11. The remaining figures, and the data contained within, were produced by me.

Abstract

We conducted a yeast two-hybrid screen to identify ligands of Ena/VASP proteins and discovered a novel scaffold molecule called Tuba. Via a C-terminal SH3 domain, Tuba binds a variety of actin regulatory proteins, including N-WASP, CR16, WAVE1, WIRE, PIR121, NAP1, Lamellipodin, and Ena/VASP proteins. Direct binding partners include N-WASP and Mena. Forced targeting of the COOH-terminal SH3 domain to the mitochondrial surface can promote accumulation of F-actin around mitochondria. Four N-terminal SH3 domains bind to dynamin, and Tuba is found at synapses in the brain. A Dbl homology (DH) present in the middle of Tuba upstream of a Bin/Amphiphysin/Rvs (BAR) domain activates Cdc42, but not Rac and Rho, and may thus cooperate with the C-terminus of the protein in regulating actin assembly. The BAR domain, a lipid binding module, may functionally replace the Pleckstrin homology (PH) domain that typically follows a DH domain. The properties of Tuba provide new evidence for a close functional link between dynamin, Rho-GTPase signaling and the actin cytoskeleton.

Introduction

Ena/VASP proteins participate in the formation of Rho-family GTPase induced actin structures, including Cdc42 stimulated filopodia and Rac regulated lamellipodia (Rho GTPases are described in detail in Chapter 1). However, a molecular link between Rho GTPases and Ena/VASP proteins has not been established. In addition to their role in cell motility, Rho GTPases are implicated in the regulation of actin-dependent processes, including endocytosis and vesicle trafficking. While the importance of Rho GTPases in endocytosis is still being determined, the importance of another GTPase, dynamin, is better established.

Fission of clathrin-coated and other endocytic vesicles from the plasma membrane involves the cooperation of several membrane-associated proteins, among which the GTPase dynamin plays a key role (Conner and Schmid, 2003; Slepnev and De Camilli, 2000). The participation of dynamin in the fission of endocytic vesicles has been established by a variety of experimental approaches in *Drosophila*, cultured cells and cell free systems, although the precise mechanism of fission and the role of dynamin in this reaction remain unclear (Hinshaw, 2000).

Several dynamin partners thought to participate in its recruitment or in its function have been identified (Gout et al., 1993; Hinshaw, 2000). At the synapse, where endocytosis plays a key role in the recycling of synaptic vesicle membranes, two prominent dynamin partners are amphiphysin and endophilin (David et al., 1996; Ramjaun et al., 1997; Ringstad et al., 1997). Amphiphysin has a three

Chapter 3

domain structure with an evolutionary conserved NH₂-terminal module of approximately 250 amino acids called the BAR (BIN, Amphiphysin, Rvs) domain, a variable central region and a COOH-terminal SH3 domain that binds dynamin. Endophilin has a similar domain structure (Slepnev and De Camilli, 2000). Although endophilin's NH₂-terminal domain is substantially divergent in amino acid composition from the BAR domain of amphiphysin, it shares some similarity at critical sites, leading to its classification as a BAR domain (Farsad et al., 2001). Accordingly, the BAR domains of amphiphysin and endophilin share functional similarities because they both can bind and deform lipid bilayers and mediate homo- and heterodimerization (Farsad et al., 2001; Ringstad et al., 1997; Takei et al., 1999; Wigge et al., 1997a). Dynamin also can bind and deform lipid bilayers, and it has been proposed that endophilin and amphiphysin might help to recruit and possibly assist dynamin in the generation of membrane curvature at endocytic pits (Farsad et al., 2001; Takei et al., 1999).

The closest homologue of amphiphysin and endophilin in *Saccharomyces cerevisiae* is Rvs167 that forms a stable heterodimer with Rvs161. Rvs167 has a domain structure like amphiphysin, while Rvs161 (homologous to the mammalian protein BIN3) is represented nearly exclusively by a BAR domain. Mutation of either one or both components of this heterodimer in yeast produces defects in endocytosis and actin function (Lombardi and Riezman, 2001). Such a dual phenotype is typical of most mutations in actin regulatory and endocytosis genes in yeast (Munn, 2001). These observations, together with results from a variety of

Chapter 3

studies in mammalian cells, have suggested a link between endocytosis and actin, although such a link has remained mechanistically elusive (Qualmann et al., 2000; Schafer, 2002). Foci of actin can often be seen at endocytic sites (Merrifield et al., 2002), and endocytic vesicles with actin tails have also been observed (Merrifield et al., 1999). Interestingly, these actin tails contain both dynamin and dynamin interacting proteins (Lee and De Camilli, 2002; Orth et al., 2002).

Several binding partners of dynamin are either physically or functionally linked to actin or actin regulatory proteins. These include, among others, syndapin/pacsin and intersectin/DAP160 (Qualmann et al., 2000; Schafer, 2002). Intersectin, in particular, represents a striking example of a multi-domain protein that links dynamin to proteins that directly or indirectly control actin polymerization, such as the PI(4,5)P₂ phosphatase, synaptojanin, N-WASP, and the Rho-family GTPase Cdc42 (Hussain et al., 2001; Roos and Kelly, 1998). The role of these proteins in the regulation of actin assembly is discussed in Chapter 1. Intersectin functions to bring together N-WASP and, through the guanyl nucleotide exchange activity of its Dbl homology (DH) domain, activated GTP-bound Cdc42, thus activating Arp2/3 and promoting actin nucleation (Hussain et al., 2001). The endocytic protein syndapin/pacsin, that like intersectin binds both dynamin and N-WASP, can promote N-WASP-dependent actin nucleation (Kessels and Qualmann, 2002). Thus, intersectin and syndapin function as molecular links between endocytosis and actin assembly.

Chapter 3

Ena/VASP proteins, despite their role in regulating actin assembly have never been implicated in endocytosis or vesicle trafficking, though a role for Ena/VASP proteins in macrophage phagocytosis has been described (Coppolino et al., 2001). Likewise, no biochemical or genetic link between Ena/VASP proteins and dynamin has been identified. Here we describe the identification and characterization of a novel protein, Tuba, that links Ena/VASP proteins to dynamin. In addition, Tuba activates Cdc42, and is thus one of the first established links between Ena/VASP proteins and Rho GTPase signaling. Overall, the results of this study suggest that Tuba functions as an important link between dynamin function, Rho-GTPase signaling, and actin dynamics.

Results

Tuba is a novel guanine nucleotide exchange factor that binds Ena/VASP proteins

We conducted a yeast two-hybrid screen to identify ligands of Ena/VASP proteins using full length EVL to screen a mouse embryo cDNA library. A number of potential binding partners were identified, many of them previously unknown. Potential ligands included proteins implicated in endocytosis, protein scaffolding, and signaling (data not shown). Two independent clones that were highly homologous to the C-terminus of an uncharacterized cDNA termed KIAA1010 were isolated. KIAA1010 is a partial cDNA isolated from human brain that encodes a putative guanine nucleotide exchange factor (GEF) for Rho-family GTPases and contains an SH3 domain at the very C-terminus. Given the role of

Chapter 3

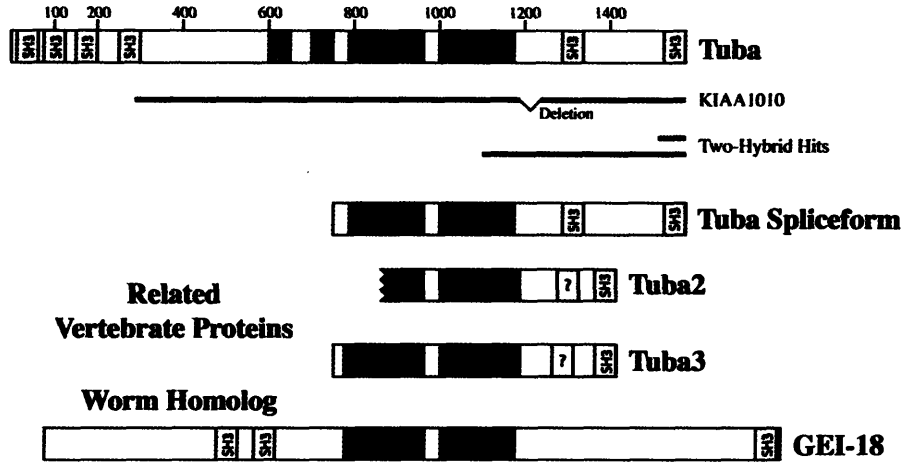
Rho-GTPases in regulating the actin cytoskeleton and the presence of an SH3 domain, a domain known to bind Ena/VASP proteins, we focused on characterizing this protein and its interaction with Ena/VASP proteins.

RT-PCR using a mouse embryonic cDNA library was carried out to obtain the full-length gene. The protein, which we have named Tuba in line with the tradition of naming large synaptic proteins after musical instruments (Cases-Langhoff et al., 1996), comprises 1580 amino acids with a predicted molecular mass of 175 kDa. The mouse gene is located on mouse chromosome 19, and the human gene is located on chromosome 10. The domain structure of Tuba (Fig. 1A) includes four N-terminal SH3 domains (referred to as SH3-1, SH3-2, SH3-3 and SH3-4), a predicted coiled-coil domain, a Rho GTPase family GEF Dbl homology (DH) domain, and two additional C-terminal SH3 domains (SH3-5 and SH3-6). In addition, a proline-rich low complexity region containing putative SH3 domain binding sites is present upstream of the coiled-coil region (Fig. 1A).

In an independent line of study, a BLAST search for proteins containing a domain related to the BAR domain of amphiphysin 1 revealed a large number of sequences, including KIAA1010. However, the putative BAR domain in KIAA1010 is not located at the N-terminus as in most of these sequences, but is instead found in the middle of the protein downstream of the DH domain (Fig. 1A). While the overall homology to the amphiphysin 1 BAR domain is limited - 24% identical, 39% similar (Fig. 1B) - similarities are concentrated in regions generally conserved amongst the amphiphysin/BIN family. This region in KIAA1010 is currently

identified as a BAR domain by protein module recognizing algorithms, such as those of the Pfam and SMART programs.

A.



B.

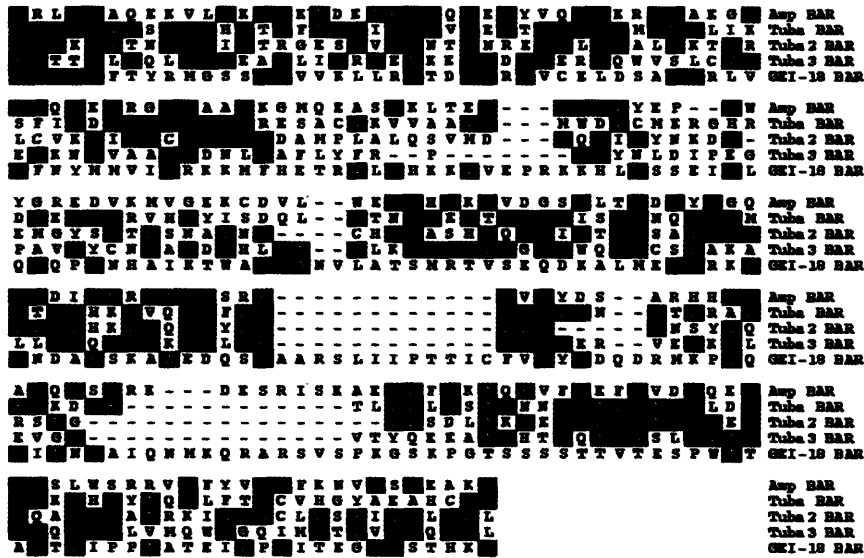


Figure 1. Domain structure of Tuba and related proteins. A. Tuba, Tuba2, and Tuba3 are shown with domains of interest noted. Thick lines below Tuba indicate the portion of Tuba encoded by KIAA1010 and the partial clones isolated in the yeast two-hybrid screen for EVL binding partners. Also shown is the shorter isoform of Tuba, as well as the *C. elegans* Tuba homolog, GEI-18. B. Alignment of the BAR domains of the Tuba family of proteins. The amphiphysin, Tuba and Tuba3 BAR domains are from human, the Tuba2 sequence is from monkey, and the GEI-18 sequence is from *C. elegans*.

Chapter 3

Tuba does not contain a Pleckstrin Homology (PH) domain that is typically found downstream of the DH domain in Rho-family GEFs. Instead, as noted above, a BAR domain is located downstream of the DH domain. BAR domains bind to membranes and can both sense and induce membrane curvature (Peter et al., 2004). PH domains are membrane-binding modules, and play an important role in localizing signaling proteins, including GEFs, to the plasma membrane (Rossman et al., 2003). The BAR domain downstream of catalytic DH region in Tuba may serve a functional replacement of the standard PH domain and mediate intracellular localization.

Searches through genomic and EST databases revealed numerous ESTs to two genes that encode proteins homologous to C-terminal half of Tuba in both human and mouse. We have named these proteins Tuba2 and Tuba3 (Fig. 1A). Tuba2 is located on human chromosome 4 and mouse chromosome 3, and Tuba3 is located on human chromosome 5 and mouse chromosome 8. Tuba2 is 41% identical and 60% similar to Tuba, and Tuba3 is 25% identical and 41% similar to Tuba. Tuba 2 is 31% identical and 48% similar to Tuba 3. Recent searches have also revealed what appears to be an alternate spliceform of Tuba that is similar in structure to Tuba2 and Tuba3 (see Fig. 1A).

A putative orthologue of Tuba, *gei-18* (GEX interactor-18), was identified in *Caenorhabditis elegans* (Fig. 1A) (Tsuboi et al., 2002). Two alternate transcripts of *gei-18* are described that comprise the N-terminal and C-terminal halves of the protein. While not recognized by Pfam or SMART, the region C-terminal of the DH

domain in GEI-18 appears to be very similar to a BAR domain. A comparison of the BAR domains of the Tuba family of proteins with each other and human amphiphysin1 is shown in Fig. 1B.

Tuba is ubiquitous

Northern blot analysis of human tissues with a probe corresponding to the C-terminus of human Tuba (nucleotides 4035-4540) revealed two transcripts of 7.3 and 6 kilobases (Fig. 2A) whose levels

varied in different tissues. A probe directed against the N-terminal half of the protein (nucleotides 1246-1696) recognized only the larger transcript (data not shown). A third transcript of 4.5

kilobases was observed in a number of mouse tissues with a larger probe corresponding to the C-terminus of mouse Tuba (nucleotides 2971-4742) (data not shown). This Tuba mRNA likely encodes

only the second half of the protein, i.e. a Tuba splice variant similar in domain structure to the homologous proteins

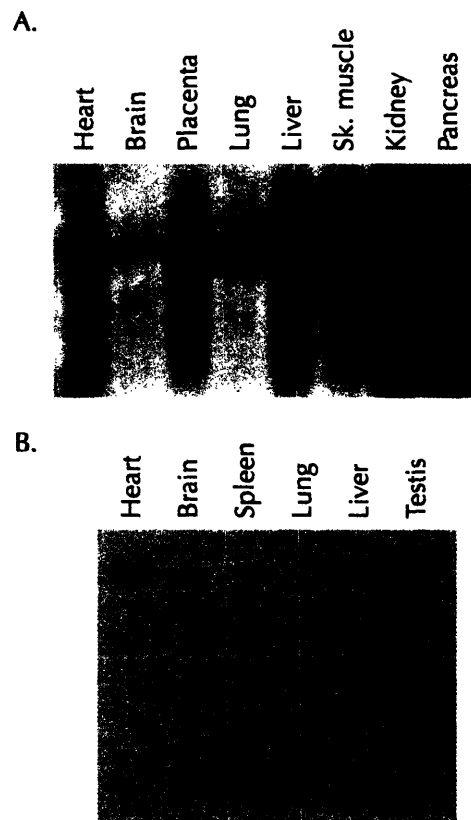


Figure 2. Ubiquitous expression of Tuba transcripts and their protein products. A. Multiple tissue northern blot using a probe directed against the 3' end of Tuba. B. Multiple tissue western blot. Western blot of rat tissue postnuclear supernatants with affinity-purified Tuba-specific antibodies.

Tuba2 and Tuba3 (Fig. 1A).

When tested by western blotting against various rat tissues, affinity-purified antibodies generated against the C-terminus of Tuba recognized a band at the expected molecular weight of full length Tuba (~185 kDa) (Fig. 2B). The band was the strongest in testis, followed by brain, heart, liver, spleen and lung. The same antibodies also recognized lower molecular weight bands at approximately 105 kDa and 75 kDa with differential tissue distribution that may represent alternatively spliced forms of Tuba or proteolytic C-terminal fragments (Fig. 3B). The 75 kDa band may also represent cross-reactivity of the antibodies against either Tuba2 or Tuba3, whose molecular weights are predicted to be in this range. Collectively, these data indicate that Tuba has a broad tissue distribution and may exist in multiple isoforms.

The N-terminus of Tuba binds Dynamin

To identify binding partners to the N-terminal SH3 domains of Tuba, a GST fusion protein comprising the four N-terminal SH3 domains (SH3-1,2,3,4) was generated and incubated with Triton X-100 rat brain extracts in affinity chromatography experiments. As shown by coomassie blue staining of SDS gels of the material retained by the beads, the fusion protein, but not GST alone, specifically and efficiently retained a protein of 100kD (Fig. 3A). This protein was identified as dynamin 1 by Matrix-Assisted Laser Desorption/Ionization-Time-of-Flight (MALDI-TOF) (data not shown) and immunoblotting (Fig. 3B). The

Chapter 3

interaction between the SH3 domains of Tuba and dynamin 1 is direct, because it could be confirmed by far western blotting using HA-tagged SH3-1,2,3,4 as a probe (data not shown). Furthermore, dynamin, but not synaptotagmin, could be co-precipitated with Tuba from Triton X-100 rat brain extracts, demonstrating that the interaction can occur *in vivo* (Fig. 3C). The separate analysis of each of the four SH3 domains in affinity-purification experiments revealed that all of them bound dynamin and that SH3-4 had the highest affinity for dynamin, followed, in order of decreasing affinity, by SH3-1, SH3-3 and SH3-2 (data not shown). We conclude that dynamin is the main ligand of Tuba's N-terminal region.

To better determine if the interaction between dynamin and the N-terminus of Tuba is relevant *in vivo*, we expressed HA-tagged SH3-1,2,3,4 in CHO cells and determined its effect on transferrin uptake, a dynamin dependent endocytic reaction. It was shown previously that SH3 domains that bind dynamin can function as potent inhibitors of this process, probably by titrating out dynamin (Shupliakov et al., 1997; Wigge et al., 1997b). When expressed in CHO cells, SH3-1,2,3,4, had a cytosolic distribution and inhibited transferrin internalization (Fig. 3D), suggesting that the N-terminus of Tuba can interact with dynamin *in vivo*. Cytosolic expression of the C-terminal SH3 domain (that does not bind dynamin - see below) had no effect on transferrin uptake (data not shown).

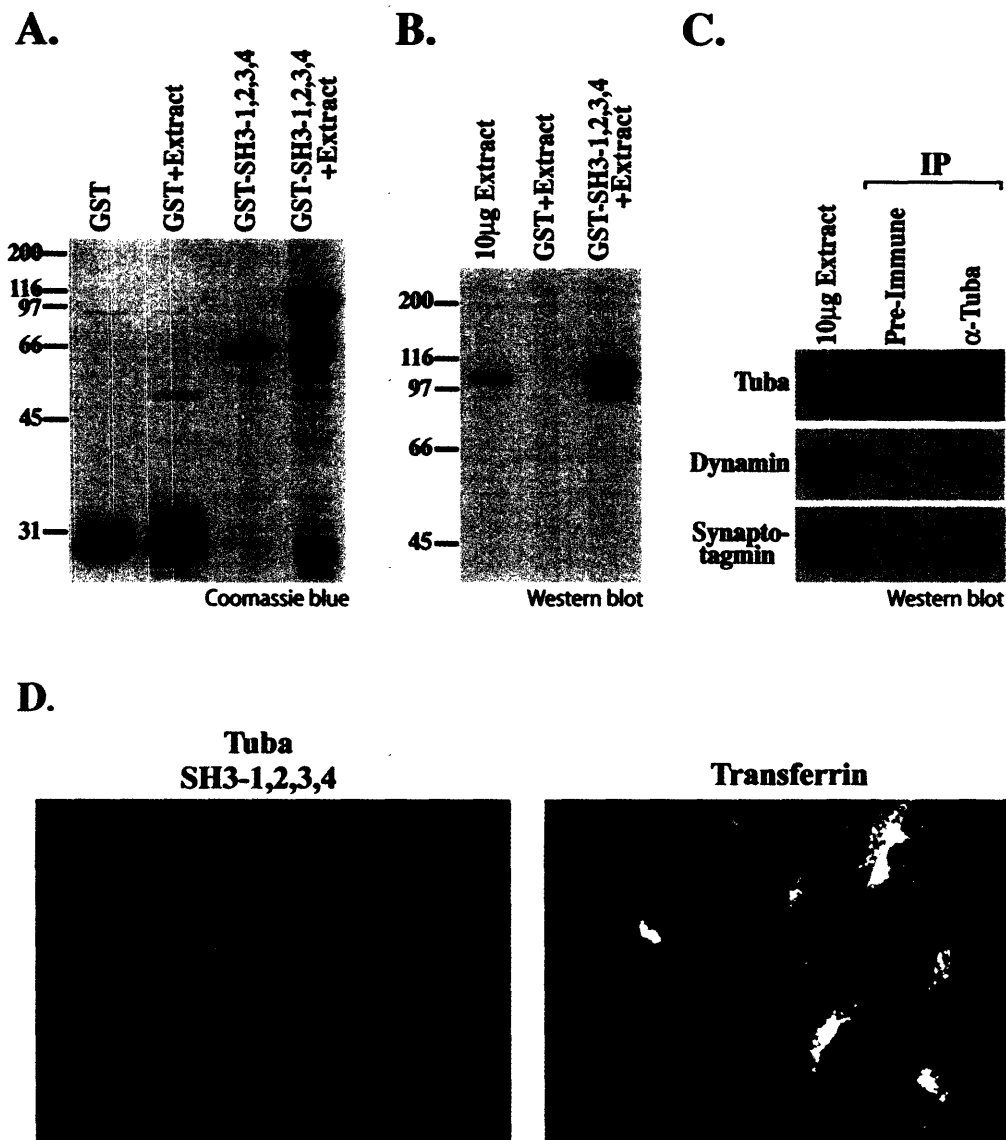


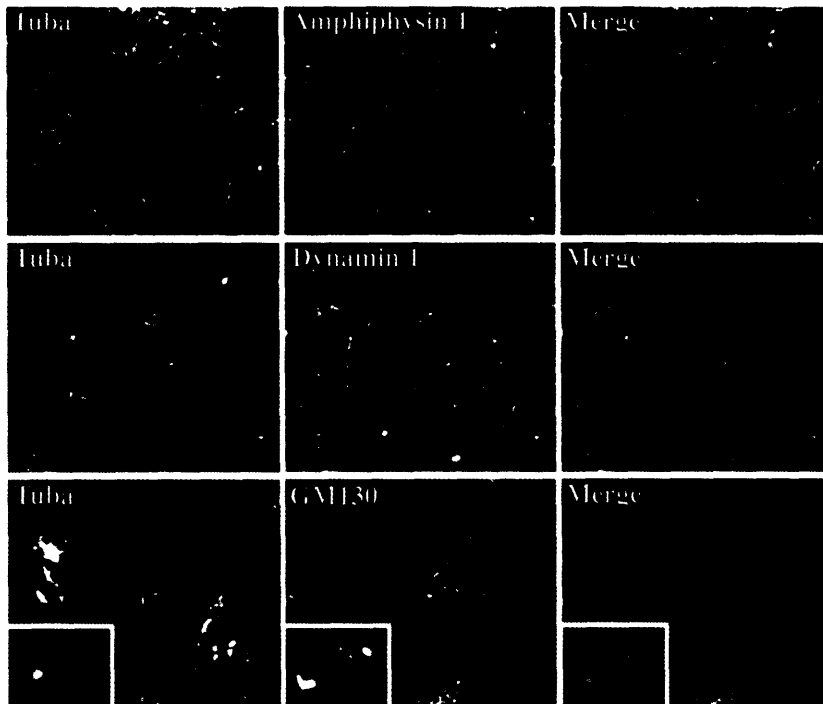
Figure 3. The N-terminal SH3 domains of Tuba bind Dynamin 1. A. Bead immobilized GST and a GST fusion protein of the N-terminal region of Tuba (SH3-1,2,3,4) were incubated with a Triton X-100 solubilized rat brain extract, and the bound material was analyzed by SDS-PAGE and coomassie staining. A band of 100 kDa (dynamin) was selectively affinity-purified. The greater abundance of dynamin than of the fusion protein used as bait is likely to reflect the oligomerization state of dynamin. B. Anti-dynamin western blot of the material affinity-purified by GST or the GST fusion protein. C. Control or anti-Tuba antibodies were used to generate immunoprecipitates from a Triton X-100 rat brain extract. The panel shows western blots for Tuba, dynamin, and synaptotagmin of the immunoprecipitates. D. CHO cells were transfected with HA-tagged Tuba SH3-1,2,3,4 and then incubated for 7 min with alexa-transferrin prior to fixation in 4% formaldehyde followed by anti-HA immunofluorescence. Overexpression of Tuba SH3-1,2,3,4 inhibits transferrin uptake, as demonstrated by the lack of the intracellular transferrin fluorescence in the transfected cell.

Tuba is found at the synapse

To determine the localization of Tuba in brain, where dynamin participates in the clathrin-mediated endocytosis of synaptic vesicles, rat brain cryosections were stained for Tuba by immunofluorescence. Tuba immunostaining yielded a punctate pattern outlining the surface of neuronal perikarya and dendrites that colocalized with immunoreactivity for the synaptic markers amphiphysin 1 and dynamin 1 (Hudy-1 antibodies) (Fig. 4A). In addition, Tuba immunoreactivity was observed within neuronal cell bodies at locations that corresponded to the Golgi complex, as shown by counterstaining for the Golgi marker GM-130 (Nakamura et al., 1995). High magnification observation, however, indicated that GM-130 and Tuba did not have an overlapping distribution, suggesting that the two antigens localized to distinct Golgi complex subcompartments (Fig. 4A).

To analyze the synaptic localization of Tuba in more detail, lysed synaptosomes were processed for anti-Tuba immunogold electron microscopy using a pre-plastic embedding procedure. Gold immunolabeling was detected in the presynaptic compartment where it was primarily concentrated at the periphery of synaptic vesicle clusters (Fig. 4B). These are the regions where clathrin-mediated endocytosis occurs (for example, see a clathrin coated vesicle in Fig. 4B) and where presynaptic actin is concentrated. This localization is consistent with a role of Tuba in endocytosis and actin function, as proposed for other BAR domain containing proteins.

A.



B.



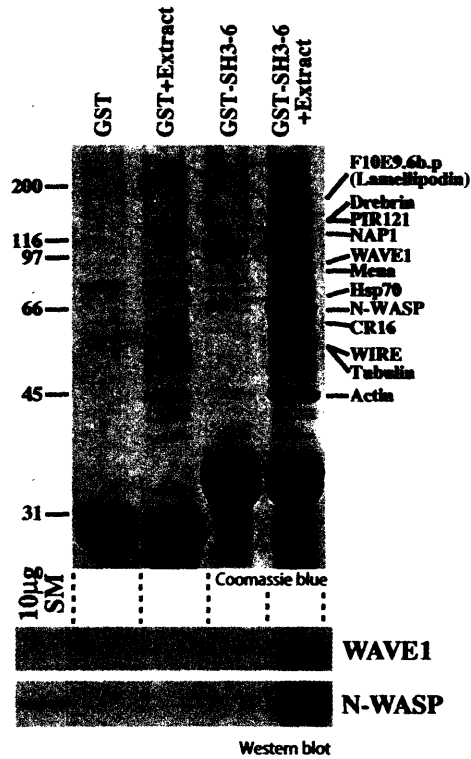
Figure 4. Tuba is found at the synapse in brain. A. Double immunofluorescence of rat brain stem frozen sections with antibodies directed against Tuba and other antigens as indicated. Tuba co-localizes with the synaptically enriched proteins amphiphysin 1 and dynamin 1. Synapses appear as bright fluorescent puncta that outline the surface of perikarya and dendrites. In addition, Tuba immunoreactivity is present in the Golgi complex area, as shown in section counterstained for the Golgi complex marker GM-130. Within the Golgi complex, however, Tuba and GM-130 do not have an overlapping distribution. B. Immunogold labeling of a lysed synaptosome demonstrating the concentration of Tuba at the periphery of the synaptic vesicle cluster in the presynaptic compartment. An arrow points to a clathrin coated vesicle.

The C-terminal SH3 domain of Tuba binds to an actin regulatory complex

We next searched for ligands of the C-terminal SH3 domains of Tuba. GST-fusion proteins of SH3 domains 5 and 6 were generated and used in pull-down experiments from Triton X-100 rat brain extracts. No major interactors were found for SH3-5 (data not shown). However, SH3-6, but not GST alone, pulled down a variety of proteins as revealed by the coomassie-stained SDS-gel of the affinity purified material (Fig. 5A). Each of the major protein bands was excised, trypsin digested, and analyzed by MALDI-TOF. The identified proteins are listed in Fig. 5A (top panel). For some proteins the interaction was validated further by western blotting (Fig. 5A, bottom panel and data not shown). Two of the major bands were actin and tubulin. Another was Hsp70, which is often found in eluates of pull-down experiments, possibly reflecting the promiscuous role of this ATPase in protein folding reactions. All other bands represent proteins that are either directly or indirectly linked to the regulation of actin dynamics.

Mena, the most highly expressed Ena/VASP protein in the brain (Lanier et al., 1999), was present in the affinity purified material as expected. However, the most abundant protein was N-WASP, the ubiquitous and brain enriched homolog of the Wiskott-Aldrich syndrome protein (WASP) (Miki et al., 1996). CR16 and WIRE (also known as WICH) are both related to WIP, a proline rich protein that binds to actin and interacts with N-terminal WH1 domain of N-WASP (Aspenstrom, 2002; Ho et al., 2001; Kato et al., 2002; Martinez-Quiles et al., 2001).

A.



B.

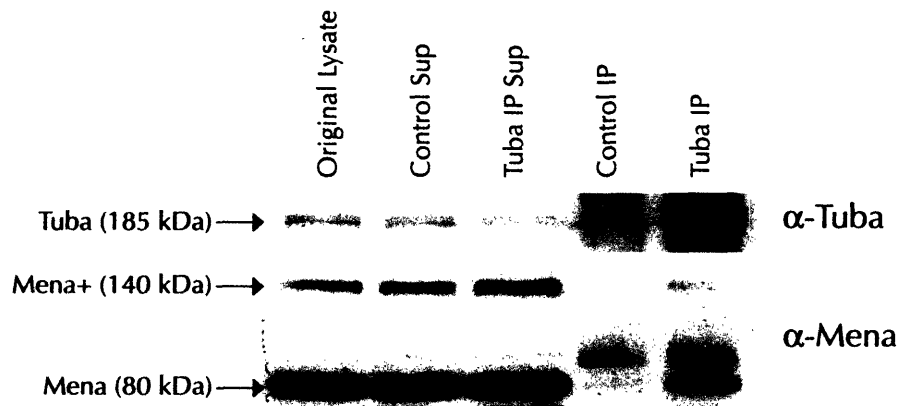


Figure 5. The C-terminal SH3 domain (SH3-6) of Tuba binds actin regulatory proteins. A. Bead immobilized GST and a GST fusion protein of SH3-6 were incubated with a Triton X-100 solubilized rat brain extract, and the bound material was analyzed by SDS-PAGE and coomassie staining (upper panel). The identities of the proteins were determined by MALDI and Q-TOF Mass Spectrometry analysis. Binding of Wave1 and N-WASP was confirmed by a western blot analysis (bottom panel). B. Control or affinity purified anti-Tuba antibodies were used for immunoprecipitation from E16 mouse embryo lysates. The top panel is a western blot for Tuba; the bottom panel is a western blot for Mena.

Chapter 3

WAVE1 is a neuronal specific SCAR/WAVE protein and a member of the WASP superfamily (Miki et al., 1998) that, like N-WASP, regulates actin assembly through binding and activation of the Arp2/3 complex (Machesky et al., 1999). Isolated WAVE1, unlike N-WASP, is constitutively active (Machesky et al., 1999), but is kept in an inhibited state while bound to a protein complex that includes PIR121 and NAP1 (Eden et al., 2002), two proteins present in the affinity-purified material. Drebrin, an F-actin binding protein (Ishikawa et al., 1994), was also present in the affinity purified material, as was Lamellipodin, a novel Ena/VASP-associated protein that regulates lamellipodial dynamics (Krause et al., 2004).

Given the large number of proteins present in the affinity purified complex, we questioned if these interactions could occur *in vivo*. When Tuba was immunoprecipitated from E15 embryo lysates, Mena was found to co-precipitate (Fig. 5B). Longer exposures revealed that the 140 kDa Mena +, a neuronal-specific isoform of Mena (Gertler et al., 1996), was also co-precipitated. N-WASP was also found in the precipitated material (data not shown). The presence of heavy chain antibody in the immunoprecipitation prevented the identification of VASP or EVL, both of which run at a similar molecular weight (data not shown). These results indicate that Tuba interacts with one or more actin regulatory proteins *in vivo*.

Since the C-terminus of Tuba was found to bind EVL in the yeast two-hybrid screen (Fig. 1A), and the co-immunoprecipitation results demonstrated that Tuba and Mena interact *in vivo*, the Ena/VASP interaction was characterized further. Pull-down experiments from lysates prepared from Ena/VASP-deficient cells

(referred to as MV^{D7} cells (Bear et al., 2000)) stably infected and sorted for equal expression of EGFP fusions of Mena, EVL or VASP showed that the SH3-6 domain of Tuba binds to each of the three proteins, but more robustly to EVL and Mena (Fig. 6A). No binding was observed from cells expressing a mutant form of Mena that lacks the proline rich region, indicating that this region, present in all Ena/VASP proteins, is essential for binding (Fig. 6A).

Lamellipodin binds to the highly conserved N-terminal

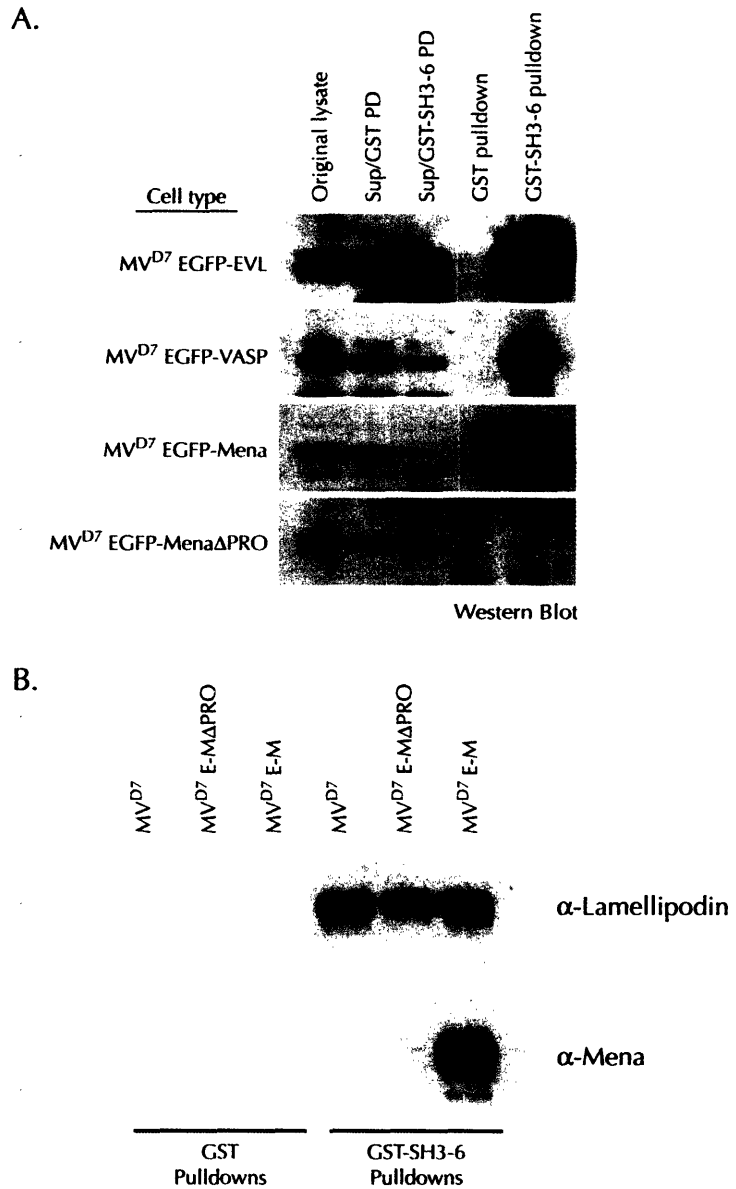


Figure 6. Tuba interacts with Ena/VASP proteins and Lamellipodin. A. MV^{D7} cells, which contain no Ena/VASP protein family members, were infected with EGFP-fusions of each member of the Ena/VASP family or of a Mena construct lacking the proline-rich domain (DPRO). Lysates from cells expressing equal levels of the fusion proteins were affinity purified on GST or GST-SH3-6. The starting lysates, as well as the supernatant and pellets of the affinity-purified material, were then processed by western blotting with anti-EGFP antibodies. B. Lysates of MV^{D7} cells and MV^{D7} stably expressing either EGFP-MenaΔPRO or EGFP-Mena were incubated with GST and GST-SH3-6. Affinity purified material was separated by SDS-PAGE and analyzed by western blot using antibodies to Mena and Lamellipodin.

Chapter 3

EVH1 domain of Ena/VASP proteins, and is thought to be an important regulator of Ena/VASP proteins and additional effectors of the actin cytoskeleton (Krause et al., 2004). We wondered whether the presence of Lamellipodin in the affinity purified material was dependent upon Ena/VASP proteins. We performed additional GST pull-down experiments using cell lysates prepared from MV^{D7} cells that lack Ena/VASP proteins and MV^{D7} cells expressing either EGFP-Mena(E-M) or EGFP-Mena Δ PRO(E-M Δ PRO), a mutant form of Mena that lacks the proline rich region. Interestingly, Lamellipodin was found in the GST-SH3-6 affinity purified material from all lysates (Fig. 6B). As expected, Mena was only recovered in the lysate from cells expressing EGFP-Mena (Fig. 6B). This result indicates that Lamellipodin is present in the affinity purified material independent of Mena, either in complex with another protein(s) or by directly binding to the SH3-6 domain.

The two-hybrid results suggested that EVL, and by association, all Ena/VASP proteins bind to the SH3-6 domain of Tuba directly. To test this further, lysates from MV^{D7} cells and MV^{D7} cells expressing EGFP-Mena were blotted and overlaid with ³²P-labeled GST-SH3-6. A band around 115 kDa (the expected size of EGFP-Mena) was only observed in the MV^{D7} EGFP-Mena (MV^{D7} E-M) lysate lane (Fig. 7A). GST-SH3-6 pull-downs from the same lysates were performed and the affinity-purified material from these pull-downs was blotted and overlaid with ³²P-labeled GST-SH3-6. Again, SH3-6 bound directly to a band with the predicted molecular weight of EGFP-Mena only in cell lysates expressing EGFP-Mena (Fig. 7A). Thus, Tuba binds directly to Ena/VASP proteins, consistent with the initial two-hybrid

results. A direct interaction between SH3-6 and other proteins present in the affinity-purified material was also observed (Fig. 7A). One prominent band had the predicted electrophoretic mobility of N-WASP, and western blotting suggested that this band was indeed N-WASP (data not shown). The identity of a major band just above N-WASP remains unknown, but we speculate that it might be a member of the WIP family of proteins. Interestingly, the intensity of this band decreased in cells expressing EGFP-Mena, possibly due to competition between Mena and this protein binding to SH3-6.

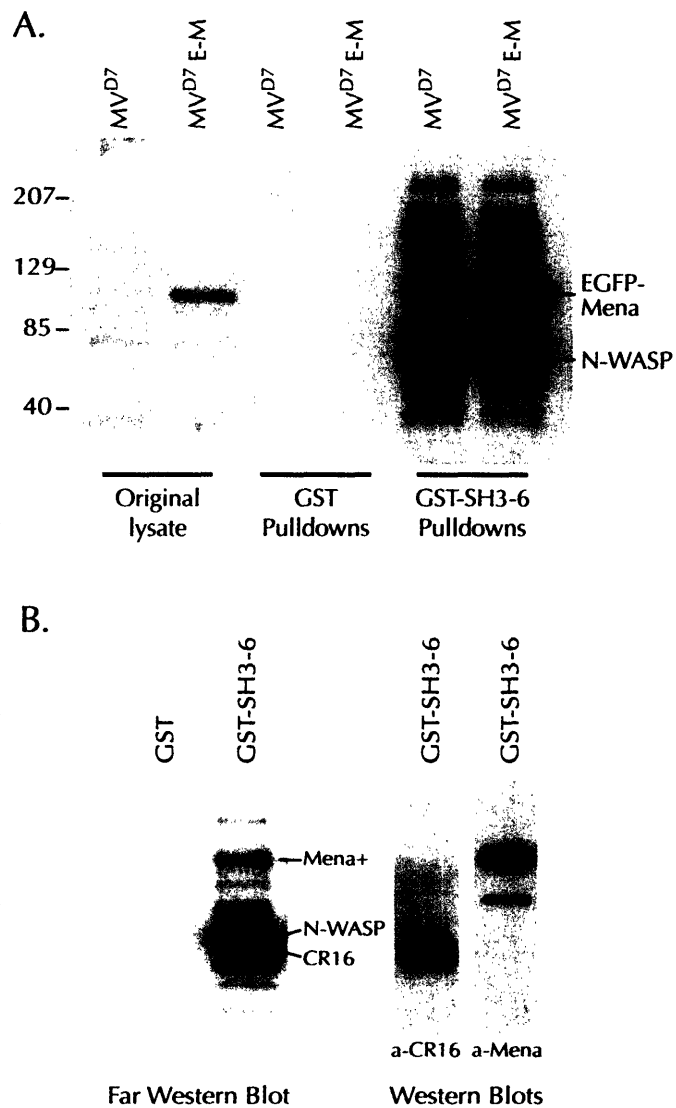


Figure 7. Tuba binds directly to Mena and N-WASP. A. Lysates of MV^{D7} cells, or of MV^{D7} cells stably infected with EGFP-Mena, were incubated with GST-SH3-6 in affinity chromatography experiments. The starting lysates and the pull-down products were separated by SDS-PAGE, blotted onto nitrocellulose, and overlaid with ³²P-labeled SH3-6. B. The affinity-purified material from mouse brain lysates by GST or GST-SH3-6 was separated by SDS-PAGE and overlaid with ³²P-labeled SH3-6 (left). The blot was stripped and reprobed with antibodies against potential ligands (right).

Chapter 3

A gel overlay with ^{32}P -labeled GST-SH3-6 was also performed on the material affinity-purified by SH3-6 from mouse brain lysate. Two prominent bands bound by SH3-6 were adjacent to the 66 kDa marker (Fig. 7B). Western blotting demonstrated that the upper band precisely co-migrated with N-WASP (data not shown), while the lower band appears to be CR16 (Fig. 7B). The overlay experiment also revealed a prominent band at around 50 kDa and a somewhat weaker signal at about 140 kDa. Western blotting indicated that the band at 140 kDa corresponded to Mena+ (Fig. 7B). The identity of the 50 kDa band remains unknown.

Since both Mena and N-WASP appear to bind directly to the SH3-6 domain of Tuba, we sought to map the binding site(s) within these proteins. A series of overlapping peptides corresponding to the proline-rich regions of N-WASP, WAVE1, EVL, and Mena were synthesized by the SPOTs method (Frank, 2002). This peptide blot was overlaid with ^{32}P -labeled GST-SH3-6 (Fig. 8A) and the resulting signal intensity at each peptide spot was measured and compared to background (Fig. 8B). N-WASP has two potential binding sites for SH3-6 (where the signal level was at least six-fold over background), while EVL and Mena each have one. Strong binding was not observed to any peptide in WAVE1. The four peptides demonstrating the strongest binding are listed in Fig 8C. These results provide further evidence for direct and specific binding between SH3-6 and N-WASP and Ena/VASP proteins.

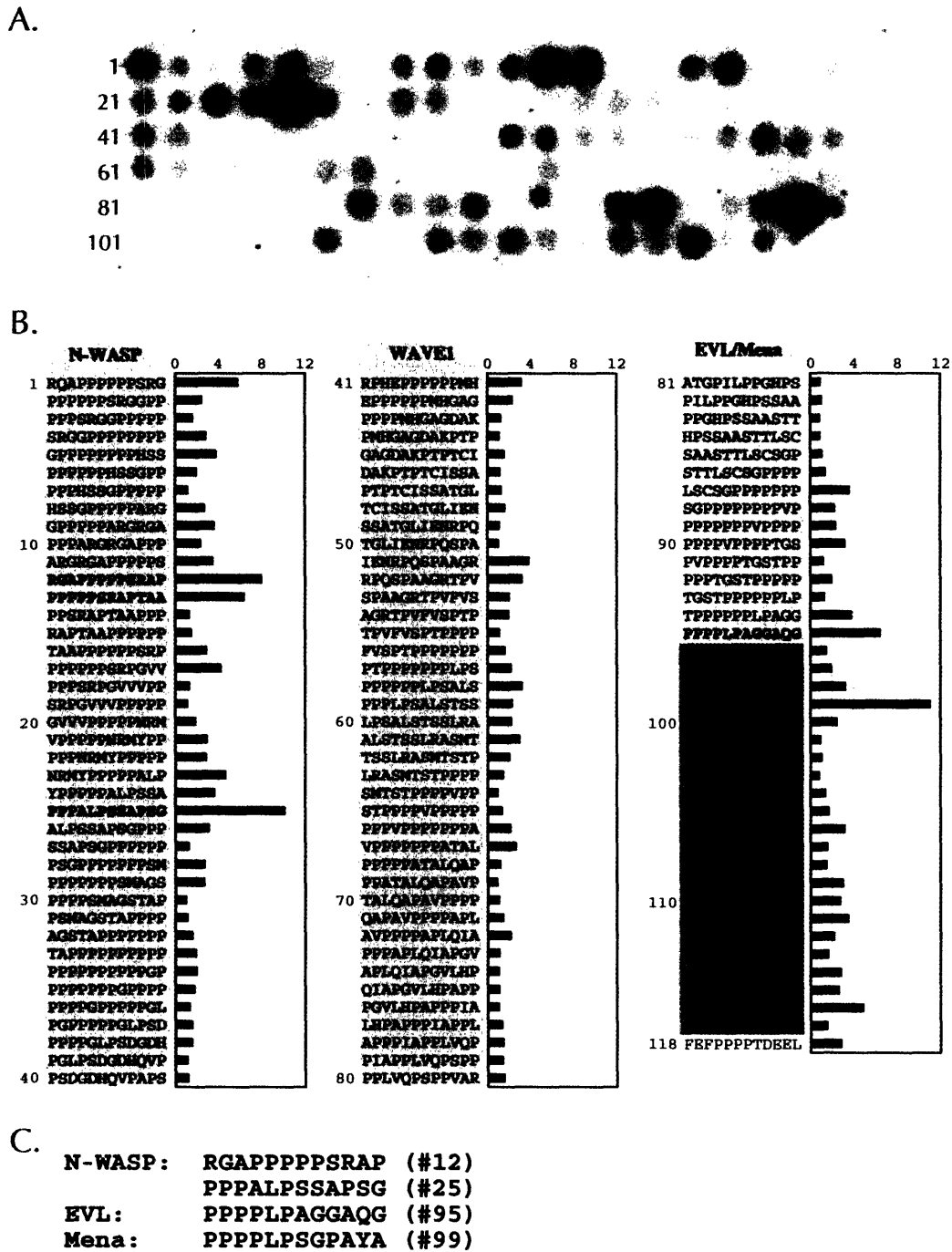


Figure 8. Mapping of SH3-6 binding sites. A. SPOTs membrane containing an array of overlapping peptides corresponding to the proline-rich regions of N-WASP, WAVE1, EVL and Mena overlaid with ³²P-labeled GST-SH3-6. B. Individual peptide spots are listed with intensity value demonstrated graphically as value/background. N-WASP peptides are shaded in blue, WAVE1 in orange, EVL in green and Mena in purple. Peptide #118 is a negative control proline-rich sequence that binds Ena/VASP proteins but not SH3 domains. Peptides in which the intensity/background is greater than 6 are in bold. C. Potential binding sites for SH3-6 in N-WASP, EVL, and Mena are listed with their corresponding peptide spot number.

The DH-BAR region of Tuba catalyzes the formation of active Cdc42

The results described above indicate that the C-terminal SH3 domain of Tuba can promote actin nucleation and/or recruitment. The presence of a DH domain in Tuba, a protein module involved in the activation of Rho family GTPases, suggests a further link to the actin cytoskeleton. The function of this domain was investigated.

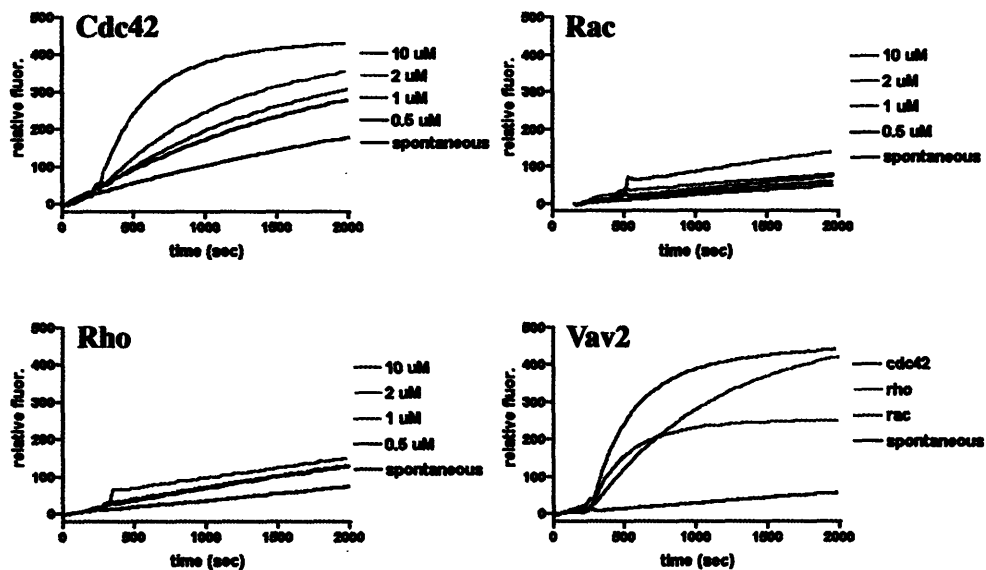


Figure 9. The DH domain of Tuba specifically catalyzes the activation of Cdc42. Indicated GTPases (2 μM) were incubated with 400 nM of mant-GTP for 200 seconds prior to addition of the indicated concentrations of his-tagged Tuba DH domain. Exchange activity was followed by the increase in fluorescence, normalized to its starting value, and reflects the binding of mant-GTP onto the GTPases. To verify the integrity of the GTPases, a fragment of Vav2 (0.2 μM) containing the DH and PH domains and previously shown to be active on Rho, Rac, and Cdc42 was used to load mant-GTP onto the GTPases under identical conditions.

Rho family GTPases, like other GTPases, cycle between a GTP-bound active state and a GDP-bound inactive state. DH domains form the core catalytic domains of enzymes that activate Rho family GTPases by catalyzing the exchange

Chapter 3

of GDP for GTP (Hoffman and Cerione, 2002). We studied the substrate specificity of the DH domain of Tuba by testing its guanyl nucleotide exchange activity on three major representative members of the Rho family: RhoA, Rac1 and Cdc42. A His-tagged Tuba DH domain was used in a mant-GTP-based assay, which allows the guanyl nucleotide exchange reaction to be monitored fluorimetrically (Snyder et al., 2002). The DH domain of Tuba specifically catalyzed, in a concentration-dependent manner, the activation of Cdc42, but not Rho or Rac (Fig. 9). The His-tagged DH-PH domain of Vav2, a DH domain known to have a promiscuous exchange activity on Rho, Rac, and Cdc42 (Liu and Burrridge, 2000), was used as a control to demonstrate that all three GTPases used were competent for exchange (Fig. 9). The DH domain of Tuba, while specific for Cdc42, displayed relatively low activity compared to the DH-PH domain of VAV - approximately 10 μ M of Tuba DH domain was comparable to 200 nM of VAV DH-PH. DH domains without associated PH domains are generally less active than DH-PH fragments (Whitehead et al., 1997). Since BAR domains of other proteins have been shown to bind lipids (Farsad et al., 2001; Lee and De Camilli, 2002; Takei et al., 1999), the BAR domain of Tuba may functionally replace a PH domain (see also Discussion). Thus, the absence of the BAR domain could account for the low activity of the DH domain of Tuba. Unfortunately, the insolubility of the BAR domain prevented us from testing the DH-BAR fragment in this assay and, more generally, the properties of Tuba's BAR domain.

The C-terminal SH3 domain of Tuba can promote F-actin recruitment

Tuba SH3-6 can bind to a number of actin-regulatory proteins. We wondered whether concentrating this domain on a surface within the cell would result in recruitment or nucleation of F-actin. To accomplish this aim, we fused the SH3-6 domain to a mitochondrial anchoring sequence (SH3-6-mito), a method that has been used successfully to map protein domains that induce actin recruitment within living cells (Kessels and Qualmann, 2002; Pistor et al., 1995). Since Tuba is expressed in the brain and localizes to synapses, we used CAD cells, a neuronal-like cell line, to express SH3-6-mito. Interestingly, in roughly 15 to 20 percent of transfected cells expressing high levels of SH3-6-Mito, F-actin was found to co-localize with the SH3-6-Mito fusion (Fig. 10, panels D, E, F). Therefore,

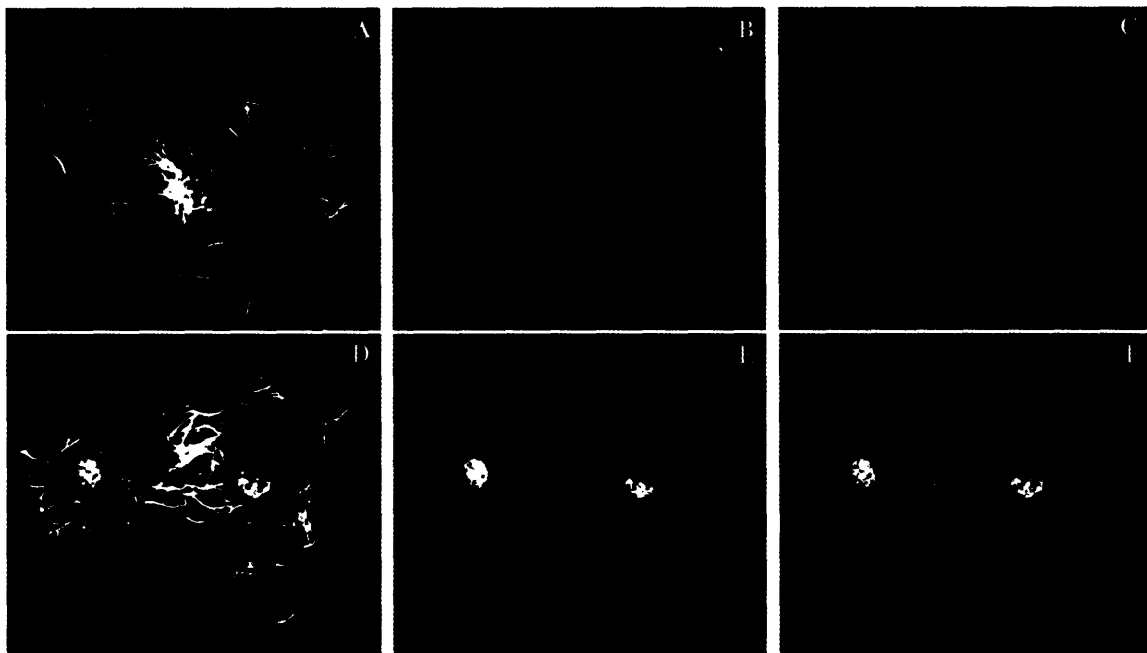


Figure 10. The C-terminal SH3 domain of Tuba recruits F-actin. SH3-6-mito, a DsRed2 fusion protein of SH3-6 with a mitochondrial targeting sequence at the C-terminus, was transiently transfected into CAD cells. The top row shows control cells stained for F-actin (A) that lacks any notable DsRed2 signal (B, merge in C). The bottom row demonstrates the colocalization of F-actin (D) with SH3-6-mito (E, merge in F) in two high-expressing cells.

overexpression of the SH3-6 domain can promote F-actin nucleation and/or recruitment within cells, presumably via a one or more of the actin regulatory proteins it is known to bind *in vitro*.

Tuba colocalizes with Mena in growth factor-induced actin ruffles

Western blot analysis indicated that Tuba is expressed in a number of cultured cell lines, including the fibroblastic Ena/VASP-deficient MV^{D7} cell line (data not shown). When the intracellular localization of Tuba was examined in unstimulated MV^{D7} cells expressing EGFP-Mena, it was found to be punctate and diffuse (data not shown). Furthermore, Tuba did not colocalize with Mena at the leading edge of lamellipodia or at focal adhesions. Since Tuba is a putative Rho GEF, we postulated that stimulating Rho GTPase activity might affect subcellular localization and/or Ena/VASP binding. MV^{D7} cells expressing EGFP-Mena were serum-starved and treated with PDGF, a growth factor known to activate Rho GTPase signaling and induce the formation of dorsal actin ruffles (Hawkins et al., 1995; Ridley et al., 1992). Mena and Tuba were found to colocalize at the tips of these actin ruffles (Fig. 11), suggesting that these proteins may associate during specific signaling events.

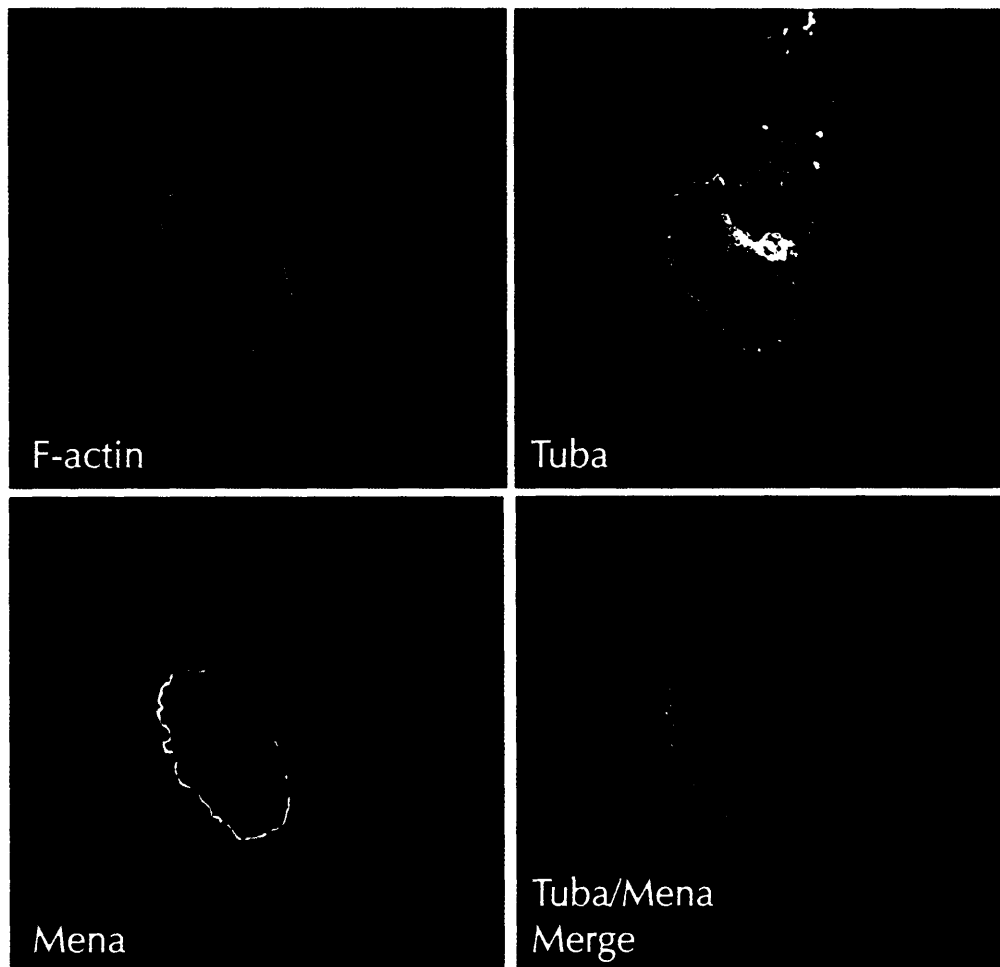


Figure 11. Tuba colocalizes with Mena in growth factor-induced dorsal ruffles. MVD7 cells expressing EGFP-Mena were serum starved for 6 hours before treatment with 50 ng/ml of PDGF for 10 minutes before fixation. Cells were stained for F-actin and Tuba. Individual stains are shown, and the bottom right panel shows the merge between the Mena and Tuba stain.

Discussion

The striking phenotype of *shibire* (dynamin) mutants of *Drosophila* (Koenig and Ikeda, 1989) and the many subsequent studies demonstrating a block of endocytosis in cells harboring dynamin mutations have strongly implicated this GTPase in the fission reaction of endocytosis (Hinshaw and Schmid, 1995; Marks et al., 2001; Takei et al., 1999). There is also strong evidence from studies in living

Chapter 3

cells and in cell free systems for a role for dynamin in the regulation of the actin cytoskeleton. For example, disruption of dynamin function impairs neurite outgrowth (an actin dependent process) (Masur et al., 1990) and perturbs actin dynamics in a variety of cellular contexts (Krueger et al., 2003; Ochoa et al., 2000; Schafer, 2002). Dynamin is present in actin tails (Lee and De Camilli, 2002; Orth et al., 2002), and many dynamin binding proteins, like intersectin (Hussain et al., 2001) and syndapin (Modregger et al., 2000; Qualmann et al., 2000), are also regulatory components of the actin cytoskeleton. This study details the discovery and characterization of a novel protein, Tuba, and its potential role as a molecular link between dynamin and actin.

The NH₂-terminal domain of Tuba binds dynamin via multiple SH3 domains, each of which can bind independently, thus increasing the overall avidity of Tuba for this GTPase. The interaction between Tuba and dynamin could be important for both dynamin localization and dynamin regulation, as has been shown for other SH3 domain containing dynamin ligands (Gout et al., 1993; Slepnev and De Camilli, 2000).

The COOH-terminal half of Tuba is linked to actin assembly via two independent mechanisms. First, the DH domain of Tuba activates Cdc42, a Rho family GTPase that binds and activates N-WASP, thereby triggering Arp2/3-mediated actin nucleation (Rohatgi et al., 1999). Second, the COOH-terminal SH3 domain binds a number of key actin regulatory proteins, including Ena/VASP, N-WASP and the N-WASP interacting protein WIRE and CR16. Based on the effects

Chapter 3

of other SH3 domain interactors of N-WASP (Hussain et al., 2001; Rohatgi et al., 2001), it is possible that Tuba binding activates N-WASP and that this activation may cooperate synergistically with Tuba-mediated activation of Cdc42 in promoting actin nucleation.

It is interesting to note that a Tuba isoform and Tuba relatives (Tuba 2 and Tuba 3) lack the NH₂-terminal dynamin-binding module, suggesting that Tuba family proteins may regulate the actin cytoskeleton in processes other than endocytosis. For example, recent models for filopodial formation propose that filopods emerge from clouds of Arp2/3-generated actin nuclei by elongation of filaments that are protected from capping and subsequently bundled (Vignjevic et al., 2003). The Tuba COOH-terminal SH3 domain binds to Ena/VASP proteins. Since Ena/VASP proteins function to promote actin filament elongation and have a potential role in filopodia formation (Svitkina et al., 2003), we speculate that Ena/VASP proteins are recruited by Tuba to promote actin filament growth after N-WASP-dependent actin nucleation. Therefore, Tuba is well positioned to promote filopodia formation by coordinating the activation of N-WASP (directly and via Cdc42) with the recruitment of Ena/VASP family members to antagonize capping protein, thus permitting filament elongation. The presence of predicted coiled-coil regions both in the BAR domain of Tuba (Ringstad et al., 2001; Wigge et al., 1997a) and upstream of this domain (see Fig. 1A) suggests a potential multimerization of the molecule as seen for other BAR and SH3 domain containing

Chapter 3

proteins (Ringstad et al., 2001; Wigge et al., 1997a), thus providing a further mechanism for the functional coordination of multiple binding partners.

The material affinity purified by this SH3-6 domain also includes the Wave1-PIR121-NAP125 complex, which is involved in the regulation of Arp2/3-mediated actin nucleation via Rac1 (Eden et al., 2002). Interestingly GEI-18, the worm TUBA homolog, was identified in a two-hybrid screen for binding partners of GEX3, the worm homolog of NAP125 (Soto et al., 2002; Tsuboi et al., 2002), suggesting that interactions between Tuba and the WAVE-inhibitory complex are evolutionarily conserved. It will be interesting to see what role, if any, Tuba plays in Rac-mediated signaling.

The SPOTs peptide binding provided further evidence for a direct and specific interaction between SH3-6 and N-WASP and Ena/VASP proteins. Four potential proline-rich SH3-6 binding sites were identified. The first site in N-WASP (RAGPPPPSRAP, #12) is very similar to a site found in the N-WASP interacting protein WIRE (RGKPPPPSRTP), a protein that is also found in the Tuba SH3-6 affinity purified complex. Far western data suggested that SH3-6 binds directly to more than N-WASP and Mena. Given that WIRE has a molecular weight of around 50 kDa, the fastest migrating band in the brain far western (Fig. 5B) is likely to be WIRE. Interestingly, the second site in N-WASP and the sites in Mena and EVL all contain "PPXLP".

The presence of binding sites for both N-WASP and dynamin, together with the presence of a Cdc42-specific DH domain, is also a characteristic of intersectin

Chapter 3

(Hussain et al., 2001). However, in Tuba the dynamin and the actin cytoskeleton binding domains are segregated at opposite ends of the protein. In intersectin, an intramolecular regulatory mechanism has been demonstrated showing that the binding of N-WASP stimulates the DH domain to activate Cdc42, thus resulting in a synergistic activation of Arp2/3-mediated actin nucleation (Hussain et al., 2001). The poor solubility of recombinant Tuba has prevented us from testing whether N-WASP binding can stimulate nucleotide exchange activity. The presence of putative consensus sites for SH3 domain binding in Tuba raises the possibility that inhibitory intramolecular SH3 domain-mediated interactions may occur (Zamanian and Kelly, 2003). These interactions might be released by the binding of appropriate SH3 domain ligands.

An additional unique feature of the Tuba family is the presence of a BAR domain, rather than of a PH domain, downstream of a DH domain. This is an exception to a nearly absolute rule (Hoffman and Cerione, 2002; Rossman et al., 2003). PH domains bind phosphoinositides (Lemmon et al., 2002), and their interaction with lipids in the bilayer recruits catalytic DH domains to their sites of action. In some cases, PH domains also have a direct regulatory role, such that PH domain binding to the membrane results in stimulation of exchange activity from the DH domain (Rossman et al., 2003; Rossman et al., 2002). As mentioned before, the absence of the BAR domain from the DH domain of Tuba in the GEF assays could account for its low activity. The crystal structure of the BAR domain from the *Drosophila* amphiphysin protein has been solved, and the domain forms

Chapter 3

an interesting crescent shaped-dimer that binds to negatively charged, highly curved membranes, and in some instances, may induce membrane curvature (Peter et al., 2004). Thus, the BAR domain of Tuba may functionally replace a PH domain. It is possible that the BAR domain functions to localize Tuba, and associated ligands, not membranes with a specific lipid content but to membranes with a specific curvature. Finally, it is worth noting that other BAR-containing proteins, like Tuba, can bind dynamin, have a putative role in membrane traffic and often contain modules associated with the actin cytoskeleton), suggesting an evolutionary relationship between this class of proteins (David et al., 1996; Ringstad et al., 1997).

Materials and Methods

Antibodies and Reagents

The following antibodies were used in this study. Rat monoclonal anti-HA epitope (clone 3F10 from Roche); anti-dynamin polyclonal antibody DG1 (our lab) and monoclonal antibody Hudy 1 (Upstate); anti-amphiphysin 1 monoclonal antibody #3 (Floyd et al., 2001); anti-N-WASP polyclonal antibody (gifts of P. Aspenstrom [Uppsala, Sweden] and M. Kirschner [Harvard Medical School]); anti-CR16 polyclonal (gift of H. Ho and M. Kirschner); anti-WAVE1 polyclonal antibody (gift of John Scott [Vollum Institute]); anti-Mena monoclonal antibody (our lab); anti-GFP polyclonal (Clontech); anti-actin monoclonal antibody (Sigma); anti-

Chapter 3

synaptotagmin monoclonal antibody (gift of Reinhard Jahn [Göttingen, Germany]); anti GM-130 from Graham Warren [Yale University]; anti-Lamellipodin polyclonal antibody (our lab). Polyclonal anti-Tuba antibodies were generated by injecting rabbits with a GST fusion protein encompassing the final 292 amino acids of human Tuba. The antibodies were affinity-purified on the antigen coupled to SulfoLink Beads (Pierce) according to the manufacturers instructions. A GST fusion protein of the PH domain of PLC δ was kind gift of Antonella De Matteis (Italy). A GST-fusion protein of the BAR domain of amphiphysin 1 was previously described (Takei et al., 1999). The KIAA1010 clone was obtained from the Kazusa Institute (Japan).

Cloning of human Tuba

To obtain Tuba's full-length sequence from the KIAA1010 clone (a gift of the Kazusa Institute), human skeletal muscle Marathon-Ready cDNAs (Clontech) were utilized for 5'-RACE using KIAA1010-specific primers and the Advantage 2 PCR Enzyme System (Clontech). Based on this sequence, a full-length clone was generated by PCR using probes corresponding to the 5' and 3' ending of the Tuba sequence and human brain Marathon Ready cDNAs (Clontech) as a template. Nucleotide sequencing confirmed the sequence of KIAA1010 and of the N-terminal region of the protein obtained by 5'-RACE with the exception of the absence in KIAA1010 of 40 amino acids in the second half of the BAR domain (see Fig. 1A). Multiple clones generated by PCR in different amplification cycles only yielded

Chapter 3

sequences including the 40 amino acids. The nucleotide sequence of human Tuba has been deposited in the GenBank database under the GenBank Accession Number AY196211.

Yeast 2-Hybrid and cloning of mouse Tuba

Full-length EVL was used as bait in the LexA 2-hybrid system (Clontech) to probe an E19 mouse embryo library. Greater than 1×10^6 independent clones were screened. From these, two independent clones of Tuba, comprising amino acids 1502-1577 and 1092-1577 (Fig. 1A), were identified as strong interactors. Full-length murine Tuba was constructed by ligating the larger of the two clones with fragments generated by RT-PCR using Tuba-specific primers and a mouse cDNA library. The nucleotide sequence of mouse Tuba has been deposited in the GenBank database under the GenBank Accession Number AY383729.

Affinity chromatography

GST or GST-fusion proteins of SH3 domain containing regions of Tuba were bound to glutathione beads (Pharmacia) and incubated with a Triton-X-100 rat brain extract prepared as described. Bound material was recovered by centrifugation followed by elution with SDS and separation by SDS-PAGE.

For the biochemical analysis of the interaction of Tuba SH3-6 with actin regulatory proteins in non-neuronal cell extracts, MV^{D7} fibroblastic cells that lack endogenous expression of all Ena/VASP proteins were used (Bear et al., 2000).

Chapter 3

Uninfected or infected MV^{D7} cells were grown to confluency and extracted in NP-40 lysis buffer. Cell extracts were clarified by centrifugation and used for affinity chromatography experiments as described above. 10 to 15µg of GST or GST-fusion protein was incubated with 1 mg of lysate.

Immunocytochemistry of Brain Tissue

Immunofluorescence of rat brain frozen sections was performed by standard procedures on formaldehyde perfuse brains. Anti-Tuba immunogold labeling was performed on lysed synaptosomes embedded in agarose followed by Epon embedding and thin sectioning as described (De Camilli et al., 1983).

Guanine Nucleotide Exchange Assays

Exchange assays using bacterially-expressed and purified Rho GTPases were performed essentially as described (Snyder et al., 2002). In particular, 2 µM RhoA (C190S), Rac1 (C188S), or Cdc42 (C188S), were added to a buffer containing 20 mM Tris, pH 7.5, 100 mM NaCl, 5 mM MgCl₂, 1 mM DTT, 10% glycerol and 400 nM mant-GTP (Molecular Probes) and allowed to equilibrate for 5 min before adding the indicated concentrations of his-tagged Tuba DH domain or 200 nM of his-tagged Vav2 DH-PH fragment. Increased fluorescence indicative of mant-GTP binding to GTPases was monitored using an LS-55 Perkin-Elmer spectrophotometer (λ_{ex} =360 nm; λ_{em} =440 nm, slits = 5/5 nm) thermostatted to 25°C. Fluorescence was normalized to the initial value at the start of the experiment. A fragment

Chapter 3

containing the DH and BAR domains of Tuba is insoluble upon expression in *E. coli*, preventing a comparison of exchange rates between this larger portion of Tuba and the isolated DH domain of Tuba.

Transferrin Uptake

CHO cells were transfected with pcHA (pcDNA3-based vector)-full length Tuba or pcHA-Tuba SH3-1,2,3,4 using FuGENE 6 Transfection Reagent (Roche) and incubated overnight. They were then washed into serum-free medium and incubated in serum-free medium for 24 hrs, with the presence of alexa-transferrin (Molecular Probes) during the last 7 minutes before a brief wash in PBS followed by fixation with 4% formaldehyde. Cells were stained by immunofluorescence according to standard procedures.

Peptide Binding

Overlapping SPOTs peptides corresponding to the proline-rich regions of mouse N-WASP (aa 217-399), SCAR/WAVE1 (aa 274-402), EVL (aa 157-210) and Mena (aa 277-351) were custom synthesized by SIGMA-GENOSYS. All peptides are 12-mers offset by three amino acids, and each spot carries an equivalent amount of peptide (5 nmol) covalently attached to the membrane. A negative control peptide was added (#118 on the blot) that contains a known proline-rich binding site for Ena/VASP proteins that does not bind SH3 domains. Tuba SH3-6 in pGEX-2TK was labeled by phosphorylating with PKA and [γ - 32 P] ATP. The relative

Chapter 3

intensity of each spot was calculated by converting the phosphoimager scan into an 8-bit image and measuring the average pixel intensity in a 74 pixel circle centered over each spot in Scion Image. This value was then divided by the background (the average intensity value of the 10 lowest spots) for comparison.

Mitochondrial Targeting of Tuba SH3-6

Mouse Tuba SH3-6 was fused in frame to a modified retroviral expression vector downstream of an ATG start codon and upstream of a fusion between DsRed2 and the mitochondrial targeting sequence from the *L. monocytogenes* protein ActA (excluding Ena/VASP-binding regions) (Pistor et al., 1994). This construct, referred to as SH3-6-mito, was used to transiently transfect CAD cells. Cells were plated onto poly-D-lysine coated coverslips 24 hours post-transfection. The media was replaced with serum-free media to induce differentiation 3- 4 hours after plating. Cells were incubated for an additional 24 to 36 hours before fixation with 4% formaldehyde. Previously established procedures were used to visualize cells by immunofluorescence.

Intracellular Localization of Tuba

MV^{D7} fibroblasts expressing EGFP-Mena were plated onto fibronectin coated coverslips and allowed to adhere and spread overnight in DME plus 15% fetal calf serum(FCS). Cells were serum starved in 0.5% FCS for 6 hours and then stimulated with 50-100 ng/ml of PDGF for 10 minutes before fixation in 4%

Chapter 3

paraformaldehyde. Fixed cells were permeabilized and stained for F-actin (Alexa Fluor 350 phalloidin) and Tuba (anti-Tuba polyclonal).

Miscellaneous Procedures

Western and northern blotting were carried out using standard procedures. For northern blotting, human multiple tissue RNA blots were obtained from Clontech. For multiple tissue western blots, tissues were isolated and prepared as previously described (McPherson et al., 1996). Far-western assays and gel overlays were carried out using standard procedures. Immunoprecipitations were carried out as previously described (McPherson et al., 1996).

References

- Aspenstrom, P. (2002). The WASP-binding protein WIRE has a role in the regulation of the actin filament system downstream of the platelet-derived growth factor receptor. *Exp Cell Res* 279, 21-33.
- Bear, J. E., Loureiro, J. J., Libova, I., Fassler, R., Wehland, J., and Gertler, F. B. (2000). Negative regulation of fibroblast motility by Ena/VASP proteins. *Cell* 101, 717-728.
- Cases-Langhoff, C., Voss, B., Garner, A. M., Appeltauer, U., Takei, K., Kindler, S., Veh, R. W., De Camilli, P., Gundelfinger, E. D., and Garner, C. C. (1996). Piccolo, a novel 420 kDa protein associated with the presynaptic cytomatrix. *European Journal of Cell Biology* 69, 214-223.
- Conner, S. D., and Schmid, S. L. (2003). Regulated portals of entry into the cell. *Nature* 422, 37-44.
- Coppolino, M. G., Krause, M., Hagendorff, P., Monner, D. A., Trimble, W., Grinstein, S., Wehland, J., and Sechi, A. S. (2001). Evidence for a molecular complex consisting of Fyb/SLAP, SLP-76, Nck, VASP and WASP that links the actin cytoskeleton to Fcγ receptor signalling during phagocytosis. *J Cell Sci* 114, 4307-4318.
- David, C., McPherson, P. S., Mundigl, O., and De Camilli, P. (1996). A role of amphiphysin in synaptic vesicle endocytosis suggested by its binding to dynamin in nerve terminals. *Proceedings of the National Academy of Sciences of the United States of America* 93, 331-335.
- De Camilli, P., Harris, S. M., Jr., Huttner, W. B., and Greengard, P. (1983). Synapsin I (Protein I), a nerve terminal-specific phosphoprotein. *Journal of Cell Biology* 96, 1355-1373.
- Eden, S., Rohatgi, R., Podtelejnikov, A. V., Mann, M., and Kirschner, M. W. (2002). Mechanism of regulation of WAVE1-induced actin nucleation by Rac1 and Nck. *Nature* 418, 790-793.
- Farsad, K., Ringstad, N., Takei, K., Floyd, S. R., Rose, K., and De Camilli, P. (2001). Generation of high curvature membranes mediated by direct endophilin bilayer interactions. *J Cell Biol* 155, 193-200.
- Floyd, S. R., Porro, E. B., Slepnev, V. I., Ochoa, G. C., Tsai, L. H., and De Camilli, P. (2001). Amphiphysin 1 binds the cyclin-dependent kinase (cdk) 5 regulatory subunit p35 and is phosphorylated by cdk5 and cdc2. *J Biol Chem* 276, 8104-8110.

Chapter 3

- Frank, R. (2002). The SPOT-synthesis technique. Synthetic peptide arrays on membrane supports--principles and applications. *J Immunol Methods* 267, 13-26.
- Gertler, F. B., Niebuhr, K., Reinhard, M., Wehland, J., and Soriano, P. (1996). Mena, a relative of VASP and *Drosophila Enabled*, is implicated in the control of microfilament dynamics. *Cell* 87, 227-239.
- Gout, I., Dhand, R., Hiles, I. D., Fry, M. J., Panayotou, G., Das, P., Truong, O., Totty, N. F., Hsuan, J., Booker, G. W., et al. (1993). The GTPase dynamin binds to and is activated by a subset of SH3 domains. *Cell* 75, 25-36.
- Hawkins, P. T., Eguinoa, A., Qiu, R. G., Stokoe, D., Cooke, F. T., Walters, R., Wennstrom, S., Claesson-Welsh, L., Evans, T., and Symons, M. (1995). PDGF stimulates an increase in GTP-Rac via activation of phosphoinositide 3-kinase. *Curr Biol* 5, 393-403.
- Hinshaw, J. E. (2000). Dynamin and its role in membrane fission. *Annu Rev Cell Dev Biol* 16, 483-519.
- Hinshaw, J. E., and Schmid, S. L. (1995). Dynamin self-assembles into rings suggesting a mechanism for coated vesicle budding. *Nature* 374, 190-192.
- Ho, H. Y., Rohatgi, R., Ma, L., and Kirschner, M. W. (2001). CR16 forms a complex with N-WASP in brain and is a novel member of a conserved proline-rich actin-binding protein family. *Proc Natl Acad Sci U S A* 98, 11306-11311.
- Hoffman, G. R., and Cerione, R. A. (2002). Signaling to the Rho GTPases: networking with the DH domain. *FEBS Lett* 513, 85-91.
- Hussain, N. K., Jenna, S., Glogauer, M., Quinn, C. C., Wasiak, S., Guipponi, M., Antonarakis, S. E., Kay, B. K., Stossel, T. P., Lamarche-Vane, N., and McPherson, P. S. (2001). Endocytic protein intersectin-1 regulates actin assembly via Cdc42 and N-WASP. *Nat Cell Biol* 3, 927-932.
- Ishikawa, R., Hayashi, K., Shirao, T., Xue, Y., Takagi, T., Sasaki, Y., and Kohama, K. (1994). Drebrin, a development-associated brain protein from rat embryo, causes the dissociation of tropomyosin from actin filaments. *J Biol Chem* 269, 29928-29933.
- Kato, M., Miki, H., Kurita, S., Endo, T., Nakagawa, H., Miyamoto, S., and Takenawa, T. (2002). WICH, a novel verprolin homology domain-containing protein that functions cooperatively with N-WASP in actin-microspike formation. *Biochem Biophys Res Commun* 291, 41-47.

Chapter 3

- Kessels, M. M., and Qualmann, B. (2002). Syndapins integrate N-WASP in receptor-mediated endocytosis. *Embo J* 21, 6083-6094.
- Koenig, J. H., and Ikeda, K. (1989). Disappearance and reformation of synaptic vesicle membrane upon transmitter release observed under reversible blockage of membrane retrieval. *Journal of Neuroscience* 9, 3844-3860.
- Krause, M., Leslie, J. D., Stewart, M., Lafuente, E. M., Valderrama, F., Jagannathan, R., Strasser, G. A., Rubinson, D. A., Liu, H., Way, M., et al. (2004). Lamellipodin, an Ena/VASP Ligand, Is Implicated in the Regulation of Lamellipodial Dynamics. *Dev Cell* 7, 571-583.
- Krueger, E. W., Orth, J. D., Cao, H., and McNiven, M. A. (2003). A Dynamin-Cortactin-Arp2/3 Complex Mediates Actin Reorganization in Growth Factor-stimulated Cells. *Mol Biol Cell* 14, 1085-1096.
- Lanier, L. M., Gates, M. A., Witke, W., Menzies, A. S., Wehman, A. M., Macklis, J. D., Kwiatkowski, D., Soriano, P., and Gertler, F. B. (1999). Mena is required for neurulation and commissure formation. *Neuron* 22, 313-325.
- Lee, E., and De Camilli, P. (2002). From the Cover: Dynamin at actin tails. *Proc Natl Acad Sci U S A* 99, 161-166.
- Lemmon, M. A., Ferguson, K. M., and Abrams, C. S. (2002). Pleckstrin homology domains and the cytoskeleton. *FEBS Lett* 513, 71-76.
- Liu, B. P., and Burridge, K. (2000). Vav2 activates Rac1, Cdc42, and RhoA downstream from growth factor receptors but not beta1 integrins. *Mol Cell Biol* 20, 7160-7169.
- Lombardi, R., and Riezman, H. (2001). Rvs161p and Rvs167p, the two yeast amphiphysin homologs, function together in vivo. *J Biol Chem* 276, 6016-6022.
- Machesky, L. M., Mullins, R. D., Higgs, H. N., Kaiser, D. A., Blanchoin, L., May, R. C., Hall, M. E., and Pollard, T. D. (1999). Scar, a WASP-related protein, activates nucleation of actin filaments by the Arp2/3 complex. *Proc Natl Acad Sci U S A* 96, 3739-3744.
- Marks, B., Stowell, M. H., Vallis, Y., Mills, I. G., Gibson, A., Hopkins, C. R., and McMahon, H. T. (2001). GTPase activity of dynamin and resulting conformation change are essential for endocytosis. *Nature* 410, 231-235.
- Martinez-Quiles, N., Rohatgi, R., Anton, I. M., Medina, M., Saville, S. P., Miki, H., Yamaguchi, H., Takenawa, T., Hartwig, J. H., Geha, R. S., and Ramesh, N. (2001).

Chapter 3

WIP regulates N-WASP-mediated actin polymerization and filopodium formation. *Nat Cell Biol* 3, 484-491.

Masur, S. K., Kim, Y. T., and Wu, C. F. (1990). Reversible inhibition of endocytosis in cultured neurons from the *Drosophila* temperature-sensitive mutant shibirets1. *J Neurogenet* 6, 191-206.

McPherson, P. S., Garcia, E. P., Slepnev, V. I., David, C., Zhang, X., Grabs, D., Sossin, W. S., Bauerfeind, R., Nemoto, Y., and De Camilli, P. (1996). A presynaptic inositol-5-phosphatase. *Nature* 379, 353-357.

Merrifield, C. J., Feldman, M. E., Wan, L., and Almers, W. (2002). Imaging actin and dynamin recruitment during invagination of single clathrin-coated pits. *Nat Cell Biol* 4, 691-698.

Merrifield, C. J., Moss, S. E., Ballestrem, C., Imhof, B. A., Giese, G., Wunderlich, I., and Almers, W. (1999). Endocytic vesicles move at the tips of actin tails in cultured mast cells. *Nat Cell Biol* 1, 72-74.

Miki, H., Miura, K., and Takenawa, T. (1996). N-WASP, a novel actin-depolymerizing protein, regulates the cortical cytoskeletal rearrangement in a PIP₂-dependent manner downstream of tyrosine kinases. *EMBO Journal* 15, 5326-5335.

Miki, H., Suetsugu, S., and Takenawa, T. (1998). WAVE, a novel WASP-family protein involved in actin reorganization induced by Rac. *Embo J* 17, 6932-6941.

Modregger, J., Ritter, B., Witter, B., Paulsson, M., and Plomann, M. (2000). All three PACSIN isoforms bind to endocytic proteins and inhibit endocytosis. *J Cell Sci* 113, 4511-4521.

Munn, A. L. (2001). Molecular requirements for the internalisation step of endocytosis: insights from yeast. *Biochim Biophys Acta* 1535, 236-257.

Nakamura, N., Rabouille, C., Watson, R., Nilsson, T., Hui, N., Slusarewicz, P., Kreis, T. E., and Warren, G. (1995). Characterization of a cis-Golgi matrix protein, GM130. *J Cell Biol* 131, 1715-1726.

Ochoa, G. C., Slepnev, V. I., Neff, L., Ringstad, N., Takei, K., Daniell, L., Kim, W., Cao, H., McNiven, M., Baron, R., and De Camilli, P. (2000). A functional link between dynamin and the actin cytoskeleton at podosomes. *J Cell Biol* 150, 377-389.

Orth, J. D., Krueger, E. W., Cao, H., and McNiven, M. A. (2002). From the Cover: The large GTPase dynamin regulates actin comet formation and movement in living cells. *Proc Natl Acad Sci U S A* 99, 167-172.

Chapter 3

- Peter, B. J., Kent, H. M., Mills, I. G., Vallis, Y., Butler, P. J., Evans, P. R., and McMahon, H. T. (2004). BAR domains as sensors of membrane curvature: the amphiphysin BAR structure. *Science* 303, 495-499.
- Pistor, S., Chakraborty, T., Niebuhr, K., Domann, E., and Wehland, J. (1994). The ActA protein of *Listeria monocytogenes* acts as a nucleator inducing reorganization of the actin cytoskeleton. *Embo J* 13, 758-763.
- Pistor, S., Chakraborty, T., Walter, U., and Wehland, J. (1995). The bacterial actin nucleator protein ActA of *Listeria monocytogenes* contains multiple binding sites for host microfilament proteins. *Curr Biol* 5, 517-525.
- Qualmann, B., Kessels, M. M., and Kelly, R. B. (2000). Molecular links between endocytosis and the actin cytoskeleton. *J Cell Biol* 150, F111-116.
- Ramjaun, A. R., Micheva, K. D., Bouchelet, I., and McPherson, P. S. (1997). Identification and characterization of a nerve terminal-enriched amphiphysin isoform. *J Biol Chem* 272, 16700-16706.
- Ridley, A. J., Paterson, H. F., Johnston, C. L., Diekmann, D., and Hall, A. (1992). The small GTP-binding protein rac regulates growth factor-induced membrane ruffling. *Cell* 70, 401-410.
- Ringstad, N., Nemoto, Y., and De Camilli, P. (1997). The SH3p4/Sh3p8/SH3p13 protein family: binding partners for synaptojanin and dynamin via a Grb2-like Src homology 3 domain. *Proc Natl Acad Sci U S A* 94, 8569-8574.
- Ringstad, N., Nemoto, Y., and De Camilli, P. (2001). Differential expression of endophilin 1 and 2 dimers at central nervous system synapses. *J Biol Chem* 276, 40424-40430.
- Rohatgi, R., Ma, L., Miki, H., Lopez, M., Kirchhausen, T., Takenawa, T., and Kirschner, M. W. (1999). The interaction between N-WASP and the Arp2/3 complex links Cdc42-dependent signals to actin assembly. *Cell* 97, 221-231.
- Rohatgi, R., Nollau, P., Ho, H. Y., Kirschner, M. W., and Mayer, B. J. (2001). Nck and phosphatidylinositol 4,5-bisphosphate synergistically activate actin polymerization through the N-WASP-Arp2/3 pathway. *J Biol Chem* 276, 26448-26452.
- Roos, J., and Kelly, R. B. (1998). Dap160, a neural-specific Eps15 homology and multiple SH3 domain-containing protein that interacts with *Drosophila* dynamin. *J Biol Chem* 273, 19108-19119.

Chapter 3

- Rossman, K. L., Cheng, L., Mahon, G. M., Rojas, R. J., Snyder, J. T., Whitehead, I. P., and Sondek, J. (2003). Multifunctional roles for the PH domain of Dbs in regulating Rho GTPase activation. *J Biol Chem* *13*, 13.
- Rossman, K. L., Worthylake, D. K., Snyder, J. T., Siderovski, D. P., Campbell, S. L., and Sondek, J. (2002). A crystallographic view of interactions between Dbs and Cdc42: PH domain-assisted guanine nucleotide exchange. *Embo J* *21*, 1315-1326.
- Schafer, D. A. (2002). Coupling actin dynamics and membrane dynamics during endocytosis. *Curr Opin Cell Biol* *14*, 76-81.
- Shupliakov, O., Low, P., Grabs, D., Gad, H., Chen, H., David, C., Takei, K., De Camilli, P., and Brodin, L. (1997). Synaptic vesicle endocytosis impaired by disruption of dynamin-SH3 domain interactions. *Science* *276*, 259-263.
- Slepnev, V. I., and De Camilli, P. (2000). Accessory factors in clathrin-dependent synaptic vesicle endocytosis. *Nat Rev Neurosci* *1*, 161-172.
- Snyder, J. T., Worthylake, D. K., Rossman, K. L., Betts, L., Pruitt, W. M., Siderovski, D. P., Der, C. J., and Sondek, J. (2002). Structural basis for the selective activation of Rho GTPases by Dbl exchange factors. *Nat Struct Biol* *9*, 468-475.
- Soto, M. C., Qadota, H., Kasuya, K., Inoue, M., Tsuboi, D., Mello, C. C., and Kaibuchi, K. (2002). The GEX-2 and GEX-3 proteins are required for tissue morphogenesis and cell migrations in *C. elegans*. *Genes Dev* *16*, 620-632.
- Svitkina, T. M., Bulanova, E. A., Chaga, O. Y., Vignjevic, D. M., Kojima, S., Vasiliev, J. M., and Borisy, G. G. (2003). Mechanism of filopodia initiation by reorganization of a dendritic network. *J Cell Biol* *160*, 409-421.
- Takei, K., Slepnev, V. I., Haucke, V., and De Camilli, P. (1999). Functional partnership between amphiphysin and dynamin in clathrin-mediated endocytosis. *Nature Cell Biology* *1*, 33-39.
- Tsuboi, D., Qadota, H., Kasuya, K., Amano, M., and Kaibuchi, K. (2002). Isolation of the interacting molecules with GEX-3 by a novel functional screening. *Biochem Biophys Res Commun* *292*, 697-701.
- Vignjevic, D., Yarar, D., Welch, M. D., Peloquin, J., Svitkina, T., and Borisy, G. G. (2003). Formation of filopodia-like bundles in vitro from a dendritic network. *J Cell Biol* *160*, 951-962.
- Whitehead, I. P., Campbell, S., Rossman, K. L., and Der, C. J. (1997). Dbl family proteins. *Biochim Biophys Acta* *1332*, F1-23.

Chapter 3

Wigge, P., Kohler, K., Vallis, Y., Doyle, C. A., Owen, D., Hunt, S. P., and McMahon, H. T. (1997a). Amphiphysin heterodimers: potential role in clathrin-mediated endocytosis. *Mol Biol Cell* 8, 2003-2015.

Wigge, P., Vallis, Y., and McMahon, H. T. (1997b). Inhibition of receptor-mediated endocytosis by the amphiphysin SH3 domain. *Curr Biol* 7, 554-560.

Zamanian, J. L., and Kelly, R. B. (2003). Intersectin 1L Guanine Nucleotide Exchange Activity Is Regulated by Adjacent src Homology 3 Domains That Are Also Involved in Endocytosis. *Mol Biol Cell* 14, 1624-1637.

Chapter 4

Role of Ena/VASP Proteins in Mouse Development

Note: Jon Leslie and I worked together to make the targeting construct used to generate the EVL knockout. Doug Rubinson and I have worked together to analyze the phenotypes of the knockout mice.

Abstract

Loss of Ena/VASP function in invertebrates causes defects in axon guidance and epithelial morphogenesis. In vertebrates, analysis of Ena/VASP function is complicated by the overlapping expression of three functionally interchangeable Ena/VASP proteins – Mena, VASP, and EVL. Mena-deficient mice display defects in nervous system development, and loss of VASP in mice affects platelet aggregation. Analysis of Mena/VASP double mutants revealed a requirement for Ena/VASP function in neurulation, and analysis of triple mutants is expected to reveal new requirements for Ena/VASP function. To accomplish this, a knockout of EVL was constructed and crossed to Mena and VASP mutant lines. Analysis of compound mutants has revealed new functions for Ena/VASP proteins, including roles in cerebellar development, sensory nerve formation, neuronal layering and cardiovascular function.

Introduction

Coordinated cell movement is required for vertebrate embryo morphogenesis. During embryogenesis, cells migrate individually and collectively, driving critical development processes ranging from gastrulation to neural crest cell movement. For example, neuronal precursors navigate through the developing brain to form specific layers, and send out cellular processes (axons and dendrites) that migrate throughout the brain to establish synaptic connections required for brain function.

Tissue formation and morphogenesis during embryogenesis requires coordinated regulation of cell motility, adhesion, and morphology. As discussed in Chapter 1, cell movement requires changes in the underlying actin cytoskeleton in response to extracellular guidance cues. Guidance cues and extracellular signals direct cell movement and promote cell adhesion and positioning during embryogenesis. Understanding how the actin cytoskeleton is regulated in response to the cues and signals during embryonic development is of great interest. Many proteins known to regulate actin assembly are required for vertebrate embryogenesis, such as N-WASP and Wave2 (Snapper et al., 2001; Yamazaki et al., 2003).

Ena/VASP proteins regulate actin assembly and regulate cell movement, as discussed in Chapter 1. The *Drosophila* ortholog Ena has been implicated in nervous system development downstream of known axon guidance receptors

Chapter 4

(Bashaw et al., 2000; Wills et al., 1999). Similarly, the Ena/VASP ortholog Unc-34 in worms functions in axon guidance receptor-mediated signaling pathways (Gitai et al., 2003; Withee et al., 2004; Yu et al., 2002). Ena also functions to regulate epithelial morphogenesis in flies (Grevengoed et al., 2001).

Analysis of Ena/VASP function in vertebrates is complicated by the presence of three highly related proteins – Mena, VASP, and EVL – that display overlapping patterns of expression in the developing and adult mouse. In mice, loss of Mena produces defects in the formation of the corpus callosum, hippocampal commissure and retinal axon tracts, indicative of defects in axon outgrowth and pathfinding (Lanier et al., 1999; Menzies et al., 2004). Loss of VASP in mice produces a defect in cyclic-nucleotide dependent attenuation of platelet activation *in vitro* and increase in platelet adhesion *in vivo* (Aszodi et al., 1999; Massberg et al., 2004). $Mena^{-/-}$; $VASP^{-/-}$ mice die perinatally with a high incidence of neural tube defects that result in exencephaly and cleft palate. $Mena^{-/-}$; $VASP^{-/-}$ mutants also display defects in anterior commissure formation not observed in Mena-null mice, as well as problems in formation of the peripheral nervous system (Menzies et al., 2004).

We hypothesized that the presence of the third Ena/VASP protein, EVL, in Mena/VASP single and double mutants masked additional requirements for Ena/VASP function for mouse development and physiology. Therefore, we generated a mouse knockout of EVL and crossed it to existing Mena and VASP mutants. Mice lacking EVL are viable and do not display any gross defects, as are mice lacking both EVL and VASP. $Mena^{-/-}$; $EVL^{-/-}$ mice are not viable and display

defects in nervous system development. Analysis of viable mutants that contain only one copy of EVL and VASP and lack Mena revealed a requirement for Ena/VASP function in cerebellar development. A majority of Mena^{+/-}; VASP^{+/-}; EVL^{-/-} embryos survive through development, but show signs of edema, possibly due to a defect in endothelial function or heart formation and/or function. Further analysis of Mena^{+/-}; VASP^{+/-}; EVL^{-/-} revealed defects in formation of multiple nerve tracts in the central and peripheral nervous system.

Results

EVL knockout – construction and analysis

We generated a targeted disruption of the EVL locus. Exons 2 and 3 were replaced with a cassette encoding neomycin resistance under the control of the PGK promoter (Fig. 1A). This strategy should remove most of the N-terminal coding region of EVL and produce a frameshift downstream, effectively eliminating EVL function.

The EVL locus was targeted in embryonic stem cells, and recombination determined by PCR and southern blot (data not shown). Five independent targeted ES clones were isolated and used to generate chimeric mice. One EVL^{+/-} clone went germline, and was used for all further analysis. Mice homozygous for the EVL disruption are fully viable and observed at the expected Mendelian ratios (data not shown). Western blot analysis of brain lysates from wild type (EVL^{+/+}), heterozygous (EVL^{+/-}), and homozygous mutant (EVL^{-/-}) animals, as determined by

PCR genotyping (Fig. 1B), was performed to determine if the targeted locus produced any protein. There are two isoforms of EVL (48 and 52 kDa) found in the brain. As expected, expression of both EVL isoforms was reduced in the heterozygous animal and eliminated in the homozygous mutant animal (Fig. 1C).

Gross morphological analysis of mice lacking EVL did not reveal any apparent defects. EVL is highly expressed in the developing embryonic nervous system, and Ena/VASP proteins are known to play an important role in nervous system development (Lanier et al.,

1999; Menzies et al., 2004); however, brain architecture appeared unperturbed in EVL mutants (data not shown). EVL is also highly expressed in cells of the immune system; however, immune cell development and organization appeared normal in

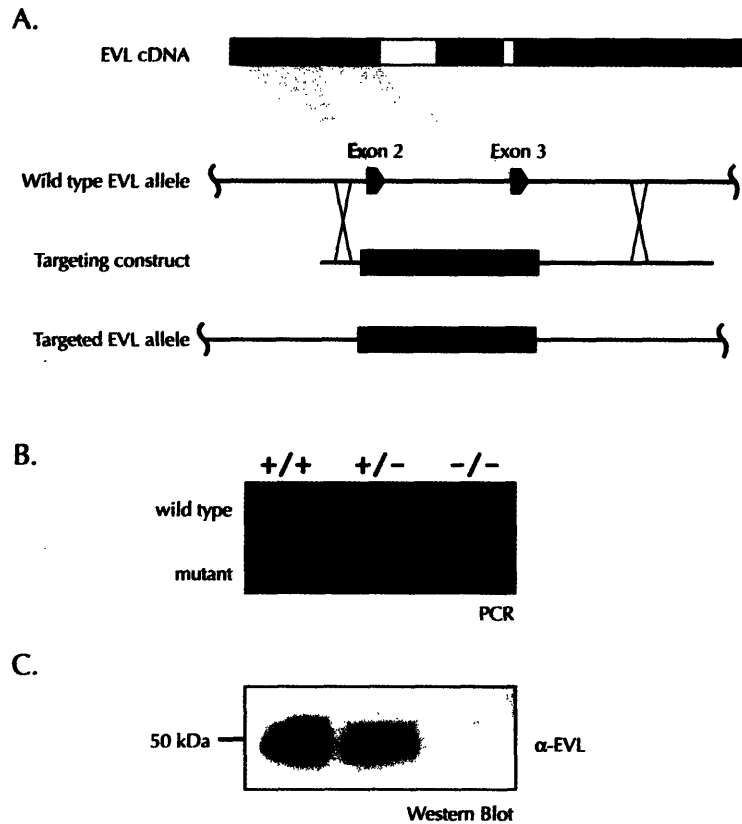


Figure 1. Generation of EVL knockout mice. A. The targeting vector contained a neomycin resistance cassette flanked by genomic DNA from introns 1 and 3. Homologous recombination will delete exons 2 and 3 of the EVL locus, removing much of the N-terminal EVH1 domain and producing a downstream frameshift to prevent translation of the remaining transcript. B. PCR genotyping was performed on tail samples from adult mice. The wild type and mutant band are noted. C. Extracts were prepared from wild type (+/+), heterozygous (+/-), and homozygous mutant (-/-) brains and analyzed for EVL expression by western blot.

Chapter 4

EVL mutants (data not shown). Immune cell function was not tested; however, these experiments are currently being conducted in VASP/EVL double knockouts (discussed below).

EVL, like all Ena/VASP proteins, binds profilin, an actin binding protein that regulates actin polymerization (Lambrechts et al., 2000; Loureiro et al., 2002). Two isoforms of profilin, profilinI and profilinII, are expressed from different genes in vertebrates. Profilin II binds with a much higher affinity to EVL compared to profilin I *in vitro* (Lambrechts et al., 2000); however, profilin I was the most frequently identified binding partner of EVL in a two-hybrid screen I conducted (Kwiatkowski, A., Serna, D. and F. Gertler, unpublished data). A synthetic genetic interaction has been observed between Mena and profilin I in mice. Mice homozygous mutant for Mena and heterozygous for profilin I (Mena^{-/-}; profilin I^{+/-}) die perinatally, and nearly half of the embryos display defects in neural tube closure. Therefore, a 50% reduction in the amount of profilin I sensitizes animals to the loss of Mena, exposing requirements for these proteins in neural tube closure (Lanier et al., 1999). To test if a similar genetic interaction exists between EVL and profilin I, we crossed EVL^{-/-} mice to profilin I^{+/-} animals. We then intercrossed EVL^{+/-}; profilin I^{+/-} mice. EVL^{+/-}; profilin I^{+/-} are viable and recovered at the expected Mendelian ratio (data not shown), suggesting that profilin I levels are not limiting in the EVL knockout. However, it remains to be determined whether such animals have any additional phenotypes not apparent from superficial examination.

Chapter 4

The absence of an obvious phenotype in $EVL^{-/-}$ mice is likely due to the presence of Mena and/or VASP in tissues and cell types that express EVL.

Therefore, the EVL knockout line was crossed to mice mutant for Mena and/or VASP to study the function of Ena/VASP proteins in mouse development and physiology.

VASP/EVL-deficient mice

Mice lacking VASP are viable, fertile and appear morphologically normal (Aszodi et al., 1999). Loss of VASP produces a defect in cyclic-nucleotide dependent inhibition of platelet aggregation, as described in Chapter 1. EVL and VASP share a similar pattern of expression in the adult mouse, and are both highly expressed in the spleen and thymus. In contrast, little or no Mena is expressed in these organs (Lanier et al., 1999). *In vitro* evidence suggests that Ena/VASP proteins play a role in immune system function, in particular T cell receptor (TCR) signaling and macrophage phagocytosis (Coppolino et al., 2001; Krause et al., 2000). Therefore, we wondered what effect removing both VASP and EVL would have on mouse development and immune system development and function. $EVL^{-/-}$ mice were crossed to $VASP^{-/-}$, and resulting $VASP^{-/-}; EVL^{-/-}$ mice intercrossed. Mice lacking both VASP and EVL are viable and observed at the expected Mendelian ratio (data not shown). Furthermore, $VASP^{-/-}; EVL^{-/-}$ mice appear morphologically normal and fertile, and immune system development appears normal. Analysis of a range of immune system cells - including T cells, B cells, macrophages and

neutrophils – by FACS indicated that all major cell types are present and found in the appropriate locales within the body (data not shown). We are currently investigating if there any defects in immune cell function (i.e. T cell synapse formation, neutrophil migration) in $VASP^{+/-}; EVL^{-/-}$ mice.

Mena/EVL-deficient mice

Mena-deficient mice are viable, but display defects in axonal pathfinding and commissure formation as described in Chapter 1. We crossed mice mutant for Mena to mice lacking EVL, and then intercrossed the resulting double heterozygous ($Mena^{+/-}; EVL^{+/-}$) mutant animals to obtain double homozygous mutants. $Mena^{-/-}; EVL^{-/-}$ mutant mice were not observed at the age of genotyping (postnatal day 10), and a decrease in the number of expected $Mena^{+/-}; EVL^{+/-}$ animals was observed (Table 1). This suggests that the combined functions of Mena and EVL are required for postnatal viability. The phenotype of $Mena^{+/-}; EVL^{-/-}$ embryos is discussed below.

Genotype	# observed	# expected
$Mena^{+/+}; EVL^{+/+}$	9	11
$Mena^{+/+}; EVL^{+/-}$	36	22
$Mena^{+/+}; EVL^{-/-}$	15	11
$Mena^{+/-}; EVL^{+/+}$	30	22
$Mena^{+/-}; EVL^{+/-}$	51	45
$Mena^{+/-}; EVL^{-/-}$	29	22
$Mena^{-/-}; EVL^{+/+}$	7	11
$Mena^{-/-}; EVL^{+/-}$	2	22
$Mena^{-/-}; EVL^{-/-}$	0	11
	179	

Table 1. Results from Mena/EVL double mutant crosses.

Phenotypes observed in viable Mena/VASP/EVL-compound mutants

In the course of generating Mena/VASP/EVL triple mutants, we determined what combinations of Mena, VASP and EVL alleles were viable as adults. Triple heterozygous mutants (Mena^{+/-}; VASP^{+/-}; EVL^{+/-}) were generated by crossing EVL knockouts to animals heterozygous for mutations in Mena and VASP. Mena^{+/-}; VASP^{+/-}; EVL^{+/-} animals are viable and fertile. Mena^{+/-}; VASP^{+/-}; EVL^{+/-} mice were intercrossed and resulting progeny observed (Table 2). As expected, no triple mutant animals (Mena^{-/-}; VASP^{-/-}; EVL^{-/-}) were recovered as adults. Mena^{+/-}; VASP^{+/-}; EVL^{-/-} and Mena^{+/-}; VASP^{-/-}; EVL^{+/-} mice were observed at or near expected Mendelian ratios. Interestingly, a significant percentage of Mena^{+/-}; VASP^{-/-}; EVL^{-/-} mice were viable. Though less than 1/3 of expected Mena^{+/-}; VASP^{-/-}; EVL^{-/-} mice were observed, animals with only one Ena/VASP allele (Mena) can survive. That this one allele must be Mena suggests that it is the most critical Ena/VASP protein for viability. However, it is unclear if this is due to Mena expression levels and distribution during development or a unique function of Mena.

Genotype	# Observed	# Expected
Mena ^{+/+} ; VASP ^{+/+} ; EVL ^{+/+}	12	8
Mena ^{+/+} ; VASP ^{+/+} ; EVL ^{+/-}	23	16
Mena ^{+/+} ; VASP ^{+/-} ; EVL ^{+/+}	23	16
Mena ^{+/-} ; VASP ^{+/+} ; EVL ^{+/+}	24	16
Mena ^{+/+} ; VASP ^{+/-} ; EVL ^{+/-}	57	31
Mena ^{+/-} ; VASP ^{+/+} ; EVL ^{+/-}	58	31
Mena ^{+/-} ; VASP ^{+/-} ; EVL ^{+/+}	33	31
Mena ^{+/-} ; VASP ^{+/-} ; EVL ^{+/-}	77	63
Mena ^{+/+} ; VASP ^{+/+} ; EVL ^{-/-}	12	8
Mena ^{+/+} ; VASP ^{+/-} ; EVL ^{-/-}	21	16
Mena ^{+/-} ; VASP ^{+/+} ; EVL ^{-/-}	21	16
Mena ^{+/-} ; VASP ^{+/-} ; EVL ^{-/-}	44	31
Mena ^{+/+} ; VASP ^{-/-} ; EVL ^{+/+}	13	8
Mena ^{+/+} ; VASP ^{-/-} ; EVL ^{+/-}	19	16
Mena ^{+/-} ; VASP ^{-/-} ; EVL ^{+/+}	9	16
Mena ^{+/-} ; VASP ^{-/-} ; EVL ^{+/-}	21	31
Mena ^{-/-} ; VASP ^{+/+} ; EVL ^{+/+}	3	8
Mena ^{-/-} ; VASP ^{+/+} ; EVL ^{+/-}	9	16
Mena ^{-/-} ; VASP ^{+/-} ; EVL ^{+/+}	10	16
Mena ^{-/-} ; VASP ^{+/-} ; EVL ^{+/-}	2	31
Mena ^{+/+} ; VASP ^{-/-} ; EVL ^{-/-}	5	8
Mena ^{+/-} ; VASP ^{-/-} ; EVL ^{-/-}	5	16
Mena ^{-/-} ; VASP ^{+/+} ; EVL ^{-/-}	0	8
Mena ^{-/-} ; VASP ^{+/-} ; EVL ^{-/-}	0	16
Mena ^{-/-} ; VASP ^{-/-} ; EVL ^{+/+}	1	8
Mena ^{-/-} ; VASP ^{-/-} ; EVL ^{+/-}	0	16
Mena ^{-/-} ; VASP ^{-/-} ; EVL ^{-/-}	0	8
	502	

Table 2. Results from triple Ena/VASP mutant crosses. Mice heterozygous for Mena, VASP and EVL (Mena^{+/+}; VASP^{+/+}; EVL^{+/+}) were crossed to each other and the genotypes of the viable adult progeny counted. No adult triple homozygous mutants (Mena^{-/-}; VASP^{-/-}; EVL^{-/-}) were observed, as expected. However, roughly one third of the expected Mena^{+/+}; VASP^{+/-}; EVL^{-/-} mice were observed, while Mena^{-/-}; VASP^{+/+}; EVL^{+/-} or Mena^{-/-}; VASP^{+/-}; EVL^{+/-} were not.

Chapter 4

As noted above, $Mena^{+/-}; VASP^{+/-}; EVL^{+/-}$ mice did not display any obvious defects. Similarly, $Mena^{+/-}; VASP^{+/-}; EVL^{-/-}$ and $Mena^{+/-}; VASP^{-/-}; EVL^{+/-}$ mice are morphologically normal and fertile. However, roughly 1/3 of viable $Mena^{+/-}; VASP^{-/-}; EVL^{-/-}$ mice exhibit an eye defect not seen in other $Ena/VASP$ mutant combinations (Fig. 2). At one month of age, these mice begin to develop conjunctivitis in typically one, and sometimes both, eyes. Further examination revealed that the eyes are often recessed within the eye sockets. Over time, the irritated eye becomes completely shut and crusted over, and the skin surrounding the eye irritated (possibly from repeated scratching). This phenotype was observed in both males and females, and no other obvious physical or behavioral defect was noted.

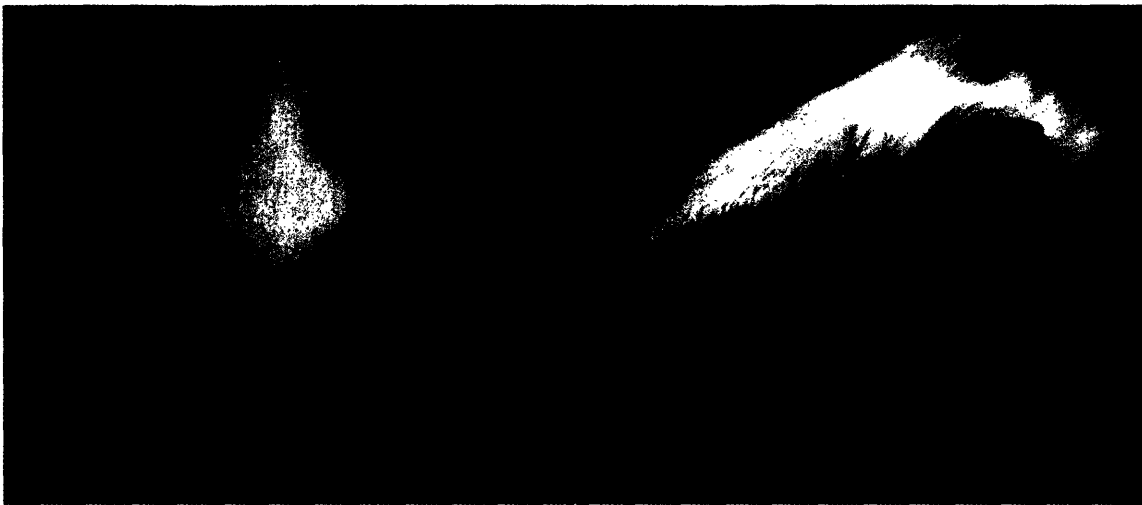


Figure 2. $Mena^{+/-}; VASP^{-/-}; EVL^{-/-}$ display periorbital abnormalities. A large percentage of $Mena^{+/-}; VASP^{-/-}; EVL^{-/-}$ mice display signs of conjunctivitis around one eye, most often the left, and occasionally in both eyes. The condition typically develops around 4-6 weeks of age and gets progressively worse with time. The pictures are of severely affected 3 month old male.

One other interesting genotype was observed from $Mena^{+/-}; VASP^{+/-}; EVL^{+/-}$ intercrosses. Two $Mena^{+/-}; VASP^{+/-}; EVL^{+/-}$ mice survived to three weeks of age.

Over 30 $Mena^{+/-}; VASP^{+/-}; EVL^{+/-}$ mice were expected from intercrosses, suggesting that most died in utero or perinatally. At roughly 10-14 days of age, both mice became ataxic and lost the ability move their hind limbs. This condition grew worse with time, and eventually animals lost all motor control. One mouse with this behavior died around three weeks of age.

A second mouse displaying this same phenotype was sacrificed and fixed to preserve brain architecture. A gross analysis of the brain

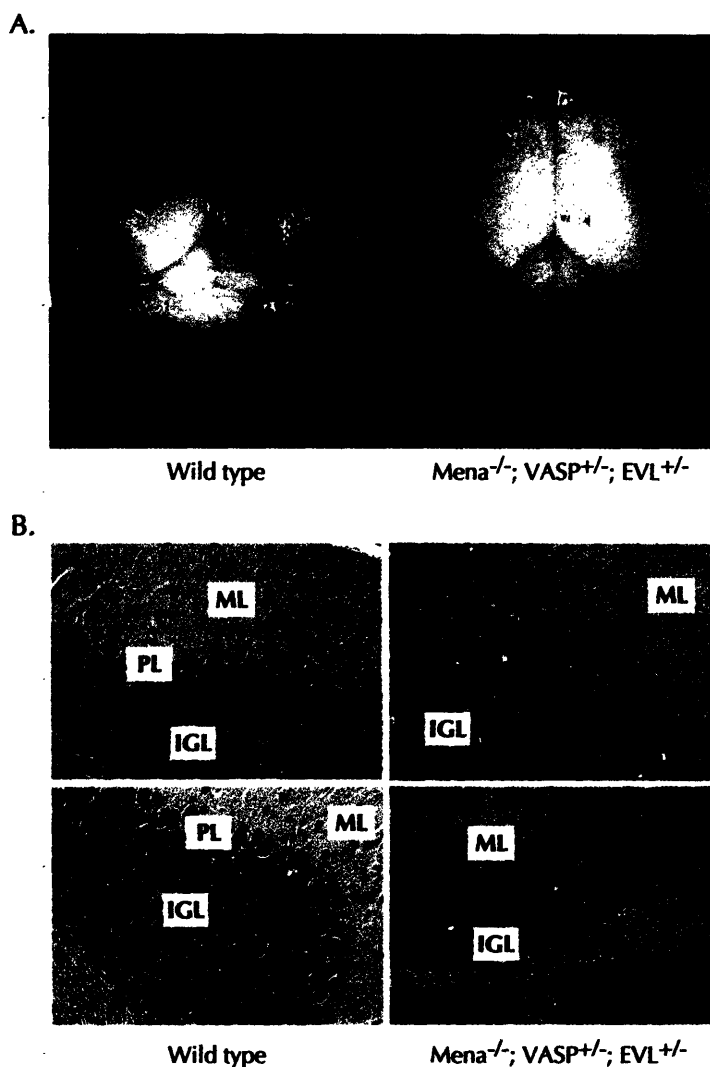


Figure 3. $Mena^{-/-}; VASP^{+/-}; EVL^{+/-}$ mice have cerebellar defects
 A. Brains were fixed and removed from a wild type and $Mena^{-/-}; VASP^{+/-}; EVL^{+/-}$ mouse at three weeks of age. Note the less developed cerebellum (above red arch) and exposed midbrain in the brain collected from the $Mena^{-/-}; VASP^{+/-}; EVL^{+/-}$ mouse.
 B. The fixed brain from the $Mena^{-/-}; VASP^{+/-}; EVL^{+/-}$ mouse shown in A. was sectioned sagittally and H/E stained to examine cerebellar morphology. A number of defects were noted in the Purkinje cell layer (PL), including clustering in regions (see arrows, top right panel) and cells located on the wrong side of the inner granule layer (IGL) (see arrow, bottom right panel). Molecular layer (ML)

revealed that the cerebellum was underdeveloped, leaving part of the midbrain exposed (Fig. 3A). The cerebellum is required for motor coordination, and mouse models with defects in cerebellar development display behavioral phenotypes similar to those observed in our mutant animals (Howell et al., 1997).

Much of cerebellar development occurs postnatally. Shortly after birth, a sheet of Purkinje cells several cells thick disperses outwards from the ventricular zone to form a well-defined monolayer. Granule cells of the external granule layer proliferate and migrate inward across the Purkinje cell monolayer to form the internal granule layer. By 25 days of age, the cerebellum consists of an outer, molecular layer, a Purkinje cell monolayer, an internal granule layer, and a layer of white matter. Histological examination of cerebellar layering revealed numerous gaps in the Purkinje cell layer, and in some instances, Purkinje cells on the wrong side of the internal granular layer (Fig. 3B, bottom right panel). Purkinje cells were also found clustered together in places, apparently having failed to form a monolayer (Fig. 3B, top right panel). There also appears to be an increase in the number of granule cells in the molecular layer as well, a possible consequence of the Purkinje cells failing to form a monolayer.

Mena/EVL-deficient mice die perinatally and display spinal nerve defects

As noted above, Mena^{-/-}; EVL^{-/-} mice were never recovered as adults. To determine how far double mutant animals make it through development, we set up timed pregnancies between Mena^{+/-}; EVL^{+/-} mice and isolated embryos at various

stages of development. At E18.5, $Mena^{+/-}; EVL^{+/-}$ mutants were recovered at the expected Mendelian ratio, suggesting that $Mena^{+/-}; EVL^{+/-}$ embryos survived development but died at birth (data not shown). At E18.5, embryo pups can be removed from the mother and physically stimulated to being respiring. $Mena^{+/-}; EVL^{+/-}$ embryos, though morphologically identical to wild type littermates, appeared to gasp but were unable to inflate their lungs, and died shortly after removal from the uterus (Fig. 4A). Greater than 40% of $Mena^{+/-}; EVL^{+/-}$ embryos displayed a similar phenotype (data not shown). Histological examination of the lungs and diaphragm suggested that both organs were formed properly in the mutant animals (data not shown). In addition, *in vitro* lung explant experiments suggested that lung bronchial branch development was not affected in $Mena^{+/-}; EVL^{+/-}$ mice (data not shown).

To look at nervous system development in $Mena^{+/-}; EVL^{+/-}$ embryos, we isolated E10.5 embryos from timed pregnant females and performed whole mount

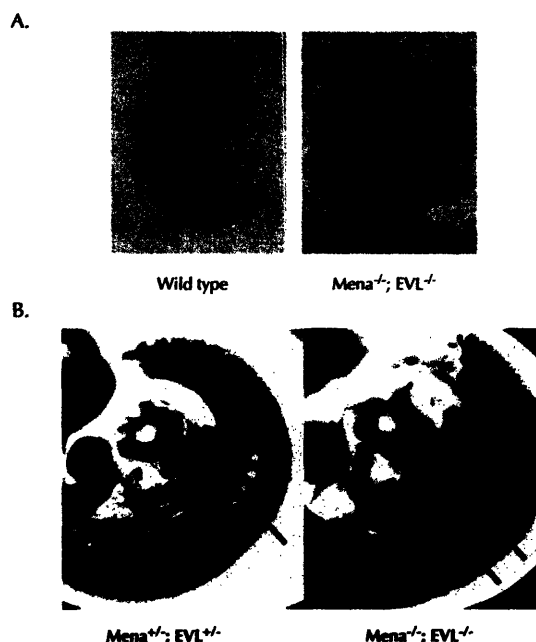


Figure 4. Mice lacking *Mena* and *EVL* die at birth and display defects in spinal nerve formation. A. Timed pregnancies between $Mena^{+/-}; EVL^{+/-}$ mice were set up and embryos collected at E18.5. Mice were stimulated to respiration and observed for 30 minutes. All wild type mice began to breathe and turned pink within 15 minutes. However, despite appearing normal, all $Mena^{+/-}; EVL^{+/-}$ embryos would never begin to respire, turned cyanotic and died shortly thereafter. B. E10.5 embryos were collected from timed matings between $Mena^{+/-}; EVL^{+/-}$ mice and whole mount neurofilament staining performed to look at nervous system development. Compared to $Mena^{+/-}; EVL^{+/-}$ control littermates, the spinal nerves (red arrows) of $Mena^{+/-}; EVL^{+/-}$ embryos appeared poorly fasciculated and misrouted.

immunohistochemistry with anti-neurofilament antibodies. Axons originating from the dorsal root ganglia (DRG) were misrouted and/or defasciculated in $Mena^{-/-}; EVL^{-/-}$ embryos (Fig. 4B). Axons that extend from the DRG combine with axons from the motor column to form the sensory and motor branches, respectively, of the spinal nerves. This defect is more severe than that noted in the absence of Mena and VASP (Menzies et al., 2004), and is consistent with the observation that Mena and EVL are highly expressed in the DRGs (A. Wehman and F. Gertler, unpublished data). While defects in DRG outgrowth are not expected to produce a breathing defect per se, they may be indicative of a more general defect in axon guidance and pathfinding.

Loss of Mena, VASP and EVL causes defects in sensory nerve formation

We hypothesized that the loss of all Ena/VASP proteins during embryogenesis would result in severe cell migration defects. Timed matings were set up between compound mutants recovered in the $Mena^{+/-}; VASP^{+/-}; EVL^{+/-}$ crosses to increase the odds of recovering triple null embryos. Embryos were examined at E10.5, and the expected number of all genotypic classes were observed, including $Mena^{-/-}; VASP^{-/-}; EVL^{-/-}$ (data not shown). Greater than 50% of $Mena^{-/-}; VASP^{-/-}; EVL^{-/-}$ embryos display neural tube defects, similar to the percentage observed in $Mena^{-/-}; VASP^{-/-}; EVL^{+/+}$ embryos (Menzies et al., 2004). We observed a similar percentage of neural tube defects in $Mena^{-/-}; VASP^{-/-}; EVL^{+/-}$ embryos. These results, and the absence of neural tube defects in either $Mena^{-/-}; EVL^{-/-}$ or $VASP^{-/-}; EVL^{-/-}$ mutant

Chapter 4

embryos, indicates that EVL does not function with Mena or VASP in neurulation. Recovery of the expected number of $Mena^{-/-}$; $VASP^{-/-}$; $EVL^{-/-}$ embryos at this stage suggests that Ena/VASP proteins are not essential for early cell migration events such as gastrulation.

We examined nervous system development in $Mena^{-/-}$; $VASP^{-/-}$; $EVL^{-/-}$ mutant embryos by performing whole mount immunostaining using anti-neurofilament antibody on E10.5 embryos. Compared to littermate controls, all $Mena^{-/-}$; $VASP^{-/-}$; $EVL^{-/-}$ embryos (n=5) exhibited a dramatic defect in spinal nerve formation (Fig. 4, top panels). Spinal nerves appeared underdeveloped, misrouted, or poorly fasciculated. The dorsal root ganglia (DRG) were present, but appeared thin and were poorly organized. These defects are more severe than those noted in $Mena^{-/-}$; $EVL^{-/-}$ embryos (see above), indicating that all three Ena/VASP proteins function in spinal nerve development.

$Mena^{-/-}$; $VASP^{-/-}$; $EVL^{-/-}$ embryos also displayed defects in cranial nerve development, particularly in the trigeminal ganglion or fifth (V) cranial nerve (Fig 4., bottom panels). The trigeminal nerve consists of three branches – the ophthalmic, maxillary, and mandibular nerves, that innervate the skin of the face. The ophthalmic and maxillary branches are comprised solely of sensory nerves, while the mandibular branch contains both sensory and motor nerves. The trigeminal ganglion, therefore, is a mixed nerve and analogous to DRGs. In $Mena^{-/-}$; $VASP^{-/-}$; $EVL^{-/-}$ embryos, the trigeminal ganglion was present but poorly structured. Outgrowth of the maxillary and mandibular branches was stunted, and there was

Chapter 4

little or no evidence of ophthalmic branch extension (Fig. 4, bottom right panel). These results, when combined with the defects in DRG formation, indicate that Ena/VASP proteins play a prominent role in the outgrowth and/or guidance of



Figure 4. Loss of Ena/VASP proteins produces severe defects in sensory nerve formation and outgrowth. E10.5 embryos were collected from timed matings between *Mena*^{+/-}; *VASP*^{+/-}; *EVL*^{-/-} males and *Mena*^{+/-}; *VASP*^{+/-}; *EVL*^{-/-} or *Mena*^{+/-}; *VASP*^{+/-}; *EVL*^{+/-} females. Whole mount immunostaining with anti-neurofilament antibody was performed to visualize the developing nervous system. Triple null embryos show severe defects in spinal nerve formation (black arrows, middle panels) and trigeminal ganglia development (bottom panels). The three branches of the trigeminal ganglia are labeled: ophthalmic (op), maxillary (mx), and mandibular (md). Note the lack of outgrowth of all three nerves, particularly the op, in the triple null embryo.

spinal nerves.

Loss of Mena, EVL and VASP causes cardiovascular defects

To determine how late in development $Mena^{-/-}$; $VASP^{-/-}$; $EVL^{-/-}$ embryos survived we collected embryos at E14.5 and E18.5 from timed matings (Table 4). Though less than the expected number of $Mena^{-/-}$; $VASP^{-/-}$; $EVL^{-/-}$ were observed at both E14.5 and E18.5, approximately 70% of $Mena^{-/-}$; $VASP^{-/-}$; $EVL^{-/-}$ embryos survive embryogenesis. At E14.5, we observed several cases of hydrops fetalis, or embryonic edema, in $Mena^{-/-}$; $VASP^{-/-}$; $EVL^{-/-}$ embryos, in addition to the expected incidence of exencephaly (data not shown).

Genotype	E14.5		E18.5	
	# Obs	# Exp	# Obs	# Exp
$Mena^{+/+}$; $VASP^{+/+}$; $EVL^{-/-}$	7	7	6	6
$Mena^{+/-}$; $VASP^{+/-}$; $EVL^{-/-}$	17	15	9	11
$Mena^{+/+}$; $VASP^{+/+}$; $EVL^{+/+}$	5	6	9	6
$Mena^{+/+}$; $VASP^{-/-}$; $EVL^{+/-}$	9	12	9	12
$Mena^{+/+}$; $VASP^{-/-}$; $EVL^{-/-}$	9	15	19	14
$Mena^{+/-}$; $VASP^{-/-}$; $EVL^{-/-}$	36	30	28	28
$Mena^{-/-}$; $VASP^{+/+}$; $EVL^{-/-}$	11	7	8	6
$Mena^{-/-}$; $VASP^{-/-}$; $EVL^{+/-}$	9	6	4	6
$Mena^{-/-}$; $VASP^{-/-}$; $EVL^{-/-}$	11	15	10	14

Table 3. Results from triple Ena/VASP mutant embryo collections. Embryos were collected at E14.5 and E18.5 from timed matings between $Mena^{+/+}$; $VASP^{+/+}$; $EVL^{-/-}$ males and $Mena^{+/-}$; $VASP^{+/-}$; $EVL^{-/-}$ or $Mena^{+/-}$; $VASP^{-/-}$; $EVL^{+/-}$ females. # Obs = number observed; # Exp = number expected.

Chapter 4

At E18.5, we observed that the amniotic sack of greater than 50% of $Mena^{-/-}$; $VASP^{-/-}$; $EVL^{-/-}$ embryos was distended and filled with blood (Fig. 5A). Upon dissection, these embryos, though developed and often possessing a beating heart, appeared pale and bloodless. Similar to E14.5, we noted a high incidence of exencephaly (approximately 70%); however, the presence of blood in the amniotic fluid and exencephaly were not linked as we observed non-exencephalic hemorrhaging embryos.

Histological examination of E18.5 $Mena^{-/-}$; $VASP^{-/-}$; $EVL^{-/-}$ mutant embryos revealed massive subdermal edema (Fig. 5B), consistent with the hydroptic skin observed at E14.5. In addition, there was evidence of distension of subdermal peripheral veins and hepatic central veins (data not shown). This spectrum of defects are frequently associated with right-sided heart failure. In right-sided heart failure, disruption of normal heart function in the right ventricle results in an increase in venous pressure, causing both venous distension and edema. Preliminary histological examination of hearts in $Mena^{-/-}$; $VASP^{-/-}$; $EVL^{-/-}$ mice revealed that the heart was morphologically normal with no evidence of myocyte disorganization, anatomic defect, or dilation (data not shown). Further analysis will be necessary to determine if the heart in triple mutant embryos forms and/or functions properly.

The source of blood found in the amnion of some triple mutant embryos is also unknown. We see no evidence of umbilical rupture, and there is little or no

evidence of hemorrhage in the embryo. Intraamniotic hemorrhage has only been observed in late stage embryos (E17.5 and E18.5), suggesting that a catastrophic event during the last stages of embryogenesis causes this phenotype.

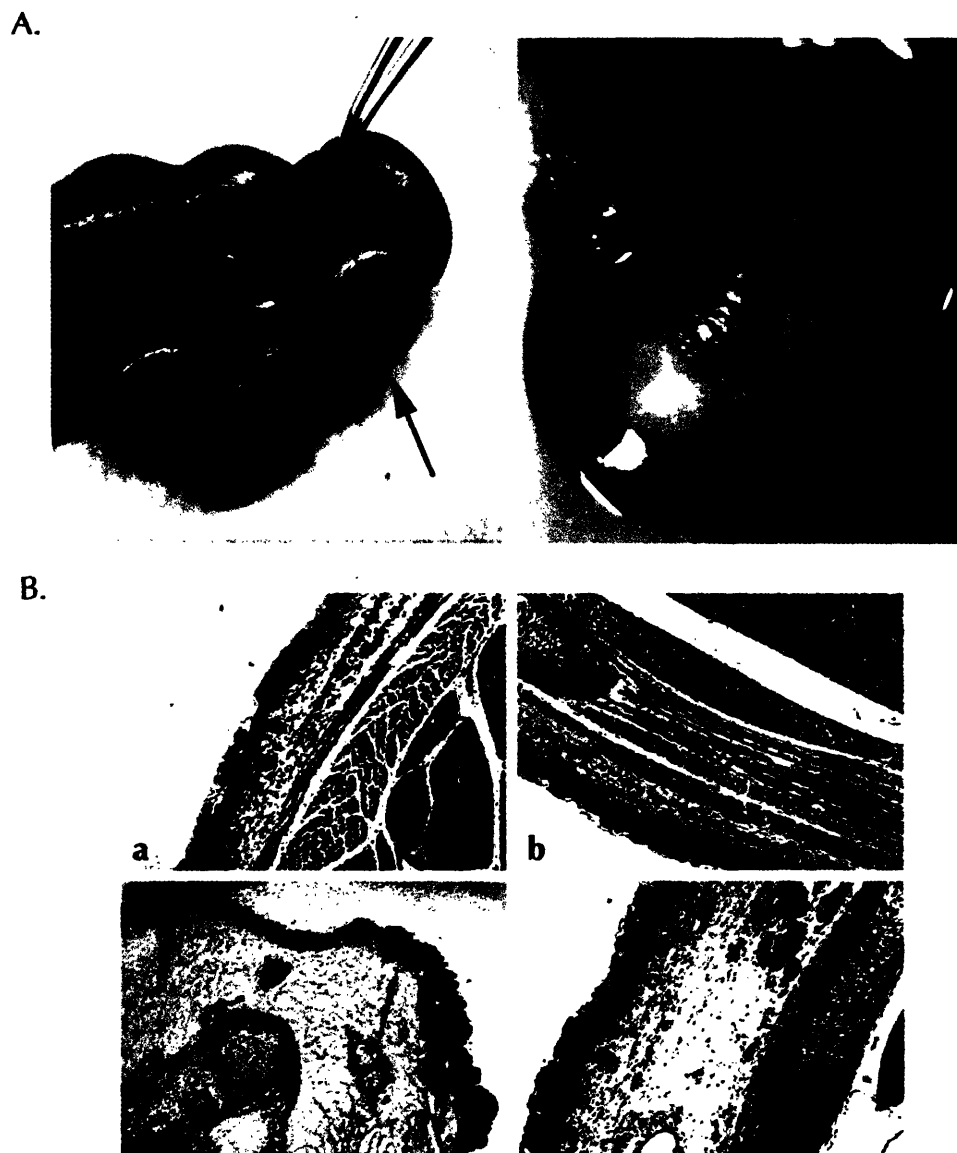


Figure 5. Intraamniotic bleeding and edema in triple mutant embryos. A. Approximately 70% of $Mena^{-/-}; VASP^{-/-}; EVL^{-/-}$ E18.5 embryos are found in blood-filled amniotic sacks upon dissection. The source of the blood is unknown. B. Histological examination of $Mena^{-/-}; VASP^{-/-}; EVL^{-/-}$ embryos (bottom panels, c(4x) & d(10x)) revealed massive subdermal edema compared to control ($Mena^{+/+}; VASP^{-/-}; EVL^{-/-}$) littermates (top panels, a(4x) & d(10x)). Sections are from the trunk region of the embryo and stained with H/E.

Loss of Ena/VASP proteins affects brain development

Though nearly 70% of $Mena^{-/-}$; $VASP^{-/-}$; $EVL^{-/-}$ embryos at E18.5 were exencephalic, remaining triple mutants developed a normal head. Histological examination of $Mena^{-/-}$; $VASP^{-/-}$; $EVL^{-/-}$ mutant forebrains revealed striking abnormalities in cellular organization and architecture (Fig. 6). Compared to control ($Mena^{+/+}$; $VASP^{-/-}$; $EVL^{-/-}$) littermates (Fig. 6, A & C), the cellularity and organization of the ventricular and intermediate zones of the cortex was defective in triple mutant embryos (Fig. 6, B & D). In addition, ventricles within the brain were enlarged, and the hippocampus appeared poorly developed.

Commissure formation was not investigated; however, based on defects observed in $Mena^{-/-}$ and $Mena^{-/-}$; $VASP^{-/-}$ animals, we expect that many midline structures will be disrupted in $Mena^{-/-}$; $VASP^{-/-}$; $EVL^{-/-}$ mutants.

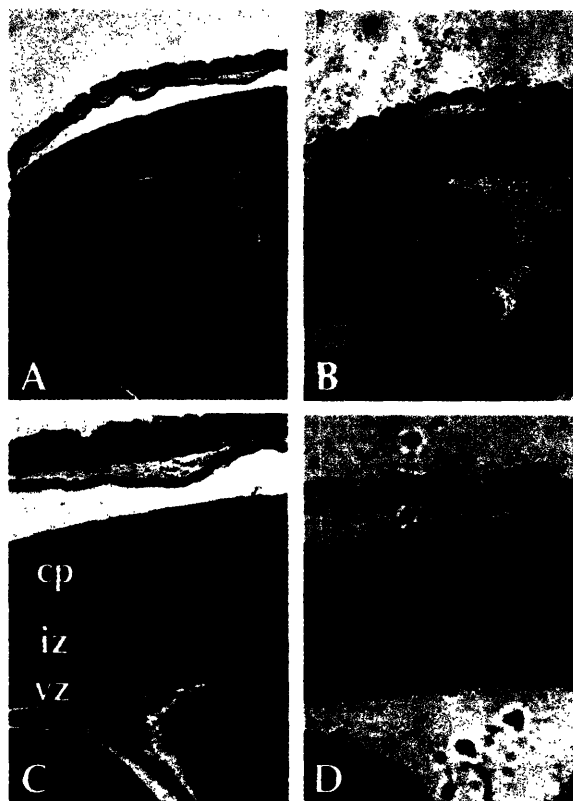


Figure 6. Loss of Ena/VASP proteins affects brain development. Coronal sections from the heads of a non-exencephalic $Mena^{-/-}$; $VASP^{-/-}$; $EVL^{-/-}$ E18.5 embryo (panels B(4x) & D(10x)) and control ($Mena^{+/+}$; $VASP^{-/-}$; $EVL^{-/-}$) littermate (panels A(4x) & C(10x)). Sections through the forebrain region are shown. Note the disorganization in the ventricular zone (vz) and intermediate zone (iz) of the cortex in the $Mena^{-/-}$; $VASP^{-/-}$; $EVL^{-/-}$ brain (panels B & D). cortical plate (cp).

Discussion

Ena/VASP function is required for a number of migration events during development. Mena, VASP and EVL cooperate to promote cranial and spinal nerve formation, cortical layering and cerebellar development. Ena/VASP proteins are also required for cardiovascular development. Loss of Mena, VASP and EVL causes massive edema and veinous extension, suggestive of a defect in endothelial function and/or heart function. However, many migration events during embryogenesis do not require Ena/VASP proteins, suggesting that the family of proteins has evolved to mediate specific actin-dependent processes.

The role of EVL

Mice lacking EVL were found to be viable and morphologically normal, and no obvious defect was observed in nervous or immune system development. This result is not surprising given the relatively subtle phenotypes of the other Ena/VASP single mutants, overlapping patterns of Mena/VASP/EVL expression, and the knowledge that Ena/VASP proteins can function interchangeably. While it is possible that continued analysis of the single knockout would have revealed a phenotype unique to EVL, we concentrated our efforts on the analysis of compound mutants.

Ena/VASP proteins function in axon guidance

A role for Ena/VASP proteins in axon guidance is well established. The invertebrate Ena/VASP orthologs, *Drosophila* Ena and *C. elegans* Unc-34, are known to function downstream of axon guidance receptor pathways (Bashaw et al., 2000; Chang et al., 2004; Gitai et al., 2003; Wills et al., 1999; Withee et al., 2004; Yu et al., 2002). In mice, loss of Mena causes defects in the formation of the hippocampal commissure, corpus callosum and optic chiasm (Lanier et al., 1999; Menzies et al., 2004). Deletion of both Mena and VASP blocks formation of the four major forebrain commissures. As demonstrated in this study, the loss of all three Ena/VASP proteins produces even more severe axon outgrowth and guidance defects.

Analysis of neural development in *Mena*^{-/-}; *VASP*^{-/-}; *EVL*^{-/-} embryos at E10.5 revealed a requirement for Ena/VASP proteins in spinal and cranial nerve development. A less penetrant and less severe spinal nerve defect was observed in both *Mena*^{-/-}; *VASP*^{-/-} and *Mena*^{-/-}; *EVL*^{-/-} (this study) mutant embryos, but no defect was noted in cranial ganglia development in either double mutant. This suggests that Mena, VASP and EVL function interchangeably in spinal nerve and cranial nerve development.

The major defects in spinal nerve formation in *Mena*^{-/-}; *VASP*^{-/-}; *EVL*^{-/-} embryos appeared to result from either the failed extension or misrouting of sensory axons originating from the DRGs. Likewise, defects in cranial nerve formation in *Mena*^{-/-}; *VASP*^{-/-}; *EVL*^{-/-} embryos were most apparent in the ophthalmic and

Chapter 4

maxillary nerves, that are pure sensory nerves. The guidance cues that direct sensory neurons to their targets remain largely unknown. Semaphorin III/D functions to repel DRG axons *in vitro*, and mice lacking semaphorin III/D display abnormalities in trigeminal and spinal nerve formation (Messersmith et al., 1995; Taniguchi et al., 1997). However, there is little biochemical or cell biological evidence to link Ena/VASP proteins to semaphorin signaling. Interestingly, a fragment of Slit was found to promote axon outgrowth from dorsal root ganglia (Nguyen Ba-Charvet et al., 2001). Ena/VASP proteins are known to function downstream of Robo, the axon guidance receptor that binds Slit (Bashaw et al., 2000; Yu et al., 2002). Future experiments will be required to determine if the defect in sensory axon outgrowth is due to lack of response to attractive and/or repulsive cues.

Blocking Ena/VASP function in hippocampal neurons inhibits filopodia formation and outgrowth (Lebrand et al., 2004). Filopodia formation is thought to be critical for sensing guidance cues and promoting growth cone motility. The defects in axon outgrowth and pathfinding could reflect requirements in these axons for Ena/VASP-dependent filopodia for guidance. Interestingly, many nerve tracts appear to have formed properly in triple mutant embryos. There are two possibilities that might explain this. The first is that filopodia formation is accomplished by another protein or proteins, such as formins. The second is filopodia formation is not required for the guidance of some axons. Further

Chapter 4

analysis of neurons from Ena/VASP dependent and independent fiber tracts will address this issue.

The periorbital defect observed in $Mena^{+/-}; VASP^{+/-}; EVL^{-/-}$ might also reflect a requirement for Ena/VASP proteins in nervous system development. A similar phenotype was observed in mice lacking neurturin (NTN), a neurotrophic factor (Heuckeroth et al., 1999). $NTN^{-/-}$ mice display periorbital abnormalities by 2 months of age, including droopy eyelids, increased eyelid thickness, and crusty drainage surrounding the eye. In addition, the eyeballs of $NTN^{-/-}$ do not protrude from the orbit, though the size of the eyeball is normal. Staining of the lacrimal gland from $NTN^{-/-}$ mice revealed an absence of parasympathetic nerve fibers, suggesting that reduced tear production from deficient lacrimal gland innervation is the cause of eye problems in $NTN^{-/-}$ mice (Heuckeroth et al., 1999). Given the similarity in phenotypes, we speculate that the eye problems in $Mena^{+/-}; VASP^{+/-}; EVL^{-/-}$ mice result from an innervation defect of the lacrimal gland. Alternatively, conjunctivitis could be caused by an infection that mutant animals are unable to fight due to a poorly developed or functioning immune system, or from an autoimmune disorder that affects lacrimal glands, such as Sjogren's syndrome. These possibilities are currently being explored.

Ena/VASP proteins are required for brain development

Defects in brain development were observed among Ena/VASP mutants. Two viable $Mena^{+/-}; VASP^{+/-}; EVL^{+/-}$ mutant mice were observed, and both were

ataxic. Analysis of brain morphology indicated that the cerebellum was poorly formed in one mutant animal, and further histological examination revealed defects in the Purkinje cell layer. Purkinje cells migrate outward radially from the cerebellar cortex to form the Purkinje cell monolayer. Proper formation of the Purkinje cell layer is thought to be critical for granule cell migration and proper cerebellar development (Goffinet, 1984; Goldowitz and Hamre, 1998), and we postulate that the ataxic phenotypes observed in $Mena^{-/-}$; $VASP^{+/-}$; $EVL^{+/-}$ mutant mice arise from defects in Purkinje cell migration. A possible defect in granule cell migration was also noted, and might either suggest a requirement for Ena/VASP function in granule cell migration or a secondary effect due to defects in Purkinje layer formation. This is the first description of Ena/VASP proteins functioning in cerebellar development.

Abnormalities were also noted in the brains of non-exencephalic E18.5 $Mena^{-/-}$; $VASP^{+/-}$; $EVL^{+/-}$ mutant embryos. The most striking of these was the disruption in the cellular organization of the cortex. Cortical neurons born in the ventricular zone migrate outward radially through the intermediate zone to form the outer layers of the cortex. Later born neurons migrate past layers established by earlier neurons, creating a cortex that is formed "inside-out": deeper layers are older than more superficial layers. In the cortex of triple mutant embryos, the ventricular zone appears thicker while the intermediate zone appears thinner and contains less cells, and the boundary between the two zones is not well defined. An earlier study showed that inhibition of Ena/VASP activity in cortical neurons led

to aberrant placement within the cortical layers (Goh et al., 2002). The observed phenotypes are consistent with that study, and provide further evidence for the role of Ena/VASP proteins in neuronal layering in the cortex.

Ena/VASP proteins in cardiovascular development

The edema and intraamniotic hemorrhaging observed at later stages of development in *Mena*^{-/-}; *VASP*^{-/-}; *EVL*^{-/-} embryos are defects never observed in any double mutant combination, suggesting a requirement for all three Ena/VASP proteins. The exact cause of the edema and intraamniotic hemorrhage are unknown, but given current *in vitro* and *in vivo* evidence for Ena/VASP function, we postulate the defects might arise from problems in endothelial barrier function and/or heart formation and function.

Endothelial function

Endothelial cells form a barrier between blood and surrounding tissues that functions to regulate the movement of fluids, macromolecules and leukocytes. Disruption of this barrier can contribute to pathological conditions such as vascular leakage and edema. The massive subdermal edema observed in *Mena*^{-/-}; *VASP*^{-/-}; *EVL*^{-/-} mutant embryos could arise from a loss of barrier function. Ena/VASP proteins have been implicated in PKA-induced endothelial junction permeability *in vitro* (Comerford et al., 2002), and involves their potential role in cell-cell adhesion.

Chapter 4

Endothelial cells form two types of cell-cell connections, adherens junctions and tight junctions, that are both linked to the actin cytoskeleton. Adherens junctions are cadherin-dependent connections linked to the cytoskeleton through catenins. Tight junctions are cadherin-independent connections and are associated with the cytoskeleton through zona occludins (ZO) proteins. The integrity of both junctions correlates with endothelial permeability. Molecular agents known to affect endothelial barrier function are thought to function through signaling pathways that control junction assembly and disassembly. Rho family GTPases regulate endothelial barrier function, as do PKA and PKG (Wojciak-Stothard and Ridley, 2002).

Cyclic nucleotide elevation, and subsequent activation of PKA and PKG, in endothelial cells increases barrier function. It was reported that one target of PKA phosphorylation in endothelial cells is VASP. VASP co-immunoprecipitated with ZO-1, and was found to colocalize with ZO-1 at tight junctions. In addition, PKA activation induced phospho-VASP localization to cell-cell junctions. Finally, expression of VASP EVH2 domain mutants affected endothelial permeability, suggesting that VASP plays a role in barrier function (Comerford et al., 2002). The loss of Ena/VASP proteins in mutant endothelial cells could affect either tight junction or adherens junction formation, which in turn would affect barrier permeability. Further experiments will be necessary to determine if the endothelium is formed or functions properly in *Mena^{+/-}*; *VASP^{+/-}*; *EVL^{+/-}* embryos.

Defect in heart formation/function

Proper heart formation and function is essential for viability during the later stages of embryogenesis. The pronounced venous distension and edema we observed in the $Mena^{-/-}$; $VASP^{-/-}$; $EVL^{-/-}$ mutant embryos could be explained by a heart defect. We have observed a beating heart in many $Mena^{-/-}$; $VASP^{-/-}$; $EVL^{-/-}$ mutant embryos at E18.5, suggesting the heart is still functioning. Furthermore, initial histological examination of the hearts from $Mena^{-/-}$; $VASP^{-/-}$; $EVL^{-/-}$ mutant embryos suggested the heart was morphologically normal. However, a more complete histological analysis will be necessary to determine if the heart has formed normally.

A role for Ena/VASP proteins in heart function has been reported (Egenthaler et al., 2003). Transgenic mice expressing the EVH1 domain of VASP in cardiac myocytes developed dilated cardiomyopathy with myocyte hypertrophy and bradycardia, and died from early heart failure (Egenthaler et al., 2003). However, the cardiovascular phenotypes observed in Ena/VASP-deficient embryos differ from those observed in the transgenic mouse. We did not observe any signs of dilated cardiomyopathy or hypertrophy in the hearts of $Mena^{-/-}$; $VASP^{-/-}$; $EVL^{-/-}$ mutants. Furthermore, these defects are not expected to produce the pronounced edema we observe in $Mena^{-/-}$; $VASP^{-/-}$; $EVL^{-/-}$ embryos. The defects in heart function in the transgenic mice could be caused by non-specific effects from overexpression of the VASP EVH1 domain.

Ena/VASP-independent functions during embryogenesis

One surprising result from the analysis of $Mena^{-/-}$; $VASP^{-/-}$; $EVL^{-/-}$ mutant embryos was the number of cell migration events that can occur independent of Ena/VASP proteins. While further examination of mutant embryos may reveal additional processes that require Ena/VASP proteins, it is clear that early migration events such as gastrulation can occur without Ena/VASP proteins.

Expression of a C-terminal fragment of VASP containing the coiled-coil region in cultured keratinocytes blocked adherens junction formation, and expression of the same construct in the epidermis of a transgenic mouse disrupted cell-cell adhesions and caused blisters (Vasioukhin et al., 2000). These results suggested that Ena/VASP proteins play an important role in adherens junction formation and skin development. However, we did not observe a skin defect in $Mena^{-/-}$; $VASP^{-/-}$; $EVL^{-/-}$ mutant embryos, and saw no evidence of the sort of defects predicted from this transgenic mouse. Similar to the EVH1 transgenic mouse discussed above, there is no data to indicate that this approach specifically blocks Ena/VASP function. While there is evidence for Ena/VASP function in the formation and regulation of adherens junctions, our genetic analysis demonstrated that Ena/VASP proteins are not required for skin formation or for the formation of epithelial junctions.

Materials and Methods

Generation of EVL knockout mouse

A BAC mouse genomic DNA clone was obtained from Genome Systems that contained the EVL locus. A standard targeting vector was constructed by subcloning regions surrounding exons two and three of the EVL locus into the vector pPGKneobpAlox2PGKDTA (a gift from Philip Soriano). The final targeting vector contained a neomycin resistance cassette under the control of the PGK promotor flanked by a 1.0 kb genomic DNA fragment upstream of exon 2 and 5.0 kb fragment downstream of exon 3. The targeting vector was electroporated into early passage R1 embryonic stem (ES) cells. Over 1000 G418 resistant ES colonies were picked and screened for homologous recombination by PCR. 5 clones were identified, and homologous recombination reconfirmed in these clones by Southern blot. All 5 clones were injected into blastocysts to generate chimeric mice. 4 of the 5 clones produced high percentage chimeras, but subsequent breeding revealed that only one clone went germline. This clone was used to establish the EVL knockout line used in this study.

Embryonic stem cell culture

R1 ES cells were cultured in DME (Specialized Media) plus 15% ES cell tested fetal calf serum (HyClone) and supplemented with L-Glutamine (Specialized Media), Penicillin/Streptomycin (Specialized Media), β -mercaptoethanol (Specialized Media) and LIF-conditioned media. When necessary, G418 was

Chapter 4

added to final concentration of 300 µg/ml. R1 cells were cultured on a monolayer of irradiated primary mouse embryonic fibroblasts (MEFs). Primary MEFs were made from E14.5 embryos isolated from timed pregnant females, expanded, and used at passage two or three. MEFs were cultured in DME (Specialized Media) plus 10% fetal calf serum (Hyclone).

Mouse colony

Chimeric mice were originally crossed to C57/B6 to determine if the clone had gone germline based on coat color. Progeny from these crosses were then backcrossed into the inbred lines 129/Sv, C57/B6, and Balb/c. All inbred lines were obtained from Taconic. Initial experiments were conducted with mutant mice on a mixed background. Later experiments used mice that had been backcrossed at least 4 times into a given inbred line.

Small (less than 1 cm) pieces of tail were cut from P10 mice for genotyping purposes. Genomic DNA was prepared from these tail samples and used for PCR. For earlier stage embryos (E8.5 to 11.5), genomic DNA was prepared from yolk sacks. Tails were taken from later stage (E12.5-E18.5) embryos.

For timed pregnancies, mating pairs were set up in the evening and checked for vaginal plugs the following morning. Plugged females were removed from the mating pair and sacrificed at the appropriate time. The day of the plug was deemed embryonic stage E0.5.

Whole mount neurofilament staining

Embryos were collected at E10.5 from timed pregnant females. Yolk sacks were taken for genotyping purposes, and embryos fixed in 80% MeOH, 20% DMSO at 4°C overnight. The following day, embryos were bleached in 60% MeOH, 20% DMSO, and 20% H₂O₂ at room temperature for 6 hours, washed in MeOH and then stored in MeOH at -20°C until staining. For staining, embryos were rehydrated by washing in a series of MeOH in PBS dilutions. After rehydration, embryos were blocked overnight at 4°C in PBS + 0.5% Triton X-100 + 2% nonfat dry milk + 3% normal donkey serum. The following day, anti-neurofilament monoclonal antibody H3 (Developmental Hybridomas) was added at 1:200 and incubated overnight at 4°C. Post-primary antibody washes were performed using PBS + 0.5% Triton X-100 + 2% nonfat dry milk. Embryos were washed at least 6 times for one hour. Embryos were then incubated with preabsorbed donkey anti-mouse antibody conjugated to horseradish peroxidase overnight at 4°C. Embryos were washed extensively before labeling with diaminobenzidine (DAB) plus NiCl₂. After staining, embryos were dehydrated in EtOH and either stored at -20°C or imaged after being cleared in methyl salicylate.

Histology

Tissues for histology were fixed in either 10% formalin or Bouin's fixative (Electron Microscopy Sciences). Tissues were embedded in paraffin, sectioned, and stained with hematoxylin and eosin (H/E) using standard techniques. Bright

Chapter 4

field images were taken on an inverted microscope using Nomarski optics and recorded with a CCD camera.

References

- Aszodi, A., Pfeifer, A., Ahmad, M., Glauner, M., Zhou, X. H., Ny, L., Andersson, K. E., Kehrel, B., Offermanns, S., and Fassler, R. (1999). The vasodilator-stimulated phosphoprotein (VASP) is involved in cGMP- and cAMP-mediated inhibition of agonist-induced platelet aggregation, but is dispensable for smooth muscle function. *Embo J* 18, 37-48.
- Bashaw, G. J., Kidd, T., Murray, D., Pawson, T., and Goodman, C. S. (2000). Repulsive axon guidance: Abelson and Enabled play opposing roles downstream of the roundabout receptor. *Cell* 101, 703-715.
- Chang, C., Yu, T. W., Bargmann, C. I., and Tessier-Lavigne, M. (2004). Inhibition of netrin-mediated axon attraction by a receptor protein tyrosine phosphatase. *Science* 305, 103-106.
- Comerford, K. M., Lawrence, D. W., Synnestvedt, K., Levi, B. P., and Colgan, S. P. (2002). Role of vasodilator-stimulated phosphoprotein in PKA-induced changes in endothelial junctional permeability. *Faseb J* 16, 583-585.
- Coppolino, M. G., Krause, M., Hagendorff, P., Monner, D. A., Trimble, W., Grinstein, S., Wehland, J., and Sechi, A. S. (2001). Evidence for a molecular complex consisting of Fyb/SLAP, SLP-76, Nck, VASP and WASP that links the actin cytoskeleton to Fcγ receptor signalling during phagocytosis. *J Cell Sci* 114, 4307-4318.
- Egenthaler, M., Engelhardt, S., Schinke, B., Kobsar, A., Schmitteckert, E., Gambaryan, S., Engelhardt, C. M., Krenn, V., Eliava, M., Jarchau, T., et al. (2003). Disruption of cardiac Ena-VASP protein localization in intercalated disks causes dilated cardiomyopathy. *Am J Physiol Heart Circ Physiol* 285, H2471-2481.
- Gitai, Z., Yu, T. W., Lundquist, E. A., Tessier-Lavigne, M., and Bargmann, C. I. (2003). The netrin receptor UNC-40/DCC stimulates axon attraction and outgrowth through enabled and, in parallel, Rac and UNC-115/AbLIM. *Neuron* 37, 53-65.
- Goffinet, A. M. (1984). Events governing organization of postmigratory neurons: studies on brain development in normal and reeler mice. *Brain Res* 319, 261-296.
- Goh, K. L., Cai, L., Cepko, C. L., and Gertler, F. B. (2002). Ena/VASP proteins regulate cortical neuronal positioning. *Curr Biol* 12, 565-569.
- Goldowitz, D., and Hamre, K. (1998). The cells and molecules that make a cerebellum. *Trends Neurosci* 21, 375-382.

Chapter 4

Grevengoed, E. E., Loureiro, J. J., Jesse, T. L., and Peifer, M. (2001). Abelson kinase regulates epithelial morphogenesis in *Drosophila*. *J Cell Biol* 155, 1185-1198.

Heuckeroth, R. O., Enomoto, H., Grider, J. R., Golden, J. P., Hanke, J. A., Jackman, A., Molliver, D. C., Bardgett, M. E., Snider, W. D., Johnson, E. M., Jr., and Milbrandt, J. (1999). Gene targeting reveals a critical role for neurturin in the development and maintenance of enteric, sensory, and parasympathetic neurons. *Neuron* 22, 253-263.

Howell, B. W., Hawkes, R., Soriano, P., and Cooper, J. A. (1997). Neuronal position in the developing brain is regulated by mouse disabled-1. *Nature* 389, 733-737.

Krause, M., Sechi, A. S., Konradt, M., Monner, D., Gertler, F. B., and Wehland, J. (2000). Fyn-binding protein (Fyb)/SLP-76-associated protein (SLAP), Ena/vasodilator-stimulated phosphoprotein (VASP) proteins and the Arp2/3 complex link T cell receptor (TCR) signaling to the actin cytoskeleton. *J Cell Biol* 149, 181-194.

Lambrechts, A., Kwiatkowski, A. V., Lanier, L. M., Bear, J. E., Vandekerckhove, J., Ampe, C., and Gertler, F. B. (2000). cAMP-dependent protein kinase phosphorylation of EVL, a Mena/VASP relative, regulates its interaction with actin and SH3 domains. *J Biol Chem* 275, 36143-36151.

Lanier, L. M., Gates, M. A., Witke, W., Menzies, A. S., Wehman, A. M., Macklis, J. D., Kwiatkowski, D., Soriano, P., and Gertler, F. B. (1999). Mena is required for neurulation and commissure formation. *Neuron* 22, 313-325.

Lebrand, C., Dent, E. W., Strasser, G. A., Lanier, L. M., Krause, M., Svitkina, T. M., Borisy, G. G., and Gertler, F. B. (2004). Critical role of Ena/VASP proteins for filopodia formation in neurons and in function downstream of netrin-1. *Neuron* 42, 37-49.

Loureiro, J. J., Rubinson, D. A., Bear, J. E., Baltus, G. A., Kwiatkowski, A. V., and Gertler, F. B. (2002). Critical roles of phosphorylation and actin binding motifs, but not the central proline-rich region, for Ena/vasodilator-stimulated phosphoprotein (VASP) function during cell migration. *Mol Biol Cell* 13, 2533-2546.

Massberg, S., Gruner, S., Konrad, I., Garcia Arguinzonis, M. I., Eigenthaler, M., Hemler, K., Kersting, J., Schulz, C., Muller, I., Besta, F., *et al.* (2004). Enhanced in vivo platelet adhesion in vasodilator-stimulated phosphoprotein (VASP)-deficient mice. *Blood* 103, 136-142.

Menzies, A. S., Aszodi, A., Williams, S. E., Pfeifer, A., Wehman, A. M., Goh, K. L., Mason, C. A., Fassler, R., and Gertler, F. B. (2004). Mena and vasodilator-

Chapter 4

stimulated phosphoprotein are required for multiple actin-dependent processes that shape the vertebrate nervous system. *J Neurosci* 24, 8029-8038.

Messersmith, E. K., Leonardo, E. D., Shatz, C. J., Tessier-Lavigne, M., Goodman, C. S., and Kolodkin, A. L. (1995). Semaphorin III can function as a selective chemorepellent to pattern sensory projections in the spinal cord. *Neuron* 14, 949-959.

Nguyen Ba-Charvet, K. T., Brose, K., Ma, L., Wang, K. H., Marillat, V., Sotelo, C., Tessier-Lavigne, M., and Chedotal, A. (2001). Diversity and specificity of actions of Slit2 proteolytic fragments in axon guidance. *J Neurosci* 21, 4281-4289.

Snapper, S. B., Takeshima, F., Anton, I., Liu, C. H., Thomas, S. M., Nguyen, D., Dudley, D., Fraser, H., Purich, D., Lopez-Illasaca, M., *et al.* (2001). N-WASP deficiency reveals distinct pathways for cell surface projections and microbial actin-based motility. *Nat Cell Biol* 3, 897-904.

Taniguchi, M., Yuasa, S., Fujisawa, H., Naruse, I., Saga, S., Mishina, M., and Yagi, T. (1997). Disruption of semaphorin III/D gene causes severe abnormality in peripheral nerve projection. *Neuron* 19, 519-530.

Vasioukhin, V., Bauer, C., Yin, M., and Fuchs, E. (2000). Directed actin polymerization is the driving force for epithelial cell-cell adhesion. *Cell* 100, 209-219.

Wills, Z., Bateman, J., Korey, C. A., Comer, A., and Van Vactor, D. (1999). The tyrosine kinase Abl and its substrate enabled collaborate with the receptor phosphatase Dlar to control motor axon guidance. *Neuron* 22, 301-312.

Withee, J., Galligan, B., Hawkins, N., and Garriga, G. (2004). *Caenorhabditis elegans* WASP and Ena/VASP proteins play compensatory roles in morphogenesis and neuronal cell migration. *Genetics* 167, 1165-1176.

Wojciak-Stothard, B., and Ridley, A. J. (2002). Rho GTPases and the regulation of endothelial permeability. *Vascul Pharmacol* 39, 187-199.

Yamazaki, D., Suetsugu, S., Miki, H., Kataoka, Y., Nishikawa, S., Fujiwara, T., Yoshida, N., and Takenawa, T. (2003). WAVE2 is required for directed cell migration and cardiovascular development. *Nature* 424, 452-456.

Yu, T. W., Hao, J. C., Lim, W., Tessier-Lavigne, M., and Bargmann, C. I. (2002). Shared receptors in axon guidance: SAX-3/Robo signals via UNC-34/Enabled and a Netrin-independent UNC-40/DCC function. *Nat Neurosci* 5, 1147-1154.

Chapter 5

Future Directions

The work presented in this thesis was performed to better understand Ena/VASP function at a molecular level, provide new insight into the signaling pathways and complexes that regulate Ena/VASP proteins, and to understand the role of Ena/VASP proteins in mammalian development. Molecular characterization of EVL revealed alternate spliceforms of the protein and demonstrated that EVL can function similar to VASP and Mena in regulating cell motility. Tuba was identified as a novel Ena/VASP ligand that links dynamin and the actin cytoskeleton to Rho GTPase signaling. A genetic analysis of Ena/VASP proteins revealed requirements for Ena/VASP function in brain development, nerve tract formation, and cardiovascular development. Still, questions remain regarding Ena/VASP function.

EVL and EVL-I

The I exon was discovered in a search for alternate isoforms of EVL. Inclusion of the 21 amino acid I exon in EVL produces the larger, 52 kDa EVL-I protein. The I exon is located in the EVH2 domain, between the conserved F-actin binding region and coiled-coil region that is required for Ena/VASP tetramerization (Bachmann et al., 1999). An exon of the same size and location is also present in the EVH2 domain of Mena.

Chapter 5

The role of the I exon is unknown, but its location may provide a clue. The EVH2 domain is critical for Ena/VASP-dependent regulation of cell motility, which requires the G-actin binding, F-actin binding and coiled-coil regions (Loureiro et al., 2002). However, inclusion of the I exon does not affect EVL localization or function in cell motility, suggesting that it does not disrupt G or F-actin binding or oligomerization, at least in the context of random fibroblast migration. As more is known about the *in vivo* requirements for EVL function, it may be possible to identify specific cellular requirements for EVL-I.

The I exon contains 6 serines that could be phosphorylated by kinases. Mena and VASP contain at least one PKA/PKG phosphorylation site, and phosphorylation is postulated to affect EVH2 activities (Kwiatkowski et al., 2003). EVL lacks any known phosphorylation sites in the EVH2 domain, and inclusion of the I exon could introduce phosphorylation sites. It will be important to determine whether one or more of these sites is phosphorylated and to identify the kinases and signaling pathways that might regulate such phosphorylation. Phosphorylation of the I exon could introduce charges that affect actin binding and potentially regulate EVL anti-capping or bundling activity.

Tuba

Identified in a yeast two-hybrid screen for Ena/VASP ligands, Tuba binds to all Ena/VASP proteins *in vitro*, and is found in complex with Mena *in vivo*. Tuba is a large protein with multiple SH3 domains and a BAR domain, and functions as a

GEF for Cdc42 *in vitro*. The N-terminus binds dynamin, and the C-terminus interacts with numerous actin regulatory proteins in addition to Ena/VASP, including N-WASP, WAVE, PIR121, NAP1, CR16, WIRE, and Lpd. The C-terminus can promote F-actin recruitment in cells, and Tuba localizes to growth factor-induced actin ruffles. These results indicate the Tuba functions to link Ena/VASP proteins and other actin binding proteins to dynamin and Rho GTPase signaling.

The ability of Tuba to bind dynamin and the presence of the BAR domain, as well as its localization to synapses, implicates Tuba in endocytosis and/or vesicle trafficking. Biochemical and genetic results link endocytic proteins to the actin cytoskeleton, but the role actin plays in endocytosis is unclear. Interestingly, activated Cdc42 has been implicated in regulating endocytosis (Garrett et al., 2000; Sokac et al., 2003). A model for Tuba function in endocytosis is illustrated in Figure 1. Through the membrane curvature sensing BAR domain, Tuba is recruited to forming or newly formed endocytic vesicles. Once at endocytic vesicles, full length Tuba might recruit dynamin; alternatively, dynamin could help to recruit and/or position Tuba. The exchange activity of the DH domain could be stimulated by the binding of the BAR domain, thus activating Cdc42. Activated GTP-bound Cdc42 would bind to and activate Tuba recruited N-WASP, that in turn would stimulate Arp2/3-mediated actin nucleation. Ena/VASP proteins might function to promote actin filament elongation and bundling after Arp2/3-mediated nucleation, and facilitate vesicle movement through the cytoplasm, analogous to their role in promoting *Listeria* motility.

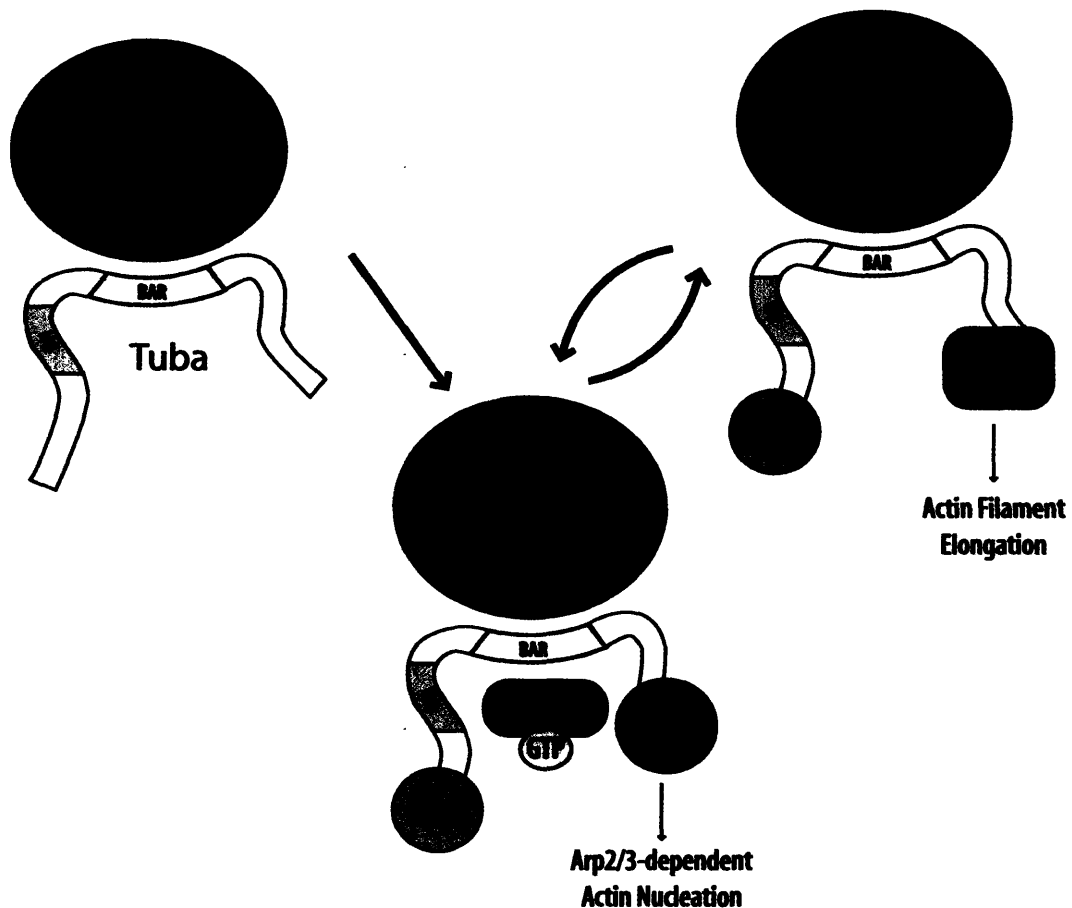


Figure 1. Model for Tuba Function in Actin Driven Vesicle Movement. Tuba is recruited to endocytic vesicles via its BAR domain. At vesicles, Tuba recruits Dynamin (Dyn) and N-WASP and/or the N-WASP/CR16/WIRE complex. The DH domain promotes GTP-bound Cdc42 that activates N-WASP, stimulating Arp2/3-dependent actin nucleation. Ena/VASP proteins also bind to the C-terminus of Tuba, and are known to promote actin filament elongation. Through Tuba, N-WASP and Ena/VASP proteins function in concert to regulate actin assembly at vesicles and promote actin-dependent vesicle movement.

This model for Tuba function could be tested through a number of biochemical and cell biological experiments. For example, the ability of Tuba to promote Cdc42-dependent actin assembly by recruiting N-WASP and/or the N-WASP/CR-16/WIRE complex could be tested *in vitro* in pyrene actin assays. Tuba should stimulate actin polymerization when combined with N-WASP, the Arp2/3 complex, Cdc42, and PIP₂, which contributes to N-WASP activation. Tuba-

Chapter 5

dependent actin assembly should require a combination of the GEF and C-terminal SH3 domains. The ability of the C-terminal SH3 domain, independent of the rest of Tuba, to activate N-WASP could also be tested in actin assembly assays. If Tuba promotes N-WASP-dependent actin assembly, the affect of other proteins found to interact with the C-terminus, including Ena/VASP proteins, on actin assembly could be tested.

The ability of Tuba to promote actin-based motility could also be tested *in vitro*. Beads coated with either full length Tuba or fragments of Tuba could be added to cell lysates or reconstituted motility media (Wiesner et al., 2003), and bead movement and actin tail formation measured. Removing known Tuba ligands from cell lysates by immuno-depleting or RNAi would define the necessary components for Tuba-mediated actin-based movement.

Visualizing Tuba in living cells should offer a clue to its function and better determine if it functions in endocytosis and/or vesicle movement. Though Tuba was found at the tips of dorsal ruffles in fixed cells, there was no way of determining the dynamics of its localization. Expression of GFP-tagged Tuba in living cells will determine where Tuba is localized, and if its localization alters with changes in cell movement, morphology and adhesion.

Another approach to determining Tuba function would be to knock down Tuba expression by RNAi and look for defects in endocytosis and vesicle movement in cultured cells. In addition, knocking down Tuba may produce defects in other Cdc42-regulated actin structures or processes, such as the

formation of filopodia. Analysis of actin-dependent processes in the absence of Tuba could better define its function.

Tuba is one member of a vertebrate family that includes two other related proteins, Tuba2 and Tuba3. All Tuba proteins share a similar DH-BAR-SH3 domain structure. Tuba 2 and Tuba 3 lack the N-terminal dynamin binding domain of Tuba, and are structurally similar to the shorter isoform of Tuba. This suggests a dynamin-independent role for the family. It will be interesting to determine if the C-terminal SH3 domains of Tuba 2 and Tuba 3 recruit a similar set of actin regulatory proteins, including Ena/VASP proteins. It will also be interesting to determine if the DH domains are specific for Cdc42 or another Rho-family GTPase. It is possible that the Tuba family has evolved to regulate actin assembly in multiple Rho GTPase signaling pathways.

Ena/VASP function *in vivo*

EV- deficient mice are viable and do not display any gross defects. Mice lacking VASP and EVL are viable with no apparent defects, whereas mice lacking Mena and EVL die perinatally and display defects in nervous system development. Loss of Mena, VASP and EVL disrupts spinal and trigeminal nerve formation, and disturbs neuronal layering in the cerebellum and cortex. Loss of Ena/VASP proteins during development also causes subdermal edema and intramniotic hemorrhaging, indicative of defects in cardiovascular function. Ena/VASP proteins function *in vivo*

to regulate specific actin-dependent migration and morphogenic events during vertebrate development.

EVL^{-/-} mice

Initial gross and histological examination of EVL^{-/-} mice did not reveal a phenotype. This was not completely unexpected given the expression pattern of EVL and the relatively subtle phenotypes of the other Ena/VASP single mutants. If the EVL knockout has a notable phenotype, it is expected to be found in a cell type that either only expresses EVL or requires a unique function of EVL. Such a cell type may be found in the immune system, where EVL is highly expressed. Analysis of immune cells in VASP^{-/-}; EVL^{-/-} mice (discussed below) could reveal an EVL-dependent phenotype, similar to that observed for VASP in platelets.

VASP^{-/-}; EVL^{-/-} mice

VASP^{-/-}; EVL^{-/-} mice are completely viable, and initial analysis suggested that the immune system develops properly in these mutant animals. However, given the evidence for Ena/VASP function in T-cell activation and macrophage phagocytosis *in vitro* (Coppolino et al., 2001; Krause et al., 2000), defects in immune system function are expected in mutant animals. To explore immune function *in vivo*, the ability of VASP^{-/-}; EVL^{-/-} mice to mount an immune response could be tested by injecting antigen and measuring immunoglobulin production. An Ena/VASP-dependent defect in immune cell function could also be pursued *in*

vitro. For example, the ability of VASP/EVL-deficient neutrophils to polarize in response to and migrate towards chemoattractants could be examined. Expression of Mena in cells of the immune could mask potential phenotypes; therefore, an Ena/VASP-deficient immune system could be rederived by injecting fetal liver cells from Mena⁺; VASP⁺; EVL⁺ embryos into irradiated mice.

Ena/VASP function in axon guidance

Mena⁺; VASP⁺; EVL⁺ mutant embryos display dramatic defects in spinal and trigeminal nerve formation. A more detailed histological analysis is required to characterize the nature and extent of these defects. Immunostaining with markers that label specific sets of neurons will reveal disrupted fibers tracts. Confocal microscopy of fluorescently labeled fibers in whole mount embryos could be used to visualize neuronal projections in 3-D. This information will be used to guide analysis on guidance pathways regulated by specific guidance factors, particularly those already known to function upstream of Ena/VASP proteins, such as Slit and Netrin.

Explants and dissociated cultures could be prepared from triple mutant embryos to study axon outgrowth and motility *in vitro*. The ability of Ena/VASP-deficient neurons to respond to attractive and repulsive cues (such as Netrin and Slit) could be tested in growth cone guidance and turning assays. Growth cone morphology and dynamics could be compared between neurons from pathways variably affected by loss of Ena/VASP function. In particular, filopodia formation

and dynamics could be examined to determine if Ena/VASP proteins are required for filopodia formation.

Ena/VASP function in brain development

$Mena^{-/-}$; $VASP^{-/-}$; $EVL^{-/-}$ mutant embryos with closed neural tubes display defects in neuronal layering in the cortex, and this phenotype can be pursued further. A more thorough histological examination of the forebrains from $Mena^{-/-}$; $VASP^{-/-}$; $EVL^{-/-}$ should reveal any additional defects in cell positioning and determine the extent of the defect hippocampus formation. Birthdate analysis of cortical neurons could also be performed to determine the stage or stages at which defects arise in mutant animals. In addition to examining layering defects, neurofilament and silver staining can be done to examine axonal pathways and fiber tracts, many of which are expected to be malformed. Axonal projections can also be visualized by Dil dye tracing.

The defect in cerebellar development in $Mena^{-/-}$; $VASP^{-/-}$; $EVL^{-/-}$ could also be explored further. Since $Mena^{-/-}$; $VASP^{-/-}$; $EVL^{-/-}$ mice appear so infrequently, use of an available EVL conditional mutant will further the investigation into the role of Ena/VASP proteins in cerebellar development. The EVL^{flxed} allele could be crossed to Cre drivers, such as the *Pcp2-Cre* line that restricts Cre expression to Purkinje cells, to determine if the cerebellar defect is specific to Purkinje cells or involves additional cell types, such as granule cells. If genetic analysis suggests the involvement of granule cells in the cerebellar defect, these cells can be studied

further. Granule cells are isolated easily, and could be used in migration assays to study guidance factor response. The ability of granule cells from mutant mice to respond to known guidance cues could be studied, and results might yield new information on signaling pathways that use Ena/VASP proteins.

Cardiovascular defects in Ena/VASP-deficient mice.

$Mena^{-/-}$; $VASP^{-/-}$; $EVL^{-/-}$ mutant embryos display subdermal edema and intraamniotic hemorrhaging, and the source of these defects should be determined. There are a number of potential causes for these phenotypes, including defects in endothelial barrier function, heart formation/function, smooth muscle function, and lymphatic system development. To begin to limit potential causes, specific Cre drivers will be used in combination with the EVL^{lox} allele to determine what cell types are involved. For example, restricting the deletion of EVL to endothelial cells using the TIE2-Cre driver will determine if the defect involves vascular development. Additional Cre drivers could be used to investigate other tissues and cell types. Once the cause of the defect has been identified with a certain tissue or cell type, the role of Ena/VASP proteins in this tissue or cell type will be pursued further. For example, if a defect is discovered in endothelial cells, the role of Ena/VASP proteins in cell-cell junction formation and endothelial barrier will be studied *in vitro*.

References

Bachmann, C., Fischer, L., Walter, U., and Reinhard, M. (1999). The EVH2 domain of the vasodilator-stimulated phosphoprotein mediates tetramerization, F-actin binding, and actin bundle formation. *J Biol Chem* 274, 23549-23557.

Coppolino, M. G., Krause, M., Hagendorff, P., Monner, D. A., Trimble, W., Grinstein, S., Wehland, J., and Sechi, A. S. (2001). Evidence for a molecular complex consisting of Fyb/SLAP, SLP-76, Nck, VASP and WASP that links the actin cytoskeleton to Fcγ receptor signalling during phagocytosis. *J Cell Sci* 114, 4307-4318.

Garrett, W. S., Chen, L. M., Kroschewski, R., Ebersold, M., Turley, S., Trombetta, S., Galan, J. E., and Mellman, I. (2000). Developmental control of endocytosis in dendritic cells by Cdc42. *Cell* 102, 325-334.

Krause, M., Sechi, A. S., Konradt, M., Monner, D., Gertler, F. B., and Wehland, J. (2000). Fyn-binding protein (Fyb)/SLP-76-associated protein (SLAP), Ena/vasodilator-stimulated phosphoprotein (VASP) proteins and the Arp2/3 complex link T cell receptor (TCR) signaling to the actin cytoskeleton. *J Cell Biol* 149, 181-194.

Kwiatkowski, A. V., Gertler, F. B., and Loureiro, J. J. (2003). Function and regulation of Ena/VASP proteins. *Trends Cell Biol* 13, 386-392.

Loureiro, J. J., Rubinson, D. A., Bear, J. E., Baltus, G. A., Kwiatkowski, A. V., and Gertler, F. B. (2002). Critical roles of phosphorylation and actin binding motifs, but not the central proline-rich region, for Ena/vasodilator-stimulated phosphoprotein (VASP) function during cell migration. *Mol Biol Cell* 13, 2533-2546.

Sokac, A. M., Co, C., Taunton, J., and Bement, W. (2003). Cdc42-dependent actin polymerization during compensatory endocytosis in *Xenopus* eggs. *Nat Cell Biol* 5, 727-732.

Wiesner, S., Helfer, E., Didry, D., Ducouret, G., Lafuma, F., Carlier, M. F., and Pantaloni, D. (2003). A biomimetic motility assay provides insight into the mechanism of actin-based motility. *J Cell Biol* 160, 387-398.